Mathematical Optimisation of the GSM-R Base Station Site Planning Problem

XINNAN LYU

A thesis submitted to

The University of Birmingham

for the degree of

DOCTOR OF PHILOSOPHY

School of Engineering

College of Engineering and Physical Sciences

The University of Birmingham

@ January 2020

Abstract

The European Railway Traffic Management System (ERTMS) has introduced a significant enhancement in the operation of the railway network, in terms of robustness and efficiency. A main characteristic of the ERTMS is the adoption of the Global System for Mobile Communication for Railway (GSM-R) as the method of train-to-ground communication. As the operation of the signalling system in ERTMS requires a reliable and seamless GSM-R connection, the site planning for the GSM-R data communication system is a critical task in the development of the ERTMS railway network. In this thesis, a mathematical GSM-R modelling methodology is proposed for formulating and solving the site planning problem for GSM-R Base Transceiver Stations (BTSs), which is aimed at providing reliable GSM-R coverage for a railway network, while reducing the construction and operation cost of the infrastructure. Optimisation algorithms are also proposed in this thesis for solving the GSM-R BTS site planning problem. In addition, an integrated simulation platform has been developed for simulating and validating the GSM-R communication system in the railway simulation environment. The result shows that the optimal result generated by the proposed methodology can provide identical reliability as that of the BTS site plan of an existing ERTMS railway network. The author of this thesis thus provides a methodology that can reduce the effort involved in BTS site surveys, when planning a GSM-R network. Mathematical optimisation and simulation validation can reduce the time required for the BTS site planning process.

Keywords: Base station site planning, GSM-R, Mathematical optimisation, Simulation

Acknowledgements

First, I would like to express my gratefulness to my supervisors, Prof Lei Chen and Prof Clive Roberts, for their generous academic support and infinite patience during my research study. This thesis would not have been possible without their continuous support.

Second, I am grateful to Dr David Kirkwood for the technical support on coding and simulation, as well as the friendship over the past few years. His guidance on the development of the railway simulator is invaluable.

Finally, I would like to thank my partner, Miss Xinzhu Zhang, for her selfless support even in the hardest times.

Contents

List of Tables

List of Figures

Lists of Symbols and Abbreviations

List of Symbols and Variables

f_D	Doppler shift frequency
f_C	Carrier frequency
v	Speed of train
c	Speed of light
θ	Angle between railway track and propagation path
N_{BTS}	Number of BTSs in site plan
L_{BTS}	Location set of the BTSs in target network
S	Set of the feasible BTS deployment solutions
C	Confidence level of the prediction
P_{RX}	Receiving power at the sampling point
P_{TH}	Minimum threshold of the receiving power
T_{ho}	Handover time in the region of the sampling point
$T_{TH,ho}$	Maximum threshold of the permissive handover time
G_{TX}	Antenna gain of the transmitter
G_{RX}	Antenna gain of the receiver
L	Path loss of transmission
L_S	System loss of transmission
dB	Decibel
$PL(dB)$	Path loss of the transmission in dB
A	Correction factor of propagation model
B	Path loss exponent
γ	Coverage probability
σ	Standard deviation of the shadow fading
F_σ	Extra fade margin to overcome the shadow fading component
P_{next}	Receiving power from the handover target BTS
$P_{current}$	Receiving power from the current BTS
X	Coordinate of BTS
$D_{handover}$	Length of the handover zone
$E_{x,y}$	Average elevation of the 1 km^2 grid cell in TRI

Gs	geographical standard deviation within a radiation area

List of Abbreviations

ABFS	Adapted Brute Force Search
ATO	Automatic Train Operation
ATP	Automatic Train Protection
BER	Bit Error Rate
BFS	Brute Force Search
BTS	Base Transceiver Stations
CBTC	Communications Based Train Control
CDF	Cumulative Distribution Function
DMI	Driver Machine Interface
DTM	Digital Terrain Model
DTMs	Digital Terrain Maps
EM	Electromagnetic
EML	Extensible Markup Language
EMW	Electromagnetic Waves
ERTMS	European Railway Traffic Management System
ETCS	European Train Control System
EVC	European Vital Computer
FDMA	Frequency Division Multiple Access
FFT	Fast Fourier Transform
GA	Genetic Algorithm
GIS	Geographic Information System
GSM	Global System for Mobile Communications
GSM-R	Global System for Mobile Communications-Railway
HO Margin	Handover Margin
HSR	High Speed Railway
kHz	kilohertz
LOS	Line of Sight
LTE	Long-Term Evolution
LTE-R	Long-Term Evolution for Railway
MA	Movement Authority

MHz	megahertz
OOB	Out of Band
OSI	Open Systems Interconnection
PER	Packet Error Rate
PL	Path Loss
PLMN	Public Land Mobile Networks
RBC	Radio Block Centre
RFR	Radio Frequency Repeater
RTM	Ray Tracing Method
TDMA	Time Division Multiple Access
TRI	Terrain Ruggedness Index
UDP	User Datagram Protocol
UI	User Interface
VOLTE	Voice Over Long-Term Evolution
WLAN	Wireless Local Area Network
TETRA	Terrestrial Trunked Radio

Chapter 1 Introduction

1.1 Research Background

The railway is one of the primary means of public transportation, offering the benefits of high capacity and low carbon emission. The signalling system is designed and installed on the railway network to guarantee the safety of the operation, and to make it possible to operate multiple trains on the same railway line.

To provide high capacity in railway network, the lineside signals display the visual instructions by signal lights, which are controlled by the control units and the interlocking system to ensure the functions and prevent any logical conflicts. The lineside signal-based railway control system is normally referred to as conventional signalling when compared with digital train control systems.

Another primary type of railway signalling system is Communication Based Train Control (CBTC), which uses wireless technology as the method of communication between trackside systems and trains. Compared with conventional signalling which displays the indication via colour lights, in CBTC, the vehicle onboard computer provides the instructions to the Driver Machine Interface (DMI) of the train. This method of train control improves the level of information made available to the driver and provides the capability of advanced features such as Automatic Train Operation (ATO). The CBTC is commonly applied in metro systems, as metro lines are closed networks where it is easier to implement and validate the CBTC system. Also, the short-range communication technology in CBTC is more suitable for metro rather than mainline railways.

In the 1990s, the European railway industry developed the European Railway Traffic Management System (ERTMS) to introduce communication-based train control on mainline railways as well as to achieve interoperability across European countries. ERTMS has two elements, the European Train Control System (ETCS), which is an Automatic Train Protection (ATP) system to achieve the safety function of railway signalling, and the Global System for Mobile Communications-Railway (GSM-R),

which is a radio system that provides communication between trains and trackside elements. It is a standard of wireless communication that was adapted from the public GSM system and expanded with railway-specific applications. Compared with the 2.4 GHz communication used in proprietary CBTC systems, GSM-R uses a dedicated 900 MHz radio system for railway operation. The GSM-R service is provided by GSM-R Base Transceiver Stations (BTS), which transmit information provided by the Radio Block Centre (RBC). Figure 1.1 shows a typical network structure of GSM-R.

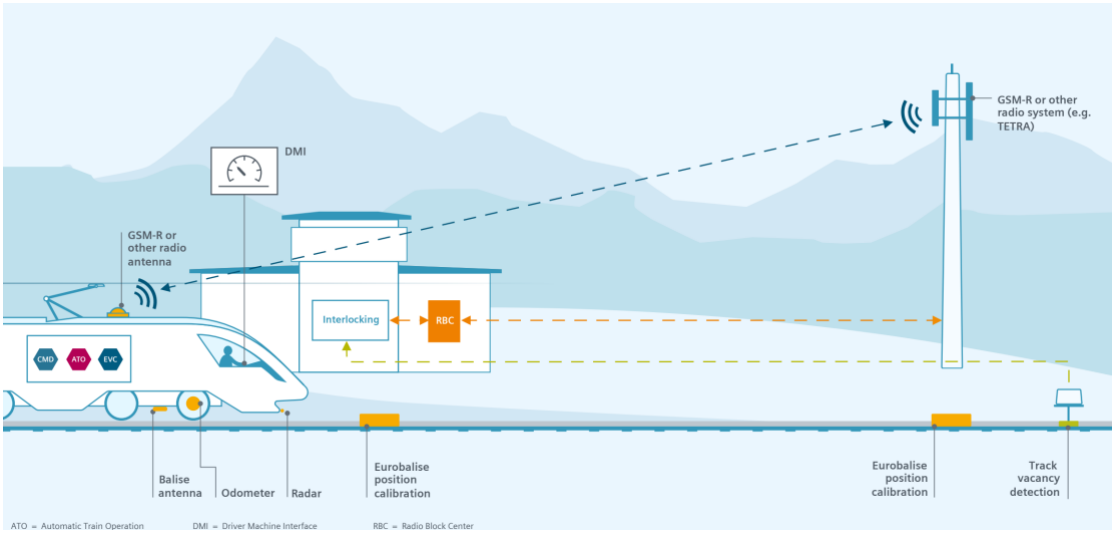

Figure 1.1 GSM-R in ERTMS (Siemens, no date)

In the operation of ETCS, the RBC uses its BTSs to transmit Movement Authorities (MA) to the trains via GSM-R communication. The MA is a permissive instruction which allows the train to enter the upcoming block section, as well as providing the properties of the railway line including location, length, gradient and speed limit. Since the information in MA contains the critical data for railway operation, the radio transmission of the GSM-R network must be guaranteed to prevent interference with railway operation. Therefore, it is important to plan the placement of the BTS to ensure robust coverage of the GSM-R radio signal.

1.2 Problem Statement

In the planning stage of a GSM-R network, several requirements must be considered in the BTS placement.

1.2.1 Coverage

The primary requirement for GSM-R site planning is full coverage of the railway network. This is because the operation of ETCS requires seamless coverage along the train route. During the operation, the on-board European Vital Computer (EVC) in the ETCS train detects the connection status of the GSM-R communication module. As the EVC follows the fail-safe operation principle, it applies a controlled stop to the train when the GSM-R communication is lost. Therefore, to prevent disruption impacts on the safe operation, it is vital to ensure the full coverage of the GSM-R signal at the site planning stage. Meanwhile, there are business and operation factors to limit the construction and operation cost. As a result, an optimised quantity of BTSs should be planned to avoid unnecessary redundancy of the radio network.

1.2.2 Propagation Model

The development of GSM-R is based on the public GSM-900 system. Even though the whole ecosystem of the GSM-900 system is fully developed and the system has been widely deployed in the world, the usage scenario is significantly different in the GSM-R network. For example, the user pattern in GSM-R network is mostly limited within the railway site area, which is unlike the GSM-900 usage pattern in public. Another difference is the environment of usage. The planning of the GSM-R network needs to consider scenarios such as mountains, tunnels and viaduct areas, as these scenarios are commonly shown in railway sites, unlike the public GSM which are mostly deployed in urban and rural areas. Such difference means that the planning of the GSM-R network requires dedicated radio propagation models which can successfully predict the transmission of the GSM-R radio signal. By far, most of the effective path loss models in 900 MHz band have been developed for urban and rural scenarios. Only limited research has been carried out in the railway environment and approaches vary in different regions. As a result, it is difficult to choose suitable propagation models to predict radio transmission.

1.2.3 Railway Operation

GSM-R is designed to operate at velocities of up to 500 km/h, while the public GSM is only available at up to 250 km/h. During the operation at high speed, the handover from one BTS cell to another should be specially considered, as it takes a certain time for the RBC to perform a handover. Therefore, the size of the overlap region for handover must ensure the successful handover in the high-speed scenario as well. On the other hand, during the movement of the train, the contact between catenary and pantograph can generate electric arcs, which generate a wide-band interference signal. This can affect the communication in a GSM-R network when the power received from the electromagnetic influence is greater than the power received from the GSM-R signal, causing requests for retransmission, therefore leading to higher end-to-end delays.

1.2.4 Optimisation Algorithms and Simulation Tools

At the site planning stage of a radio network, massive computation power is required to simulate the propagation of the electromagnetic waves (EMW). This is because ray-tracing is the most accurate method to simulate the propagation of EMW, but requires exhaustive calculation to ensure the accuracy of the prediction. To reduce the computation effort while maintaining the accuracy, using best-effort algorithms and stochastic propagation models are a more practical way to achieve the BTS site planning at an economic cost and effort.

In terms of the validation of the site planning result, most of the simulation tools used in the railway industry are based on public GSM simulators. The lack of railway features, such as simulating the movement of the trains and the effect of the GSM-R communication on the railway operation is a challenge.

1.3 Objectives and Contributions of the Thesis

The author of this thesis aims to provide a theoretical approach to modelling and optimising a GSM-R communication network. He evaluates the factors to consider during the radio site planning stage. Based on the conditions and requirements of the data communication in ERTSM, the author will propose a method to optimise the

placement of the GSM-R base stations, which considers the properties of the railway operation. This mainly includes the following objectives:

a) To create a mathematical modelling method for GSM-R base station placement in a railway network.
b) To develop efficient optimisation algorithms for solving GSM-R base station placement problems.
c) To present an integrated simulation platform for evaluating the GSM-R communication in a railway environment.

The author contributes to the following aspects:

a) He proposes a modelling and optimisation method dedicated to the GSM-R network, which provides guidance for the GSM-R site planning at an early stage and can reduce the time required for the processes of site planning.
b) He considers the factors that apply to both the railway and the communication system to generate a comprehensive method.
c) He establishes a simulation platform which integrates the radio simulation within the simulation of the railway operation.

1.4 Thesis Outline

The overall research motivations and background are addressed in Chapter 1; in particular, the problems involved in GSM-R BTS site planning are presented.

Chapter 2 gives a general introduction and review of related research carried out on GSM-R communication systems, where the requirements of the site planning and GSM-R prediction models are presented.

Chapter 3 introduces the methods of modelling, which will be carried out in two respects, the modelling of the railway network and the communication system.

Chapter 4 proposes the optimisation method and evaluation of the suitable optimisation algorithms.

Chapter 5 conducts a theoretical case study of an existing GSM-R railway line, which simulates the application of the optimisation method onto a real-world railway system.

Chapter 6 presents the deployment of a simulation platform for evaluating the impact of the GSM-R optimisation result on the railway operation. The optimisation result is compared with the site plans to evaluate the result.

Conclusions and future work are presented in Chapter 7.

Chapter 2 Research Review of GSM-R

2.1 Research Background

The Global System for Mobile Communication (GSM) is currently the most widely used communication standard for public mobile voice and data communication. Because of the high market share and the global availability of the GSM standard, it has been enhanced and adapted as a standard for railway communication for signalling and operation system, which is referred to as the Global System for Mobile Communication – Railway (GSM-R). With the advantage of the mature ecosystem and the railway specific features, GSM-R has been successfully and widely deployed in several regions in the world, including Europe, Australia, South Africa, China and India. Compared to the standard GSM which can operate at speeds of up to 250 km/h, the primary advantage of the GSM-R system is that it supports the movement at very high speeds, which can provide seamless connection when the trains operate at up to 500 km/h. In the scenario of high-speed operation, the GSM-R connection is the primary method of communication with the onboard computer. Therefore, the main aim for the site planning of the GSM-R network is to guarantee the reliability of the railway operation, as the failure of the radio communication would result in a downgrade to the fail-safe status of the signalling system, which leads to disruption of the railway services. To ensure the reliability of the GSM-R network and to always maintain the communications link, GSM-R site planning should include the propagation of the radio signal, the potential interference and a modelling and simulation tool to validate the site plan.

The aim of this chapter is to analyse the characteristics of the GSM-R radio communication system and the variety of approaches to model and simulate GSM-R. This chapter is divided into three parts. In the first part, the GSM-R propagation models and interference studies are reviewed, which include the factors to validate in GSM-R site planning. In the second part, approaches to GSM-R site planning are illustrated. The third part introduces the existing solutions for GSM-R modelling and simulation.

2.2 The GSM-R system

The GSM-R system in ERTMS is the communication system that provides a reliable and secure connection between trains and trackside elements. The specification of the GSM-R standard was developed by the EIRENE project (UIC, 2015) that defined the system requirement specification for railway operations. The GSM-R system uses 4 MHz frequency bands in the GSM-900 and DSC-1800 system. In Europe, the frequency band 876-880 MHz is allocated in GSM-R for the uplink, and 921-925 MHz for the downlink (Bouaziz *et al.*, 2016) (Briso *et al.*, 2002). To maximise the usage efficiency of the frequency bands, the GSM-R applies the following two multiple access methods to allow multiple users.

The first method is Frequency Division Multiple Access (FDMA) applied to the BTS of the GSM-R system. The 4 MHz band is allocated to the BTS as 200 kHz radio channels. To avoid co-channel interference, each GSM-R cell uses a specific GSM-R channel that differs from the adjacent cells. Each of the GSM-R channels occupies 200 kHz of the GSM-R frequency band. Therefore, a total of 20 channels is available in theory in the 4 MHz bandwidth. To consider the coexistence of the GSM-R with other communication systems, the railway operator can use up to 19 GSM-R channels by introducing a 200 kHz guard band (Lefrancq, 2016).

The second method is Time Division Multiple Access (TDMA) that is applied to the users of the GSM-R system. For each frequency band, data transmission is made in periodical TDMA frames with a period of 4.615 milliseconds. This TDMA frame is divided into 8 time slots of 577 microseconds each, which can be attributed to up to 8 users in the same frequency channel. Each time slot contains a burst composed of 156 bits, including 148 bits of information (Dudoyer *et al.*, 2011). Figure 2.1 shows the TDMA scheme in GSM-R.

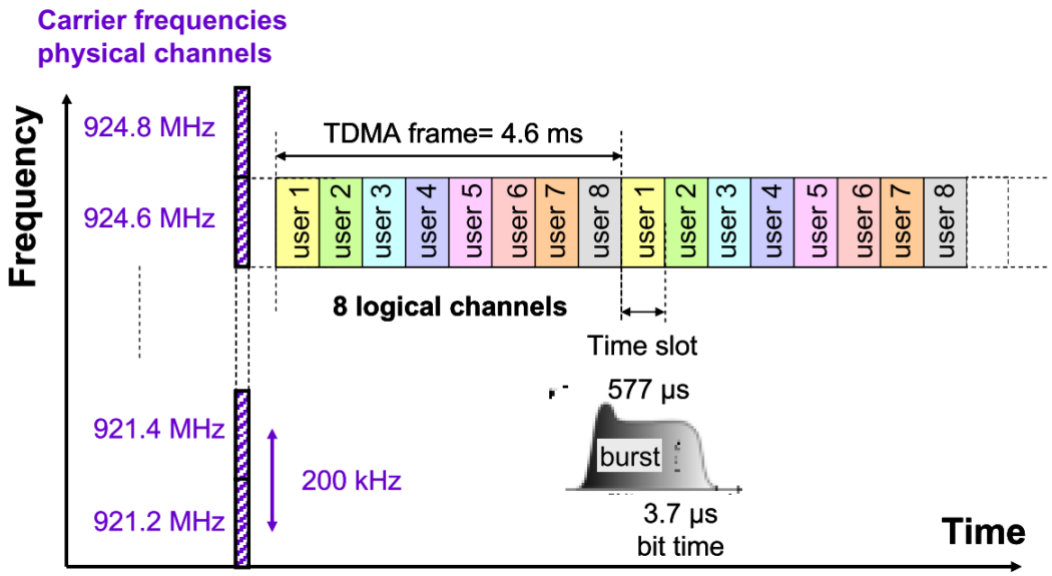

Figure 2.1 Multiple Access Scheme in GSM-R (Lefrancq, 2016)

2.3 Other Communication Systems in Railway

To understand the characteristics of the GSM-R system, a general literature review was conducted to assess the existing communication systems currently employed in the railway environment.

2.3.1 WLAN

The Wireless Local Area Network (WLAN) is the most widely used communication system in metro environment, also known as Wi-Fi. In (Wen *et al.*, 2018), the use of WLAN in metro signaling systems is introduced. In most cases, WLANs use the 2.4GHz band for wireless communication, which results in various challenges. The primary challenge is the co-channel interference caused by the limited spectrum, where some access points may need to share the same frequency. Another challenge is the limited coverage for each access point due to the limitation in transmission power. The case study conducted by the author utilizes 27 dBm as the effective transmission power, with the distance between the two adjacent access points not exceeding 65m.

2.3.2 TETRA

The Terrestrial Trunked Radio (TETRA) is another technology widely used in the railway environment. In (Wei Qi *et al.*, 2012), the application of TETRA in the urban railway environment is introduced. Due to TETRA being a generic radio communication system, the author introduces an example of a secondary developed system when deploying the system into an urban rail transit system. The TETRA system uses a frequency of 800MHz. Another example of deployment is provided in (Alamoud and Schütz, 2012), where the frequency of 400 MHz is utilized in a typical urban setting.

As of the date of this thesis, there have been several discussions about selecting TETRA as the replacement for the GSM-R network. The author in (Hsiao and Lin, 2023), introduces the TETRA as the most widely adopted choice of communication system for newly constructed railway projects worldwide. In terms of difference between TETRA and GSM-R, the author in (Hu *et al.*, 2022) compared the characteristics of the two systems. Both systems use TDMA as the access scheme and operate at the same level of transmission power. The primary difference is that TETRA uses a channel bandwidth of 25 kHz, which is narrower than the 200 kHz used in GSM-R. Therefore, the peak transmission rate in TETRA is limited to 7.2 kb/s, which is slower than the 9.6-21.4 kb/s in GSM-R. Another distinction is that TETRA can utilize a broader frequency band compared to GSM-R. The author provides an example of the frequency band, which ranges from 380 MHz to 866 MHz. Meanwhile, the GSM-R operates only at a dedicated frequency range of 876MHz to 960MHz.

Due to the similar characteristics shared by TETRA and GSM-R, the methodology of this research can also be applied to the TETRA system in railway.

2.3.3 LTE

The Long-Term Evolution (LTE) and LTE for Railway (LTE-R) are also widely deployed in the railway system. In (Tingting and Bin, 2010), a comparison of system architectures is made between GSM-R and LTE-R. The architecture of LTE-R is flatter compared to GSM-R, as LTE-R supports multiple access systems and is compatible with GSM-R.

Compared to GSM-R, LTE has several limitations. The LTE is designed to operate at speeds of up to 350 km/h and is not guaranteed to function at speeds of up to 500 km/h. Therefore, testing the operability is necessary to ensure safe operation. (Guan, Zhong and Ai, 2011) conducted simulations of LTE-R to assess its performance at speeds of 350 km/h and 500 km/h. The results indicated that LTE-R is a promising solution based on the channel quality. (Du *et al.*, 2012) propose a method to mitigate the inter-carrier interference caused by Doppler frequency shift resulting from high-speed railway operation.

The challenge of coverage is discussed in (He et al., 2016). As LTE-R uses a higher frequency band while co-existing with GSM-R, it introduces larger propagation loss and more severe fading, resulting in a cell coverage range of 4-12 km depending on the frequency availability in a region. For example, LTE can operate at 450MHz and 700MHz, providing better coverage than GSM-R. However, only limited regions in the world support the use of these frequency bands for LTE.

2.3.4 5G

As of the date of this research, there is limited research on the use of 5G in railway environments. The 5G system can mitigate the limitations of LTE and GSM-R. For example, more countries have planned to use the 700MHz band for 5G instead of LTE, which can provide better coverage in railway environments. The 5G system also natively supports operation at speeds of up to 500 km/h. The low-latency properties of 5G communication will also benefit the railway signaling system. In (Xue *et al.*, 2020), the authors discussed the potential use of 5G in railway scenarios, demonstrating a typical latency of 1ms. This is significantly shorter than the delay in GSM-R communication. A technical report in (*Evolution of GSM-R*, 2015) shows an example of an 800 ms delay in GSM-R communication, as well as 50 ms in a dedicated LTE system.

2.4 Characteristics of GSM-R

2.4.1 Differences between GSM-R and GSM

To meet the requirements of the railway operation in ETCS mode, the operations group (GSM-R Operations Group, 2012) defines the system requirements of the GSM-R for deployment and operation, including radio specifications, network reference model, and railway applications. The main differences between GSM-R and GSM lie in the following three aspects, namely, speed, security, and railway specific applications.

2.4.1.1 Speed

The main advantage of GSM-R is the support of higher speeds of up to 500 km/h. When the GSM-R users operate at high speed, the high Doppler shift and Doppler spread can impact the transmission (Zhou *et al.*, 2011). Therefore, (UIC, 2015) has defined the minimum requirements for the operation of the GSM-R network, including:

- coverage probability of 95%, based on a coverage level of -98 dBm for voice and non-safety critical data;
- coverage probability of 95%, based on a coverage level of -95 dBm on lines with ETCS levels 2/3 for speeds lower than or equal to 220 km/h;
- coverage probability of 95%, based on a coverage level of -92 dBm on lines with ETCS levels 2/3 for speeds above 280 km/h;
- coverage probability of 95%, based on a coverage level of between -95 dBm and –92 dBm on lines with ETCS levels 2/3 for speeds between 220 km/h 280 km/h.

As a higher threshold of received power is set in the GSM-R system, a more reliable guarantee is made when trains travel in high speed, which results to the 500km/h speed characteristics of the GSM-R. The requirement is also test validated by and has been proven to be operatable at 574.8km/h (Railway Signalling EU, 2013).

2.4.1.2 Security

ETCS is an Automatic Train Protection (ATP) system that transmits movement authorities to train drivers via in-cab displays and to Automatic Train Operation (ATO) equipment. The main purpose of the ATP is to avoid human errors and prevent train collisions (Cecchetti *et al.*, no date). In ETCS Level 2, the train collects position information from the trackside elements and reports the location and speed information to a Radio Block Centre or RBC. Based on this information, the RBC sends the movement authority (MA) to the onboard European Vital Computer (EVC), then the MA is applied to the ATP system to apply the permissive information. Within the process, the safety-related messages, including position report and MA, are transmitted bidirectionally by GSM-R.

As the transmission of the GSM-R radio is propagated in an open environment, a communication protocol known as EURORADIO is introduced in ERTMS to ensure the security of the GSM-R transmissions. The interfaces of the EURORADIO are shown in Fig 2.2. The messages generated by trackside and train borne applications are handled by the EURORADIO communication protocol and transmitted via a network medium. The EURORADIO acts as a safety layer in the communication system; therefore, it introduces network overhead, including processing delay and additional headers in the data packet.

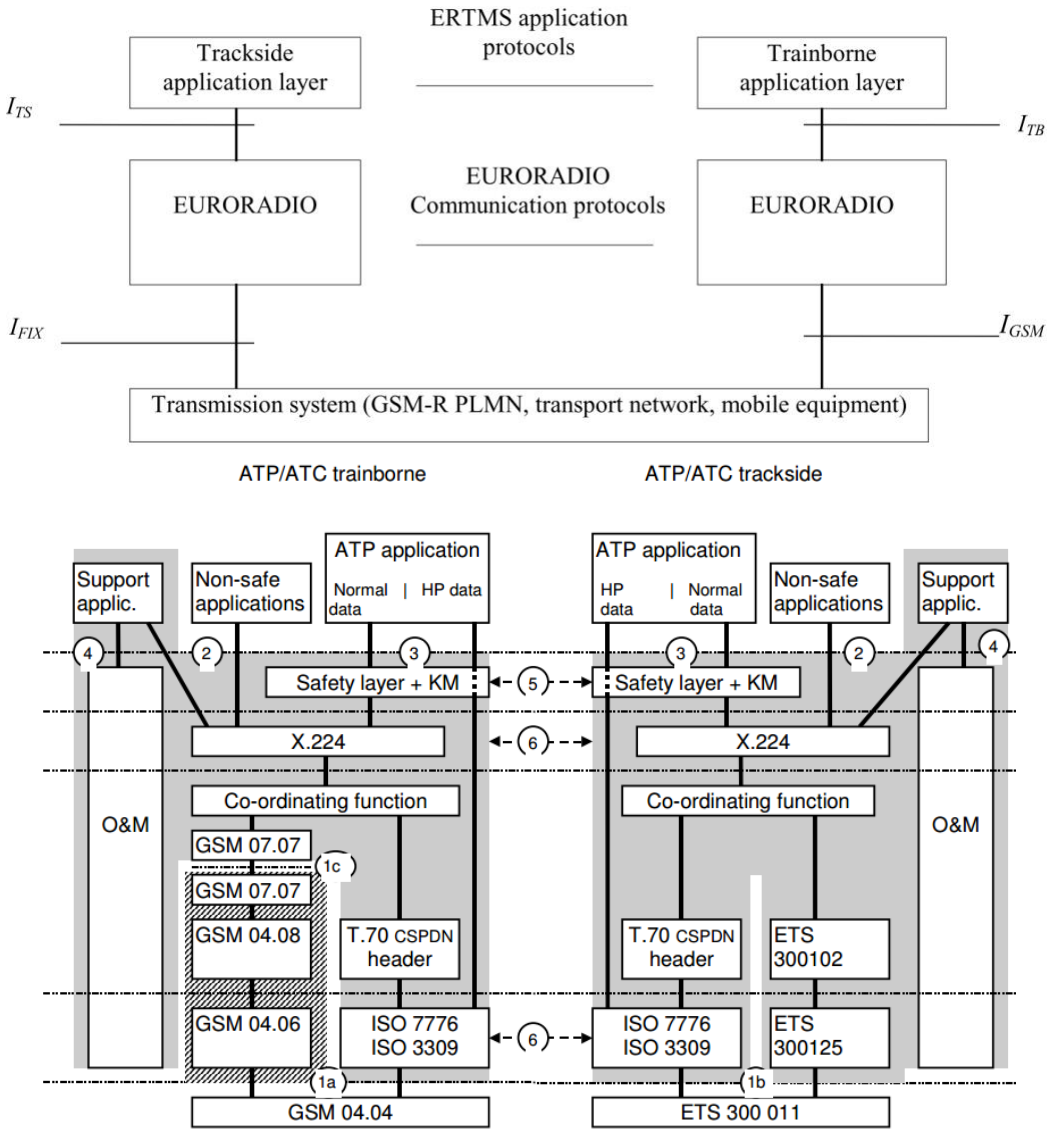

Figure 2.2 EURORADIO interfaces (UNISIG, 2012)

Figure 2.2 also shows the standard network architecture of the EURORADIO protocol. The security feature of the EURORADIO system is provided by the safety layer with Key Management, which correspond to Index 3 in the figure. As physical keys are used as the method of authentication for key management, the key management feature can ensure the exclusivity of the GSM-R network and can also ensure cyber security. X.224 is a connection transport protocol, which can request new network connections and establish transport connections with different priorities.

Since the priority of GSM-R communication is handled by the safety layer, the performance of EURORADIO needs be assessed to ensure the performance of transmission for the railway signalling system. (Chen *et al.*, 2011) applied performance

analysis to the EURORADIO safety layer. The authors created a Coloured Petri Net model for simulation to analyze the performance under intensive transmission conditions. The simulation's parameters were set by choosing data loss rates of 0.01, 0.05, and 0.1. Subsequently, confidence intervals for the probability of communication within various time frames were simulated to evaluate the performance of the EURORADIO safety layer. When a time limit of 15 seconds is set for safety connection establishment, the EURORADIO protocol can guarantee a success connection rate of 0.9673. The paper also presented a method to enhance the existing protocol by incorporating advanced schemes, which can elevate the confidence level to 0.9863. Similar research using Coloured Petri Net is also presented in (Lijie *et al.*, 2012).

In (Quan, Zhao and Zhou, 2013) , authors utilized a probabilistic model checker tool to conduct a similar evaluation. The result shows that with a message loss rate of 0.01, the probability of establishing a secure connection within an 8.5-second time frame is 0.99884.

2.4.1.3 Railway Applications

To meet the additional demand for railway applications, the designers (UIC, 2015) supplemented the GSM-R with additional features including voice broadcast service, voice group call service, railway specific applications, shunting mode, etc. The voice group call service allows several GSM-R users to participate in the same voice calling session where the standard voice broadcast service only enables the call initiator to broadcast voice message. Meanwhile, the railway specific applications are implemented by allocating different call priorities to the service. For example, the shunting mode and emergency mode can initiate a voice communication session with higher priority than a voice group call service and a voice broadcast service.

2.4.2 Propagation Models

Based on the system requirement specification discussed in section 2.2.2, research has been conducted to implement and optimise BTS site planning. The propagation can be modelled with two methods, numeric calculation and stochastic models.

2.4.2.1 Numeric Models

The propagation of the GSM-R radio signals can be simulated by calculating the reflection and diffraction of the electromagnetic waves (EMW). In the open-space

scenario, the 2-ray model is typically applied to simulate the line-of-sight (LoS) propagation and the reflected EMW on the ground. By adding the number of reflected and diffracted EMWs in 3D space, the ray-tracing method (RTM) can be used to increase the accuracy of the EMW simulation (Wei *et al.*, 2012). In RTM, the EMWs are launched in every direction of 3D space, which can then be reflected, scattered and diffracted at the objects in the 3D space. The reception of radio is calculated by summing all the EMWs propagated to the receiver in the radio system.

In (Zhang, 2013), a multi-path propagation calculation method is proposed to simulate the propagation of GSM-R in the high-speed railway environment. In this paper, the author introduces a 3-ray model to simulate the EMW propagation, including line-of-sight transmission, ground-reflection transmission, and the reflected EMW caused by the metal surface on the roof of the high-speed trains. The results from the author's case study show that the 3-ray model can provide a more accurate prediction result than the typical 2-ray model when the transmission distance is over 2 km. Based on the measurements collected in the case study, the 3-ray model can be simplified into a 2-ray model when the communication range is between 362 m and 1989 m, which can be simplified further into a Line of Sight (LoS) model when the range is within 362 m. As the multipath model introduced in this paper is based on 2D RTM, the use of the 3-ray model is limited to plain space without any primary object in the environment.

In (He *et al.*, 2017), a ray-tracing study was conducted at 3.5 GHz in a railway environment. Even though the frequency applied in the study is different from the typical 900 MHz frequency of GSM-R, the principle of the ray-tracing study is identical for the GSM-R system. In this paper, the author built a 3D railway environment in urban, cutting and viaduct type areas, with a total length of 1740 m. The RTM study was based on a high-performance computing server, and the modelling tool was based on Google Sketchup 3D modeller. In (Zhang *et al.*, 2015), an RTM study was conducted in a 163 m station environment. The study shows a conflict in that the computational cost increases exponentially with the number of surfaces in the model. Thus, the number of objects in the 3D model must be minimized; on the other hand, a high level of detail in the 3D model is required to guarantee the accuracy of the simulation results. This is because objects with a dimension that is larger than the wavelength of the communication frequency can influence the transmission. Thus, all the topology and buildings in the 3D environment must be modelled.

As the application of the GSM-R system is on the mainline railway, the GSM-R radio must be propagated in a large-scale environment. (He et al., 2016) suggests that the typical distance between two GSM-R BTS is 7 to 15 km. By considering redundancy coverage to ensure higher availability and reliability, a BTS distance of 3 to 5 km is applied. The size of a single GSM-R cell is much larger than that used in the 3D RTM study introduced in (He *et al.*, 2017) and (Zhang *et al.*, 2015). Due to the high computation cost and effort of 3D modelling, numerical calculation methods, such as RTM simulation are not appropriate for GSM-R site planning and optimisation. As RTM simulation cannot be processed efficiently when the 3D environment has a high level of detail, it would take significant amount of time to provide calculation result for each base station configuration, which is normally a few days of computation time for each area.

2.4.2.2 Stochastic Models

Stochastic models are developed from site measurements or ray-tracing studies, which have the feature of simplicity and generality (Priebe and Kurner, 2013). As GSM-R is adapted from the public GSM system, a number of standard empirical models are available for GSM-R propagation studies, including the HATA (Hata, 1980) and WINNER (Kyösti *et al.*, 2008) models.

(Lin *et al.*, 2012) proposes a novel channel model suitable for the high-speed railway environment based on the WINNER II physical channel model. Introducing the characteristics of viaducts and complex terrain, they adapted the Rician channel model to describe multipath fast fading and selected the Lognormal distribution to model the shadow fading. However, the proposed channel model has only been validated by simulation, it has not been tuned further by site measurements.

The author in (Luan *et al.*, 2013) conducted a comparison between the propagation results from WINNER II and the fitted results from measurements. The study was carried out in hilly terrain, where the WINNER II model was applied by the two-slope model with a breakpoint distance. The result shows that the fitting curve of the measurements is very close to the WINNER II path loss model over short distances. The differences arise in the breakpoint distance, as well as the slopes of the two segments in the model. This means that the estimation of scattered power caused by hilly terrain is higher than the prediction of the WINNER II model. The review in (He

et al., 2011) also shows that the WINNER II model is unable to predict the EMW propagation in the railway cutting scenario. Therefore, there is a certain limitation to the application of the WINNER II channel model.

Another widely used empirical propagation model is the Okumura-Hata model. In (Medeisis and Kajackas, 2000), the authors provide an approach to adapt the universal Okumura-Hata propagation prediction model for rural areas. The paper illustrates the corrections appliable to the propagation model and the setup requirement for tuning the model for use in a non-standard environment.

The study in (Cota *et al.*, 2013) applies a similar approach and adapts the Okumura-Hata for the railway environment. The author conducted high accuracy measurements on 560 km of urban railway in Lisbon, which were processed to tune the prediction model. The result shows that the tuned Okumura-Hata model can provide an accurate prediction in 90% of the places, which is consistent with a high correlation coefficient value of 87%. By excluding the results that are due to the inaccuracies of cartography, the final correlation coefficient and average total hit rate tend to approach the 100%.

(Usman, Sadiq and Ozovehe, 2012) also conducted a similar study on a suburban railway in Nigeria. The authors compared the measurement result with the Hata model and the 2-ray model. By adapting the Hata suburban model, the prediction model can provide a more accurate result than the 2-ray model. A similar study was also conducted by (Djomadji Eric Michel and Emmanuel, 2015), where the authors applied an iterative algorithm based on Newton second order to optimise the Okumura Hata model in an 800MHz CDMA network. Another example of modification is also demonstrated in (Akhoondzadeh-Asl and Noori, 2007) using the Levenberg-Marquardet method in a CDMA network. In (Zhang *et al.*, 2017), authors conducted an experiment with LTE network in a railway environment. The LTE network was utilized for providing passenger services rather than for train operations.

Apart from the standard propagation prediction models which are applicable to a particular frequency range, the propagation model can also be developed based on the measurement campaigns at a specific EMW frequency. As the propagation of EMW follows an exponential decay pattern when increasing the transmission distance, the propagation model can be described simply by the path loss exponent.

An example of Shadow Fading model is given in (He, Zhong, Ai and Oestges, 2015). A large set of measurements was conducted in the GSM-R system to determine the decorrelation distance and cross-correlation of shadow fading between two adjacent base stations. A heuristic model presented in the research was validated on a High-Speed Railway (HSR) line. Similar research based on measurements was also conducted in (Lu, Zhu and Briso-Rodríguez, 2011), where the GSM-R deployment in the railway terrain cutting environment was analysed. Testing of viaduct and plain scenarios was also conducted in (Wei *et al.*, 2010). The research in (Ma *et al.*, 2014) also applied measurements on an HSR train, presenting a real-time dynamic estimation algorithm for the GSM-R network.

(Lu and Bertoni, 2011) applied a different approach to determine a fading model. Instead of conducting field tests, the authors utilized Monte Carlo simulations on a typical mobile communication system in hilly and mountainous terrain. The simulation results based on a variety of databases can prove the feasibility of using simulations to determine the fading models.

The survey in (Chen *et al.*, 2015) combined the use of standard empirical propagation models with the path loss exponent models. The survey categorised the HSR environment into plain, viaduct, cutting, suburban and in-carriage scenarios, and derived the path loss model by fitting the measurement result into the WINNER II model and path loss exponent model. However, the study conducted in this paper does not cover all possible railway scenarios, such as hilly terrain and urban environments. A survey including mountain and urban environment is presented in (Ai *et al.*, 2012), which is part of the 12 railway scenarios discussed in this research.

In (C. Wang *et al.*, 2016), a survey was conducted to evaluate the path loss exponent in HSR environments. The measurements were conducted in several HSR environments, including open space, viaduct, cutting, hilly terrain, tunnel and station, where the open space scenario was further classified into rural, urban and suburban scenarios. The survey shows that most of the transmission on the railway relies on the LoS components, while the multipath components that are scattered and reflected by the surrounding obstacles will cause serious constructive or destructive effects on the received signal, thereby influencing the channel's fading characteristics. The paper also demonstrated

the encounter of more than one scenario in one GSM-R cell, such as the frequent transition between tunnel and viaduct environments.

2.4.2.3 Interference and Noise

An assessment in (Martens and Schattschneider, 2014) analysed the three potential electromagnetic (EM) interference mechanisms associated with the GSM-R system, which is Out Of Band (OOB) emissions, blocking and intermodulation. The analysis shows that the blocking and intermodulation interference are caused by the strong public land mobile network (PLMN) signals received by GSM-R radio, which can be mitigated by improving the performance of GSM-R receivers, or by limiting the PLMN emission levels. Although GSM-R uses a dedicated frequency band, the paper shows that no harmonized limits exist in the EU. Also, the OOB interference caused by PLMN can only to a very limited extent be mitigated by measures in the GSM-R network and must be resolved on the PLMN side. The report demonstrated the potential EM Interference (EMI) caused by the public network, which can be eliminated or reduced by enforcing the EM compatibility (EMC) standard but did not provide an analysis of the EMI generated by the railway system.

(Adriano *et al.*, 2008) raised the issue of the significant EM disturbance produced when sparks occur due to poor contact between the catenary and the pantograph. Measurements were carried out in the study to record the transient noise generated by the sparks. The paper presents a model to analyse the transient signal generated by electric arcs in terms of power, rise time, duration and the repetition rate. By applying a Fast Fourier Transform (FFT) to the modelled transient signal, the author noted that all the transient interferences cover the GSM-R frequency band. The analysis shows the average rise time is 1ns, and the average duration is 20 ns, which are considerably shorter than the duration of a GSM-R burst. This means the average interference of the spark is not able to block the GSM-R signal but can introduce a higher bit error rate (BER) to the GSM-R communication. However, the study only provides limited estimates for the repetition rate of the interference, as a more accurate measurement is needed.

In (Dudoyer *et al.*, 2012), the authors performed measurements on both DC and AC supplied railway systems. The results show that the distribution of the rise times and of the burst durations are similar for the two supply voltages. The duration of the transient disturbance is less than 20 ns, with an average of 5 ns, while the rise time of the

disturbance is 0.4 ns on average with a maximum measured value of 1 ns. In this paper, the repetition rate of the transient disturbance is measured, which varies significantly in different operation conditions including speed of train, nature of traversed areas, etc. Therefore, it is meaningless to try to define a typical value for the repetition rate, as it depends on the characteristics of power facilities and operation conditions. Thus, the author suggests the use of a variable for the repetition rate when performing immunity tests. The immunity tests presented in the paper indicate that the bit error rate (BER) of the GSM-R transmission increases when the time interval decreases. Also, when the repetition rate is below 150 μs, the BER is greater than 1.13%, which is the upper limit of the QoS requirement defined in (ALCATEL *et al.*, 2005).

2.4.3 **Doppler Effect**

When the railway operates at high speed, the Doppler effect can affect wireless communication. The Doppler effect can be defined in two forms: Doppler frequency shift and Doppler spread.

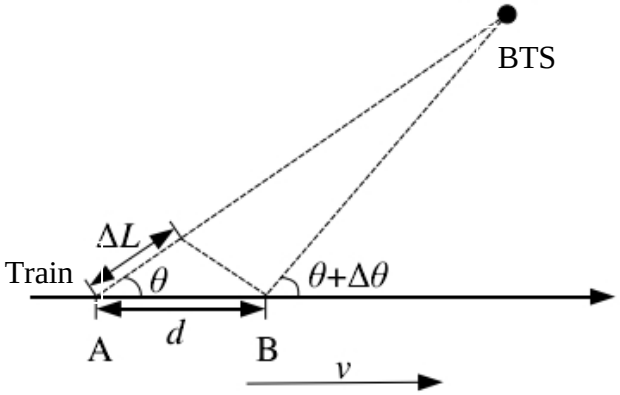

Figure 2.3 Doppler Effect in railway operation (Cai, 2017)

The Doppler frequency shift is caused by the fast movement of the train. When the train is approaching or travelling away from a BTS, the high relative speed between the BTS and the train can cause a frequency change and phase change of the GSM-R transmission band. Figure 3.8 demonstrates a typical Doppler effect in the railway scenario. The Doppler shift frequency can be modelled by:

$$f_d = \frac{v}{c} \times f_c \times \cos\theta \quad (2.1)$$

Where f_D is the Doppler shift frequency, f_C is the carrier frequency of the GSM-R network, v is the speed of the train, c is the speed of light, θ is the angle between the railway track and the LoS propagation path. In the GSM-R deployment, the placement of BTS must be within the railway corridor near the track; therefore, the angle θ can be assumed to be zero. Equation (3.24) can be thus simplified as:

$$f_D = \frac{v}{c} \times f_C \tag{2.2}$$

As the shift frequency can be determined by the GSM-R system, the effect of the Doppler frequency shift can be compensated by the transmission component of GSM-R.

The Doppler spread is caused by the Doppler frequency shift in the different direction of the multipath propagation, resulting in a spread of the power spectrum. Therefore, comparing with the propagation when the train is stationary, the received power at the compensated Doppler frequency is reduced when the train operates at high speed.

The level of the Doppler Spread is determined by the speed of operation and the roughness of the terrain. It is not possible to take measurements at high speed before the construction of the GSM-R communication system. As a result, the system requirement specification in (UIC, 2015) has added a compensating value to consider the Doppler Effect in this case. The minimum threshold is increased from -98 dBm to -95 dBm when the operation speed is over 220 km/h and further increased to -92 dBm when the operation speed is over 280 km/h.

2.5 BTS Site Planning

Although many research studies have been carried out to model the propagation of GSM-R EMW, there is limited research available to optimise the siting of BTSs for GSM-R communications.

2.5.1 General Site Planning in Railway

In (Kastell *et al.*, 2006) the authors discussed the factors influencing the GSM-R network, such as site planning to ensure handover quality, coverage at the entrance or exit of a railway tunnel, and handover during high-speed train travel. The author identified that the main cause of the problems in a GSM-R network is the high-speed operation, which can lead to poor propagation conditions. Therefore, a site planning

technique based on location information system is suggested, which can be used to estimate the cell planning. The paper only demonstrated a methodology for this approach without providing any technical details.

The technical report in (Binningsbø, Baldersheim and P., 2006) provides a set of GSM-R radio planning guidelines from the construction perspective. The report presents recommended values for minimum receiving power, base station and antenna configuration, and principles for predicting the propagation. BTS site planning is also discussed and a guideline for site location selection is proposed. The report does not provide a reference model to estimate the propagation or method of site planning to derive the optimised location.

In (He, Zhong, Ai and Guan, 2015), the author optimises the number of BTSs by improving the accuracy of the propagation prediction models. Based on measurements in a different environment, the path loss models were improved from the standard Hata model. A simulated case study was also carried out for this paper to apply the improved models on an existing high-speed railway line, which reduced the required number of base stations from 160 to 100. However, the optimisation process for the base station placement is not demonstrated in the paper.

In (Ai *et al.*, 2017), the author demonstrates the estimation of cell coverage by applying the propagation models for railway viaduct, cutting, urban, suburban and rural environments. The link budget calculation is presented to derive the required receiving power, which is applied to the path loss models to calculate the size of the BTS cell in the different types of environment. The deployment of the BTS cell is not covered in this paper.

Improper BTS location planning can result in issues such as:

- Increased cost of operation and maintenance: If a BTS fails to support a coverage probability of 95%, the transmitting power of the BTS must be increased to ensure the GSM-R users can receive enough receiving power. This increases the operation cost of the BTS and reduces the lifetime of its communication devices.
- Increased probability of handover failure: The level of receiving power cannot be guaranteed at the edges of BTS coverage areas, thus, the probability of handover failure increases when a train switches from one BTS cell to another. (Jin, Jiang

and Wu, 2010) analyse the impact of handover failure, which could cause call failure, data transmission failure or connection loss.

- Limited possibility of future railway upgrades: (UIC, 2015) defines the minimum coverage probability for the railway operation speed. This requirement is higher when applied to a network configured for high speed operation. It can also be a limiting factor for upgrades of the communication system, as new candidates for the next generation of railway communication standards tend to be more restrictive. (Martens and Schattschneider, 2014) review the operational requirement for LTE carriers, which indicates a required increase of 10 dB in the transmitting power.

2.5.2 Coverage in Tunnels

Apart from the general site planning approach shown in Section 2.5.1, there are additional configurations that need to be defined in the GSM-R system. When the train travels into a tunnel, the path loss at the entry of the tunnel can significantly affect the level of the received power within the tunnel. Therefore, extra equipment is required in the tunnel to provide extended coverage using GSM-R repeaters.

In (Briso-rodríguez, Cruz and Alonso, 2007), authors conducted measurements using 900MHz transmitters in a railway tunnel to simulate GSM-R transmission. The results indicate that 900MHz signals can propagate with significant loss for the first 300 meters. Also, a significant fade of 20 dB was observed as a train exited a tunnel. The paper concluded the research with a propagation model, which was also validated in the radio planning of a 40 km railway tunnel. Similar results were also shown in (Martí Pallarés *et al.*, 2001), where a signal power fade of up to 40 dB was measured when trains entered tunnels. (Liu *et al.*, 2017) surveyed tunnel channel measurements using various communication systems, including GSM-R and LTE.

(Siemens, 2004) provides the guideline for providing GSM-R coverage for the tunnel system. The report categorises tunnels by their length, and applies repeaters based on the configuration of the tunnel. Figure 2.4 shows a typical setup for a tunnel system using a radio frequency repeater (RFR).

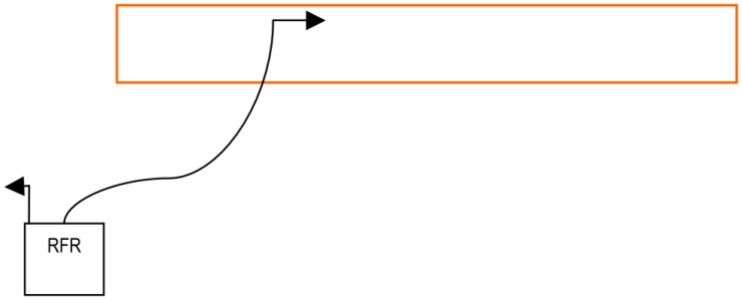

Figure 2.4 Deployment of a repeater to provide coverage in tunnels (Siemens, 2004)

Solutions for providing coverage in the tunnel system are summarised in Table 2.1.

Table 2.1 Coverage Solution in Tunnel System

Length of Tunnel	Solution	Extra Configurations
< ~100 m	N/A	Coverage is likely to be sufficient in most cases.
< ~300 m	One RFR	A single RFR is placed at one of the entries of the tunnel.
< ~1000 m	One RFR with radiating cable	A radiating cable, also known as a leaky feeder is used.
< ~1200 m	Two RFR with radiating cable	An RFR is placed at each entrance of the tunnel for providing enough power to the radiating cable
> ~1200 m	Two RFR with distributed antennas / radiating cable	Multiple antennas or radiating cables are required in a long tunnel, see Figure 3.10 for the configuration.

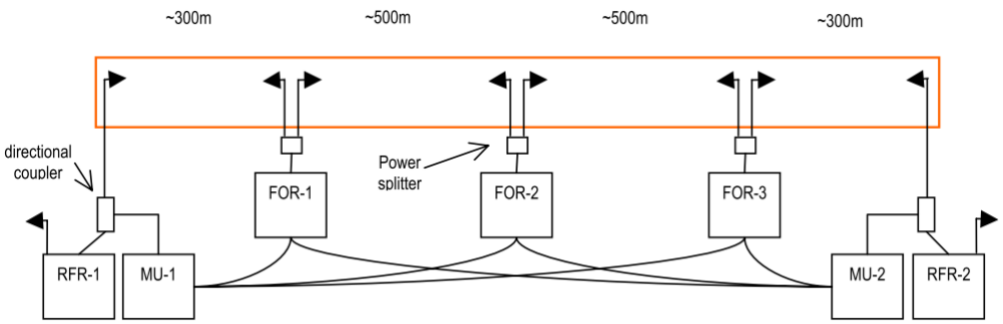

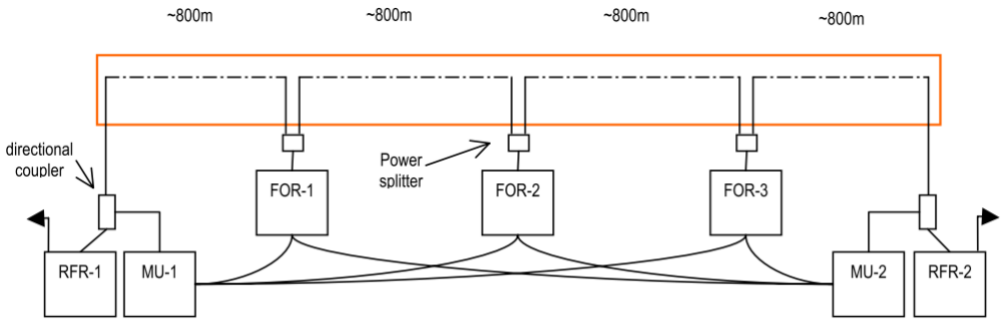

Figure 2.5 Distributed antennas and radiating cable configurations for providing coverage in long tunnels (Siemens, 2004)

2.5.3 **Coverage Redundancy**

A redundant design of the GSM-R network ensures a continuous connection when a failure occurs in the GSM-R communication system. At present, two solutions are adapted in the deployment of GSM-R to guarantee the coverage of the transmission, including a dual system in one RBC and interleaving redundancy coverage.

In (Shi, Zhang and Gao, 2010), the author provides examples for redundancy configurations in GSM-R site planning. Figure 2.6 shows an example of providing a dual system in the RBC. In this case, the RBC is fitted with two sets of communication systems, which are connected to two BTSs installed at the same location. In some railway systems, the two transmitting systems are even installed onto the same BTS tower. Therefore, when Network A fails, the ERTMS can hot-swap the communication system to Network B, leaving the railway service uninterrupted. This redundancy system has the advantage of low construction and maintenance cost.

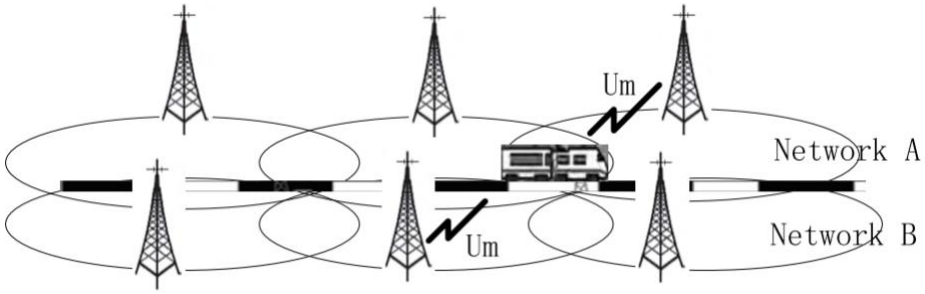

Figure 2.6 Dual system in RBCs (Shi, Zhang and Gao, 2010)

Another redundancy solution is to provide interleaving redundancy coverage using two GSM-R networks with different BTS configurations. Figure 2.7 is an example of the redundancy coverage solution.

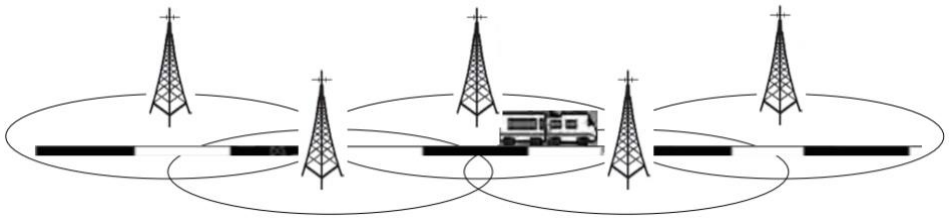

Figure 2.7 Interleaving redundancy coverage (Shi, Zhang and Gao, 2010)

In this configuration, the BTSs of the redundant network are located at the handover zones of the primary network. Both networks have the capability for providing the full coverage of the railway network. For operation, the train is equipped with two sets of communication system, which are linked to each of the GSM-R networks. Therefore, when a handover is required in the GSM-R transmission, the redundancy network can also provide support for the soft handover. However, the main disadvantage of this configuration is the construction cost of the redundancy network.

Research on evaluating different redundancy designs in a GSM-R network was conducted in (Miao, Tang and Liu, 2013). The author established a Markov Chain quantitative analysis based on system state transition models to simulate the performance of two different designs. The results show that the dual system design in RBC has higher reliability compared to the interleaving redundancy design. Meanwhile, the interleaving redundancy design has higher steady-state availability due to the common cause of failure in the same site. Therefore, the author suggested using interleaving redundancy for most of the rail network, while the dual system design should be implemented in key network segments.

2.6 Simulation Tools

Apart from numeric optimisation methods to derive the BTS placement, simulation and modelling tools are also suitable for site planning and can be used as validation tools for the optimisation result.

In (Nemţoi, Alexandrescu and Stanciu, 2010), the author undertook GSM-R site planning using the radio planning tool ICS Telecom. As ICS Telecom is a general radio

planning tool, the railway elements were converted into vectors and mobile subscribers. The environment was imported as Digital Terrain Maps (DTMs), and the standard ITU-R propagation models were selected for the simulation. The deployment of the BTS was an automatic process in the ICS Telecom software, which failed to cover all the subscriber points, leading to the need for a further manual intervention process to achieve the full coverage. (Hillenbrand, 1999) also demonstrates a radio network planning tool named TORNADO developed by Siemens. No further detail on the software is provided.

(Bouaziz *et al.*, 2016) use a discrete-event network simulator called OPNET to evaluate the performance of LTE communications operated in the GSM-R frequency band. The simulation indicated improvements in the performance of throughput and communication delay. The study described in (Sniady, Sønderskov and Soler, 2015) also selected the OPNET for simulating the use of Voice Over LTE (VOLTE) for railway operation. However, the OPNET does not support the GSM-R communication standard; therefore, all the research carried out in OPNET is limited to LTE or the public GSM system.

Several studies have utilized OMNeT++ as an IP-based radio network simulator, including (Wang, Liu and Hu, 2005), (Helgason and Kouyoumdjieva, 2012), (Khan, Kalil and Mitschele-Thiel, 2013), (Köpke *et al.*, 2008) and (Sousa and Jorge, 2013). Moreover, (Hammoud, Prof and Abdelouahab, 2012) utilised OMNeT++ for LTE simulation, demonstrating the feasibility of adapting the software for radio network simulation. There has been no research or simulation models for GSM or GSM-R simulation in OMNeT++.

2.7 Conclusions

In the previous sections, the main research on GSM-R propagation and the approaches to BTS site planning have been reviewed. Although substantial research has been carried out on the propagation study of GSM-R, the application of GSM-R propagation models is not well established in the existing literature. The limitations of the existing research can be summarised into the following three aspects:

1. **Limited support for the numeric optimisation of BTS site planning:**
   Within the author's knowledge, all the research about GSM-R site planning to date is unable to provide a numeric optimisation method for BTS site planning and optimisation.
2. **Lack of railway features in the existing site planning tools:**
   The existing site planning tools for GSM-R are adapted from those for the public GSM system. The GSM-R is emulated by generating the subscriber patterns to simulate the railway operation, which is unable to provide accurate site planning results due to the restricting requirements for radio coverage in railway operation.
3. **Incomplete support for optimisation algorithms:**
   The existing site planning tools solve the BTS placement problem by applying a built-in optimiser, where the optimisation algorithm cannot be modified by users. The use of the site planning tools is also a factor of limitation, as the existing tools are developed for commercial use, but are not available for academic research.

This chapter introduced the literature related to GSM-R modelling and planning. Based on the requirement of the GSM-R deployment and the factors that affect the transmission, a method to model the GSM-R BTS site planning problem will be introduced in the following chapters, which is able to apply the variety of optimisation algorithms available.

Chapter 3 Mathematical Modelling of the GSM-R BTS Site Planning Problem

3.1 Introduction

In the previous chapter, a review of the existing literature on GSM-R propagation and site planning was presented. The main objective of developing the modelling method presented in this thesis is to provide a numeric solution to the GSM-R BTS placement problem, that is to derive the number of BTSs required for railway networks, and the locations of the respective BTS sites.

In this chapter, a mathematical BTS site planning model for GSM-R is presented for the application of the GSM-R propagation models. This chapter begins with the analysis of the BTS site planning problem, including the preparation and analysis process for the site planning issue. Then the formulation of the BTS site planning problem is presented. Finally, the methods for preparing the data and the propagation models are illustrated.

3.2 Analysis of the BTS Site Planning Problem

In the process of site planning, the primary objective is to apply suitable propagation models to the target environment in order to achieve a certain coverage level. The key of the process is to select and tune the path loss (PL) models to provide an accurate prediction of the radio propagation. To achieve this, Digital Terrain Model (DTM) databases are used to catalogue and process the environment data, which initiates the site planning task. A summary of the BTS site planning process for GSM-R is suggested in Figure 3.1.

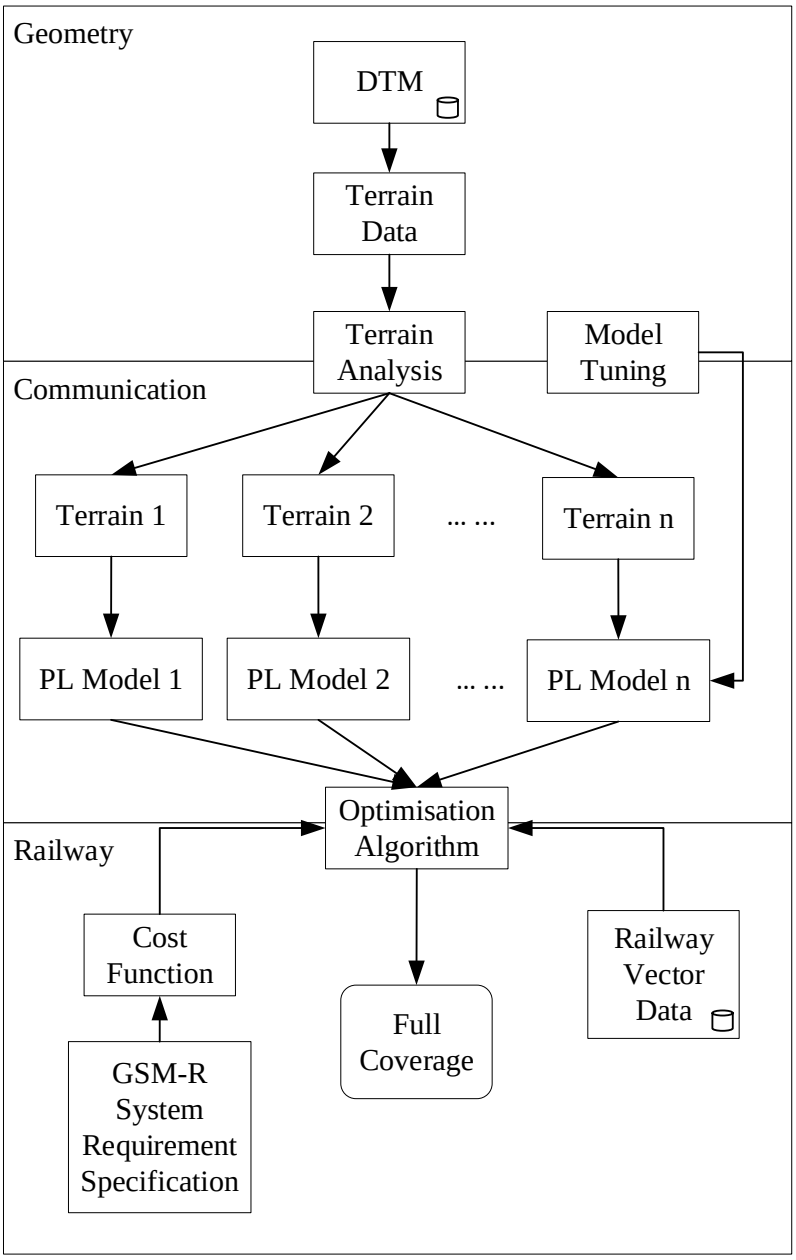

Figure 3.1 GSM-R BTS Site Planning Process

There are three topics analysed in the BTS site planning process, including geometry, communication and railway. The key to solving the BTS site planning problem is to derive the solution of the interfaces between two pairs of topics.

Geometry – Communication To ensure the propagation models selected in the communication system are suitable for the estimation of the target environment, a categorising of the target environment is required. In this process, the DTM data is sampled and converted into a suitable terrain data format for the target area. The next step is to apply a terrain analysis system to allocate the target environment to sectors,

which are catalogued by the types of terrain, such as plains, urban, mountain, etc. The model tuning process for the communication system is also a mandatory task for achieving an accurate estimation of propagation. This is normally achieved by implementing sets of radio site surveys in the target area. The expected outcome of the Terrain Analysis process is to partition the target environment into sectors by terrain types, as well as quantifying the characteristics of the terrain in each sector.

Communication – Railway By applying the tuned propagation models different types of environment, the propagation of the EMW in the target area can be simulated. The next process is to derive the placement of the BTS sites, including the number of the BTSs as well as their locations. This can be achieved by applying the optimisation algorithm to a modelled railway environment.

In this process, the sampling points of the railway are selected to represent the usage pattern of the GSM-R communication, which is achieved by sampling the continuous railway track with a sampling interval. The sampling points are provided to the optimisation algorithm to ensure all the sampling points satisfy the optimisation condition when deriving the optimal BTS site planning solution.

Another element required by the optimisation algorithm is the cost function of the target system. In the cost function, the limiting factors are defined by the GSM-R System Requirement Specification (UIC, 2015). They can also vary in different systems. More illustrations on the cost function are discussed in the following sections of this chapter.

The expected output of the optimisation process is to derive the optimal solution for BTS site planning, which can ensure the full coverage of the railway network as well as other performance requirements.

3.3 Formulation of the BTS Site Planning Problem

The aim of the BTS placement optimisation is to provide an optimal solution for the BTS deployment problem, which can provide the radio coverage that satisfies the ETCS operational standard. The solutions can be optimised by minimising the number of BTSs deployed in the network, without affecting the operation of ETCS services within the lifecycle of the target system. The objective of the BTS site planning problem can be mathematically expressed as:

$$\begin{cases} min\ \ N_{BTS}(x) = |L_{BTS}(x)| \\ s.t. x \in S \\ r \in R \\ C(r) \geq 95\% \\ P_{RX}(r) \geq P_{TH} \\ T_{ho}(r) \leq T_{TH,ho} \end{cases} \tag{3.1}$$

Where N_{BTS} is the number of BTS in the site plan, L_{BTS} is the location set of the BTS in the target network.

In the condition of the formulation,

- x is a deployment solution which represents a method of BTS deployment in a network, S is the set of the feasible BTS deployment solutions.
- r is a railway sampling point, and R is the set of all sampling points available in the railway network, C is the confidence level of the prediction. $C(r) \geq 95\%$ indicates the requirement for ensuring the minimum confidence level in the coverage area of a network.
- P_{RX} is the receiving power at the sampling point, P_{TH} is the minimum threshold of the receiving power in the system. $P_{RX}(r) \geq P_{TH}$ is to ensure the sufficient receiving power for exceeding the noise and interference in the railway environment.
- T_{ho} is the handover time in the region of the sampling point, $T_{TH,ho}$ is the maximum threshold of the permissive handover time. $T_{ho}(r) \leq T_{TH,ho}$ is to limit the handover time within the maximum duration range during the GSM-R data communication.

3.4 Data and Model Preparation

In Section 3.3, the formulation of the BTS placement problem is illustrated. Before applying the cost function into the optimisation algorithm, some data and model preparation work are required in order to define the variables in the formulation.

3.4.1 Path Loss Model

The use of the path loss models requires the receiving power Prx(r) and the confidence level c(r). The equation for deriving the receiving power can be expressed as below:

$$P_{RX} = P_{TX} + G_{TX} + G_{RX} - L - L_S \tag{3.2}$$

Where P_{TX} is the transmitted power from the transmitter, G_{TX} is the antenna gain of the transmitter, G_{RX} is the antenna gain of the receiver, L is the path loss of the transmission, L_S is the system loss, including connection and ageing loss of communication devices which increases over time.

The formulation of the path loss function can vary in different stochastic propagation models. An example formula for deriving the path loss can be expressed as in (He, Zhong, Ai and Guan, 2015):

$$PL(dB) = A + B\log_{10}(d) \tag{3.3}$$

Where $PL(dB)$ is the path loss of the transmission in dB, A is the correction factor to ensure aa sufficiently good fit of the model, B is the path loss exponent to describe the rate at which the path loss increases, d is the distance of transmission.

As the path loss functions are modelled from the mean value of the stochastic result, which is based on a 50% confidence level, the standard deviation is used in the model to describe the fluctuation of the prediction. The fluctuation is caused by the shadow fading effect of the communication, because of multipath propagation. The confidence level is also described as the coverage probability. In the Gaussian distributed radio system, the coverage probability can be calculated by:

$$1 - \gamma = \int_{F_\sigma}^{\infty} f_{SF}(x)dx = 0.5erfc\left(\frac{F_\sigma}{\sqrt{2}\sigma}\right) \tag{3.4}$$

Where γ is the coverage probability, F_σ is the extra fade margin to overcome the shadow fading component, σ is the standard deviation of the shadow fading.

Applying a confidence level of 95% for GSM-R deployment into equation (3.4), we can get:

$$F_\sigma = 1.654\sigma \tag{3.5}$$

Combining equation (3.5) with (3.3), we find the path loss function to satisfy the 95% confidence level, which is expressed as:

$$PL(dB) = A + B\log_{10}(d) + 1.654\sigma \tag{3.6}$$

Meanwhile, as the local mean power has the property of a normal or Gaussian distribution, the confidence level can be derived by the Cumulative Distribution Function (CDF), which is expressed as:

$$C = \frac{1}{2} + \frac{1}{2} erf\left(\frac{P_r - P_{TH}}{\sigma\sqrt{2}}\right) \tag{3.7}$$

Where C is the coverage probability, P_r is the mean receiving power, P_{TH} is the minimum power threshold for the GSM-R transmission, σ is the standard deviation of the propagation model.

As introduced in Chapter 2, in ETCS operation, P_{TH} can be defined by the following principle:

- coverage probability of 95% based on a coverage level of -98 dBm for voice and non-safety critical data;
- coverage probability of 95% based on a coverage level of -95 dBm on lines with ETCS levels 2/3 for speeds lower than or equal to 220 km/h;
- coverage probability of 95% based on a coverage level of -92 dBm on lines with ETCS levels 2/3 for speeds above 280 km/h;
- coverage probability of 95% based on a coverage level between -95 dBm and –92 dBm on lines with ETCS levels 2/3 for speeds above 220 km/h and lower than or equal to 280 km/h.

3.4.2 **Handover**

During the GSM-R operation, the handover between two cells must be considered specially. As GSM-R supports high-speed operation at over 280 km/h in ETCS, trains can travel a long distance within the handover time window. The handover overlap must be determined to ensure successful handover during railway operation.

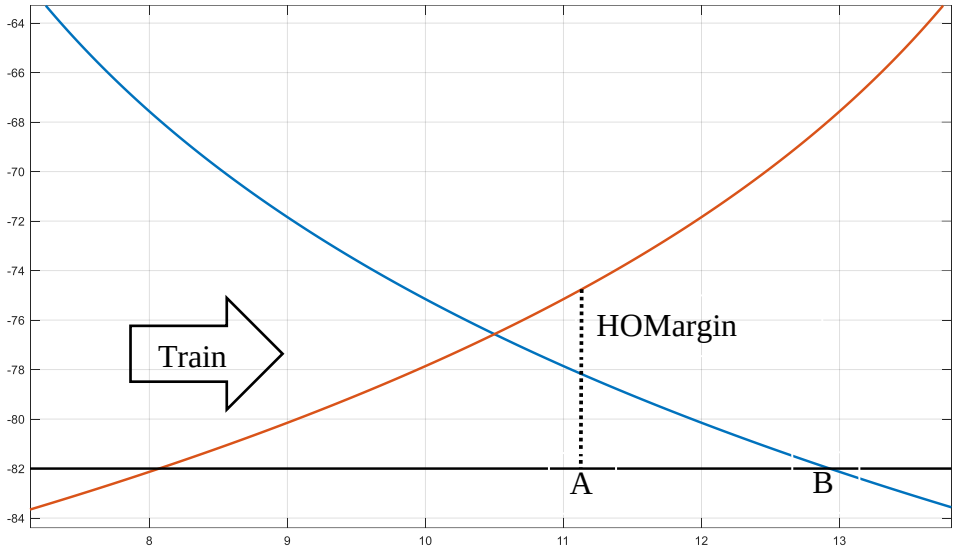

Figure 3.2 Handover in a GSM-R network

Figure 3.2 shows a generic scenario of GSM-R handover, with one train travelling from the current BTS to the target BTS on a straight railway line in the same radio environment. To eliminate the Ping-Pong effect in a GSM system, a Handover Margin (HOMargin) is applied to the handover process, to trigger the handover process when the receiving power from the target BTS is higher than the receiving power from the current BTS. This is to ensure trains are always connected to the appropriate BTS when approaching a handover area. The handover process can be started when:

$$P_{next} - P_{current} > HOMargin \tag{3.8}$$

Where P_{next} is the receiving power from the target BTS, $P_{current}$ is the receiving power from the current BTS, $HOMargin$ is a constant in the system configuration.

The handover trigger point is when:

$$P_{next,A} - P_{current,A} = HOMargin \tag{3.9}$$

This represents the Point A in Figure 3.2, where $P_{next,A}$ is the receiving power of the target BTS at Point A, $P_{next,A}$ is the receiving power of the current BTS at Point A.

By defining the path loss function as $L(d)$, where the d is the distance of transmission, the $P_{next,A}$ can be calculated by:

$$P_{next,A} = P_2 - L(|X_2 - X_A|) \tag{3.10}$$

Where P_2 is the transmitting power of the next BTS, X_2 is the coordinate of the next BTS, X_A is the coordinate of the handover initiating point, where the condition expressed by the equation (3.7) is satisfied.

By applying the same method in (3.10), The $P_{current,A}$ can be derived by:

$$P_{current,A} = P_1 - L(|X_1 - X_A|) \tag{3.11}$$

Where P_1 is the transmitting power of the current BTS, and X_1 is the coordinate of the current BTS.

This event represents the process when the train travels at Point A. As the train continues travelling towards Point B, where the received power from the current BTS starts to be lower than the minimum power threshold, the handover process must be completed before Point B. Therefore, we can get:

$$D_{handover} = D_{AB} = |X_B - X_A| \tag{3.12}$$

Where X_B is the coordinate of the Point B, where the receiving power from the source BTS is below the minimum receiving power P_{TH}.

Therefore, by defining the mean value of the train speed at the handover zone, the permissive handover time T_{ho} can be calculated by:

$$T_{ho} = \frac{D_{handover}}{v} \tag{3.13}$$

Where $D_{handover}$ is the length of the handover zone defined in (3.12), v is the average speed of the train within the handover area.

As stated in (3.1), the limiting factor for the handover is:

$$T_{ho} \leq T_{TH,ho} \tag{3.14}$$

$T_{TH,ho}$ is the maximum permitted handover time window in the system. In (UIC, 2015), this is defined as less than:

- 8 s in 95% of cases
- 12 s in 99% of cases

Because of the low acceleration rate characteristic of trains, the movement of the train during the handover process can be regarded as uniform motion. The train speed v can

be regarded as constant during the handover. This can be determined from the speed curve based on the speed limit and operational services.

In a simplified scenario, when the current BTS and target BTS are within a similar radio environment, the path loss function can be expressed as:

$$L = \alpha \log_{10}(d) + C \tag{3.15}$$

Where α is the path loss exponents, d is the transmission distance, C is the constant for fitting the path loss function.

In Equation (3.12), Position B (X_B) can be derived by:

$$P_{current,B} = P_{TH} \tag{3.16}$$

$$P_{current,B} = P_1 - L(|x_1 - x_B|) \tag{3.17}$$

Combining (3.16) with (3.17), we can get:

$$X_B = X_1 + 10^{\frac{P_1 - C - P_{n-1}}{\alpha_1}} \tag{3.18}$$

The Position A (X_A) can be derived using the same method, which is:

$$X_A = X_1 + \frac{X_2 - X_1}{1 + 10^{\frac{H + P_2 - P_1}{\alpha}}} \tag{3.19}$$

By applying the Equation (3.18) and (3.19) to (3.13), the function for determining the permissive handover time T_{ho} is:

$$T = \frac{10^{\frac{P_1 - C - P_{TH}}{\alpha}} - \frac{X_2 - X_1}{1 + 10^{\frac{H}{\alpha}}}}{V} \tag{3.20}$$

3.4.3 **Digital Terrain Models**

High accuracy Digital Terrain Models are widely used for terrain analysis and civil structures planning. In the process of GSM-R site planning, the DTM is an important reference database to analyse the terrain of the target area. In terms of GSM-R transmission, there are two factors that affect the propagation prediction, which are the type of terrain in the environment catalogue and the roughness of the terrain.

3.4.3.1 Catalogue of the Environment

The catalogue of the environment is used to identify the type of terrain within the target area. In railway sites, apart from the environment with the distinguishing characteristic such as cutting and viaduct, the open-space territory can be catalogued into the following settings:

- Urban
- Suburban
- Rural
- Mountain

Since each type of environment has its own dedicated path loss model, the Terrain Ruggedness Index (TRI) is introduced to identify the terrain roughness (Riley, DeGloria and Elliot, 1999).

To derive the TRI from a DTM, a square grid network with 1 km^2 grid cells is applied to the target area, as shown in Figure 3.3. In each of the cells, the average elevation is derived for calculating the total TRI of the centre cell.

-1,-1	0,-1	1,-1
-1,0	0,0	1,0
-1,1	0,1	1,1

Figure 3.3 Sampling system in TRI model

In this grid system, the TRI can be derived by:

$$TRI = \sqrt{\left(E_{0,0} - E_{-1,-1}\right)^2 + \left(E_{0,0} - E_{0,-1}\right)^2}$$

$$+\sqrt{\left(E_{0,0} - E_{-1,-1}\right)^2 + \left(E_{0,0} - E_{1,0}\right)^2}$$

$$+\sqrt{\left(E_{0,0} - E_{1,1}\right)^2 + \left(E_{0,0} - E_{0,1}\right)^2}$$

$$+\sqrt{\left(E_{0,0}-E_{-1,1}\right)^2+\left(E_{0,0}-E_{-1,0}\right)^2} \quad (3,21)$$

Where E_{xy} is the average elevation of the 1 km^2 grid cell at the Grid (x,y).

The range of the TRI values for each grouping are as follows:

- Level = 0 – 80 m
- Nearly Level = 81 – 116 m
- Slightly Rugged = 117 – 161 m
- Intermediately Rugged = 162 – 239 m
- Moderately Rugged = 240 – 497 m
- Highly Rugged = 498 – 958 m
- Extremely Rugged = 959 – 4367 m

Therefore, when applying the path loss models to the target area, the TRI can be used as a reference to identify the type of environment in a region. In this paper, the terrain categories are defined as:

- Plain (including urban, suburban, rural): TRI < 161m
- Mountain: TRI > 161m

The plain environment shall be further refined using other sources of information such as a satellite image database. This is because the DTM does not contain building and vegetation information, which can significantly affect the accuracy of the propagation prediction.

3.4.3.2 Roughness of the Terrain

As discussed in Section 3.4.1, the standard deviation of the propagation is described in the path loss model, which is used to calculate the fading margin of the propagation and the confidence level of the coverage. In the practice of applying the path loss models, a range for the standard deviation is provided as a guidance value for the typical environment. The value should be determined by conducting measurements on site.

As the shadow fading is caused by multipath propagation, due to the reflection and scatter of EMW at obstacles in the environment, the intensity of the shadow fading can be estimated by the roughness of the terrain in the propagation area of the GSM-R transmission.

In GSM-R communication, the BTSs are implemented with high-gain antennas configured in a directional setup. This is because the use patterns of the GSM-R communication are limited to the railway track and can be determined during the process of GSM-R site planning. As GSM-R is a dedicated system for railway operations, all the GSM-R users are located in the railway corridor, either within trains or near railway tracks. As a result, by determining the gain and the angle of the GSM-R antenna, the antenna pattern can be derived to estimate the propagation paths of the EMW. A typical antenna pattern for the high-gain antenna is shown in Figure 3.4.

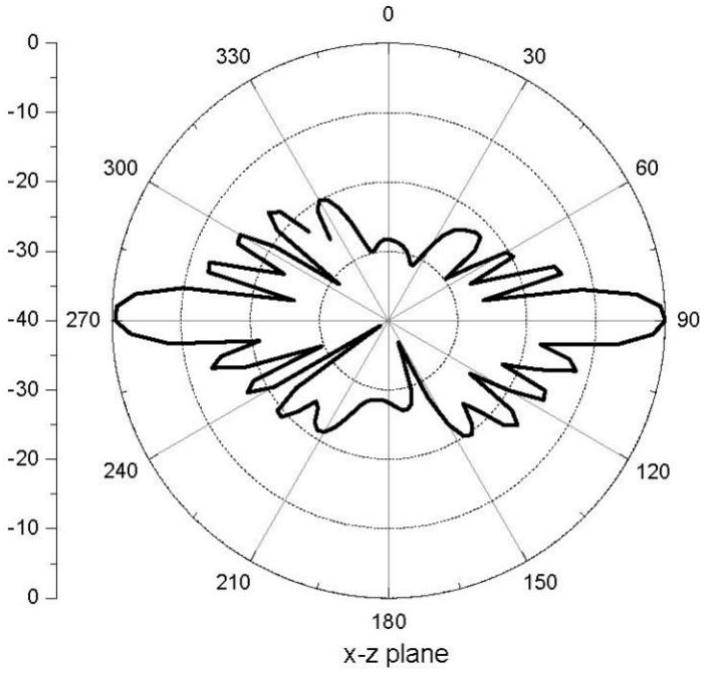

Figure 3.4 Antenna pattern for a high-gain omnidirectional antenna (Yu, Ni and Wang, 2006)

Within the radiated zone of the antenna, the roughness of the terrain can be determined by the standard deviation of the terrain elevation, which is expressed as:

$$G_s(d) = \sqrt{\frac{1}{N}\sum_{i=1}^{N}\left(h_i - \bar{h}\right)^2} \tag{3.22}$$

Where d is the distance from the BTS to the receiver, G_s is the geographical standard deviation within a radiation area with a length of d, N is the number of DTM sampling points in the area, h_i is the elevation of the sampling point i, h is the average elevation.

Within the potential coverage area of the BTS, by increasing the distance from the transmitter to the receiver, we can get an array of the geographical standard deviation within the coverage area with sampling points, expressed as:

$$G_s = \{G_s(d_1),\ G_s(d_2), \ldots,\ G_s(d_n)\} \tag{3.23}$$

G_s is the geographical pattern to describe the complexity of the terrain. The elements in G_s have a trend to increase when d is increased. This is because, when increasing the sampling area, more complexity is introduced into the area, which leads to a rise in the geographical standard deviation.

Figure 3.5 and Figure 3.6 show an example of placing a BTS within a mountain area, a complex terrain, where the railway is placed in a valley. The elevation graph and the antenna pattern for the 30 degrees high gain antenna are displayed.

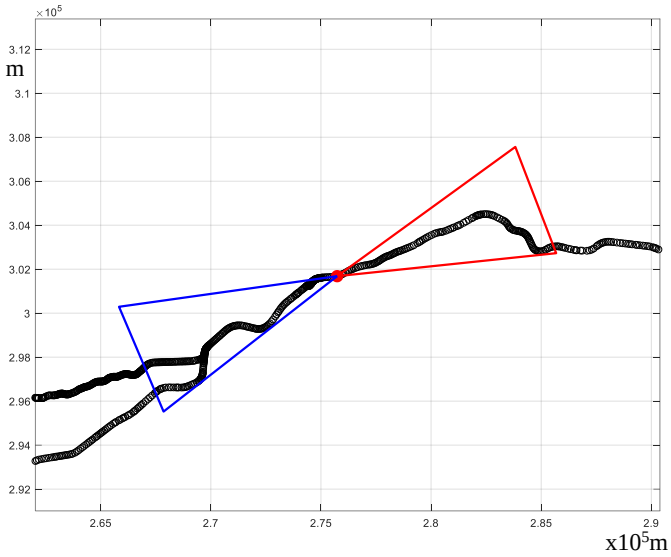

Figure 3.5 BTS placement in a valley region (i)

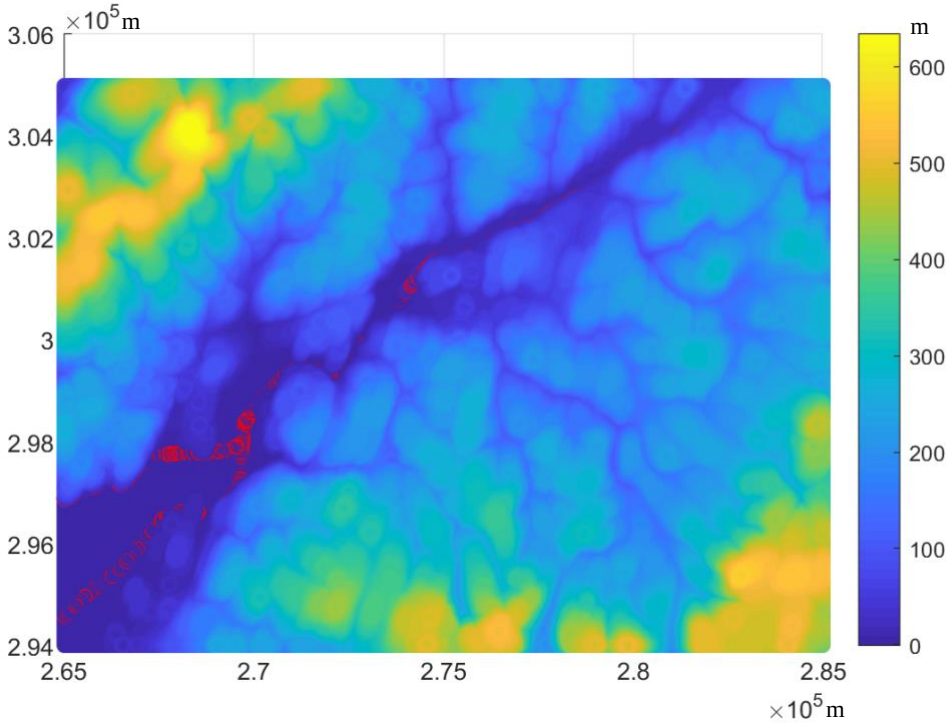

Figure 3.6 Railway tracks in a valley region (ii)

As shown in Figure 3.6, the red dots are the sampling points of the railway track, which are surrounded by a region coloured by the topology height above the sea level. This represents the railway located in a valley area.

By applying the function (3.22) and (3.23), we can get the geographical pattern G_s to describe the trend of terrain complexity when travelling away from the BTS. In Figure 3-7, the geographical patterns are calculated for each coverage area of the bi-directional antennas, in which the colour of the figure matches the coverage area representation in Figure 3-5.

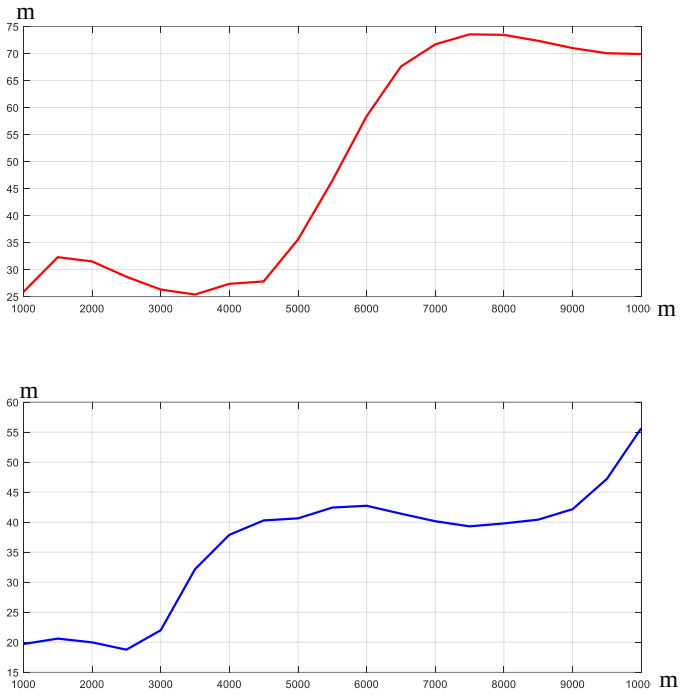

Figure 3.7 Geographical pattern in the sampled area

It is to be noted that the BTS is placed in a limited plain region at the centre of the topology map shown in Figure 3-6, which is reflected by the flat line at the beginning of the geographical pattern. When moving away from the BTS, G_s increases significantly, which is because of the valley in the region far from the BTS.

Although the standard deviation generated by shadow fading of the transmission must be determined by precise measurement, the estimation of the standard deviation, which is done by selecting a value σ in the propagation model, can be based on the slope of G_s. This is because the shadow fading effect is correlated to the terrain complexity when more complexity is introduced into the area and, thus, more transmitted power can be reflected and scattered. Therefore, before undertaking the site measurement to determine the σ in Equation (3.6) accurately, an estimation can be made by performing the G_s analysis in the target area.

3.4.4 Redundancy

As described in Section 2.5.3, there are two techniques for providing redundancy for the coverage of GSM-R network, Including dual system in RBC and interleaving redundancy. For both solutions for providing redundancy in the GSM-R network, the networks in the redundancy configuration have the capability of providing full coverage

to the railway network. Thus, no other modelling or optimisation work is required in the system model proposed in this thesis.

3.5 Conclusions

This chapter introduced the application of propagation models into the process of GSM-R BTS site planning. To apply the optimisation algorithm in the railway environment, a process for achieving the BTS site planning has been illustrated. Then the formulation of the BTS siting problem was presented for the mathematical programming and optimisation. Network configurations were discussed for providing solutions to the limiting factors of the formulation, and extra settings have been introduced to ensure the reliability of the target network. Studies for non-generic scenarios, including applications in tunnels and dual coverage, were also conducted.

Chapter 4 Optimisation of BTS Site Planning for GSM-R

4.1 Introduction

In the previous chapter, an approach to the formulation of BTS site planning is proposed, which can mathematically translate the BTS siting problem into a numeric model. This chapter introduces the application of the formulation into the optimisation algorithm.

In this chapter, the modelling of the ETCS railway system is introduced to be able to code the railway network into a mathematical method for applying the optimisation algorithm. Then, typical optimisation algorithms for solving the BTS site planning formulation are analysed. Finally, a comparison between the optimisation algorithms is discussed.

4.2 ETCS System Modelling

The primary task of ETCS modelling is to replicate the movement pattern of the GSM-R user equipment. The user equipment of the GSM-R contains an onboard communication module with antennas mounted on the train roof, as well as handheld devices used by railway operations and track worker staff. Therefore, the user movement patterns of the GSM-R communication are related to the railway corridor.

GSM-R base stations are generally located near the railway track. Because of land availability and asset management issues, the base stations should be as close to the track as possible. By taking account of the Doppler effect when the train is operating at high speed, a certain distance should be maintained from the railway track to reduce the frequency change of the Doppler-shifted frequency. A typical distance from the track is 50 meters (UIC, 2009) to guarantee both the transmission availability and construction availability.

As a result, the modelling of the GSM-R base station location can utilize the railway track as the basis of location. Compared with the coverage range of a base station and

the speed of the train when approaching the base station, the distance between the base station and the nearest track can be neglected. Therefore, the location of the base station can be associated with the railway track. By taking sampling points along the railway track with a sampling interval of 50 meters, a list of all possible locations of GSM-R base stations can be generated. The information for the sampling points includes:

- The kilometre post of the railway, which is widely used for asset management;
- Geographic Information system (GIS) coordinate of the point;
- Elevation information;
- Terrain Ruggedness Index (TRI) value.

By collecting all the sampling points into an array, we can obtain:

$$N = \{N_1, N_2, \dots, N_n\} \tag{4.1}$$

Where N is the array of all the sampling points in the ETCS network. The elements in the array N can be regarded as the sampling points for the trains in the ETCS network, as well as possible BTS locations in the GSM-R network.

Then a binary system can be introduced to define the decision of installing a base station, which can be expressed as

$$\begin{cases} 0: Not\ Installed \\ 1: Installed \end{cases} \tag{4.2}$$

By combining (4.1) with (4.2), a binary array can be created to generate a combination of base station locations, such as:

$$C_1 = \{1, 0, 1, 0\ ,0\ \dots,0\} \tag{4.4}$$

Which means C_1 is a BTS location configuration generated from the ETCS network, where Sampling Point N_1 and N_3 in (4.1) have been equipped with a BTS.

The expression (4.4) can be generated by means of an optimisation algorithm, such as Brute Force Search (BFS). As a result, a collection of all the possible BTS location solutions can be expressed as:

$$C = \{C_1, C_2, \dots, C_n\} \tag{4.5}$$

By applying the mathematical formulation introduced in Chapter 3, an optimal solution can be derived from the set in (4.5).

4.3 Optimisation Algorithms

After coding the GSM-R network into a binary decision system, optimisation algorithms can be applied to derive the optimal result.

4.3.1 **Brute Force Search (BFS)**

Brute Force Search is used to generate all possible BTS locations, which are then passed to the mathematical formulation of the BTS site planning to validate the feasibility of the result. The flow chart of the BFS algorithm is shown in Figure 4.1.

At the beginning of the optimisation, the range of the potential number of BTSs is defined. Then the set of combinations is generated for the modelled railway network to describe the location of the BTSs. The next step is to introduce all the combinations into the mathematical function of the GSM-R site planning problem. For each of the combinations, the limiting factors are evaluated. After filtering the combinations which are not feasible for providing the reliable coverage, the cost function is applied to derive the minimum number of BTSs required in the network, as well as the optimal location of the BTSs.

BFS is computation extensive and is very time consuming. However, the accuracy of the result can be used as a reference for other algorithms as well as further research. For each combination in BFS, received power at each sampling point on the railway track is calculated and compared to determine the coverage.

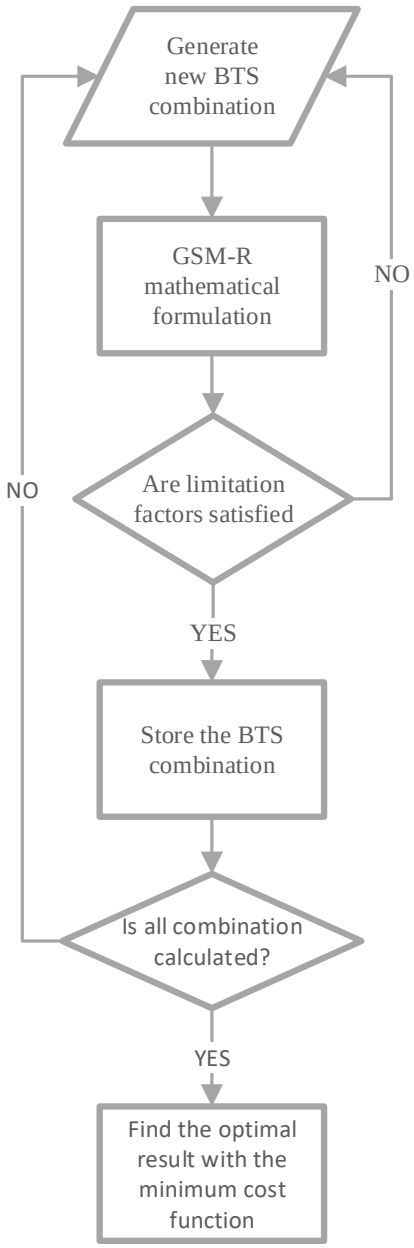

Figure 4.1 Flow chart of the BFS algorithm

As the quantity of the BTS placement combination expands exponentially when increasing the number of BTSs, the BFS becomes impractical for optimizing the whole railway network. For example, a 200 km railway network contains more than 2000 sampling points. As the typical coverage range of a BTS is 7-15 km, if we assume that each BTS can provide 10 km of coverage, by taking account of the overlap for the handover, a minimum of 21 BTSs is required in the network. The total number of BTSs combinations can be derived by:

$$C(n,r) = C(2000,21) = \frac{2000!}{21!(2000-21)!} = 3.69E + 49 \qquad (4.6)$$

which are not realistic to calculate through a BFS.

To reduce the computation effort, the railway network can be separated into sectors. For example, by separating the 200 km railway network into 5 sectors, each sector contains 400 sampling points with 4 target BTS, the total number of the combinations is:

$$C(n,r) = C(400,4) = 1.05E + 9 \tag{4.7}$$

If each combination takes 10 milliseconds to compute and all the combinations are calculated by a 64-thread workstation PC, the whole scenario would take 1.8 days to exhaust all the possible solutions, which is acceptable in the process of the radio planning. However, as the railway network is divided into sectors, the coverage between the sectors cannot be guaranteed. Extra work is required manually to optimise the handover between the boundaries of the sectors.

4.3.2 **Adapted BFS (ABFS)**

To overcome the shortcomings in the BFS algorithms, an adapted BFS can be developed for deriving the optimal result from the possible combinations. The flow chart for the algorithm is shown in Figure 4.2.

The main reason for the unrealistic level of calculation in BFS is the excessive number of combinations in the target network; this occurs for of the following three reasons:

- A large number of sampling points available;
- Exceeded number of BTSs to optimise in the same network;
- Untargeted search for the location of BTSs, causing unnecessary combinations, such as two BTSs being placed too close together

The application of the ABFS can be summarised into three steps: initialisation, evaluation, expansion.

Initialisation: The aim of the ABFS is to overcome the limitation of the BFS while maintaining the accuracy of the BFS. Similar to the feasible solution derived by the BFS algorithm being applied to the optimisation of a sector of the network, ABFS also starts in a small region of the target railway network. However, only one BTS is applied to the region in the first step of the algorithm. In this process, the combinations are

generated by locating the single BTS at all the possible locations in the region. The propagation model used in the GSM-R optimisation function is applied for each of the combinations to evaluate the robustness of the coverage.

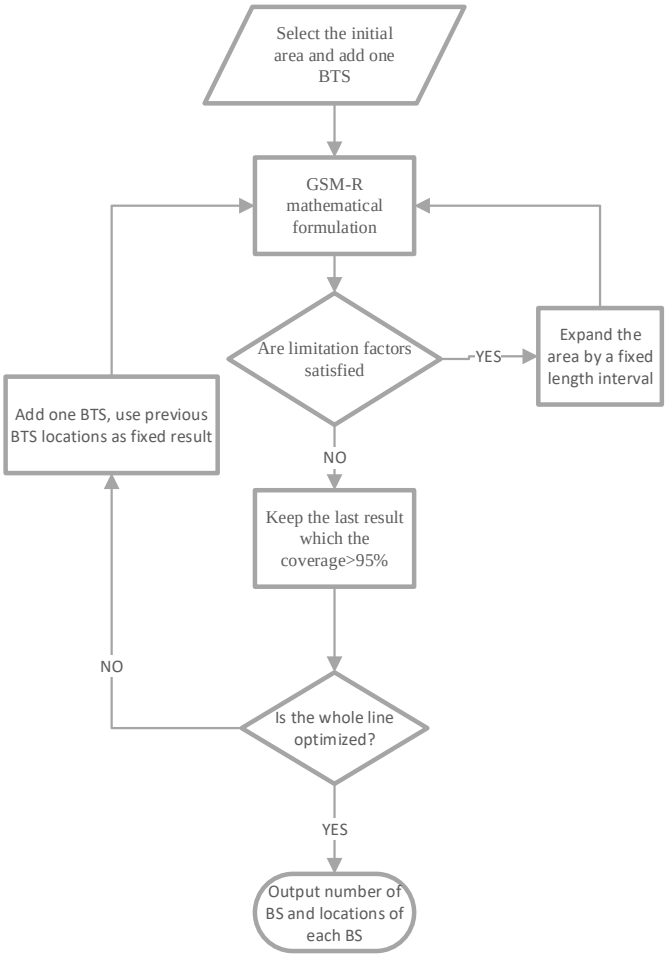

Figure 4.2 Flow chart for ABFS

Evaluation: The second step of the algorithm is to evaluate the potential for the current BTS. This is achieved by expanding the size of the target region, as indicated in Figure 4.3. As the existing BTS in the existing region can provide enough coverage, the region is expanded to evaluate the potential of the current BTS to provide further coverage while maintaining the reliability. The size of the optimisation region keeps being expanded until the BTS in the respective region is just sufficient to provide a reliable GSM-R service in the optimisation region.

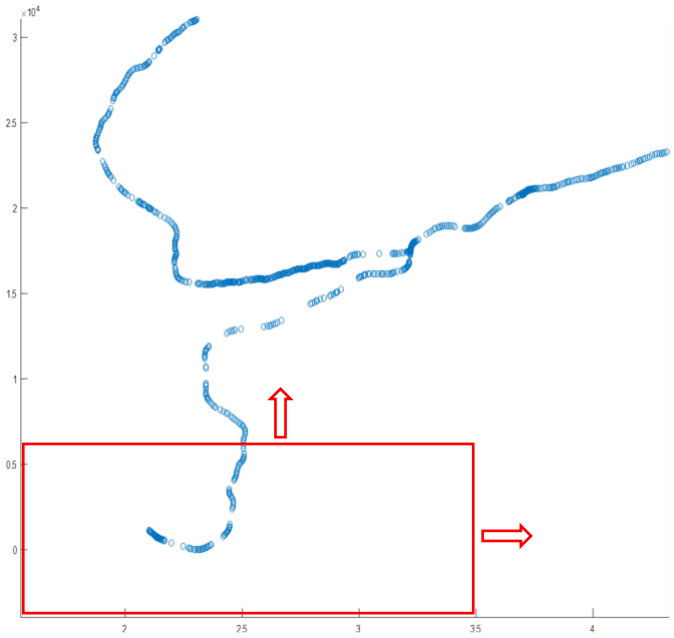

Figure 4.3 Expansion of the optimisation region

Expansion: The third step is to fix the current BTS as one of the optimal locations, and to add the second BTS into the network, since more BTSs are required in the network if we continue expanding the evaluation region. Then the **Evaluation** step is repeated by expanding the target region while searching for the optimal location for the second BTS. As the location of the first BTS is fixed by the previous iteration, it only requires the search for one BTS in the current region. Therefore, the search effort for the second BTS grows linearly when expanding the network with more sampling points and a greater number of BTSs.

Eventually, the target window of the optimisation algorithm covers the whole railway network, and the optimisation process is concluded. As the cost function is applied in each of the iterations to derive the minimum number of BTSs in the sub-region of the network, the site planning solution in the final iteration is also the optimal result derived from the optimisation formulation.

The limitation of the ABFS relates to the evaluation process. As the target region is expanded in each iteration of the optimisation, the result can be different depending on the direction of the expansion. This can be eliminated by expanding the optimised region in the same direction until this direction is exhausted, then proceeding to the other directions until the whole network is optimised. Another solution is to select the

entry or the end point of the railway network; in this case, the direction of the expansion is limited to the direction of the railway service.

The same issue also occurs during the initialisation process. As the railway network may contain multiple entry or exit points, the optimisation result may be different when selecting a different initialisation area. This can be eliminated by the following two solutions:

- Perform multiple optimisations by selecting every entry or exit as the initialisation area, then derive the optimal result from the multiple optimisations.
- If possible, identify a fixed point in the network to initiate the optimisation. This can be related to certain infrastructure in a railway, which requires the specific installation of an RBC, including depots and highly trafficked stations. These target areas can be selected as the initialisation areas.

4.3.3 Genetic Algorithm (GA)

Genetic algorithms provide a search methodology based on natural selection and on "survival of the fittest", the main idea is to behave as a natural system so that a population of individuals can adapt to the environment. This means the survival and reproduction of an individual are promoted by the elimination of useless traits and by rewarding useful behaviour (Sharma, Pathak and Sharma, 2012).

The application of the GA approach includes three types of operations: selection, cross-over and mutation. The flow chart for the GA is shown in Figure 4.4.

The procedures for applying the GA to the BTS site planning problem are as follows:

Initialisation: In the initialisation process, an initial number of the BTSs is provided in the GSM-R network. The initial population is generated by randomly placing the fixed number of BTSs into the whole network. Each of the individuals in the population is a configuration of the BTS locations, which is coded by the binary decision system and expressed as a chromosome in the population.

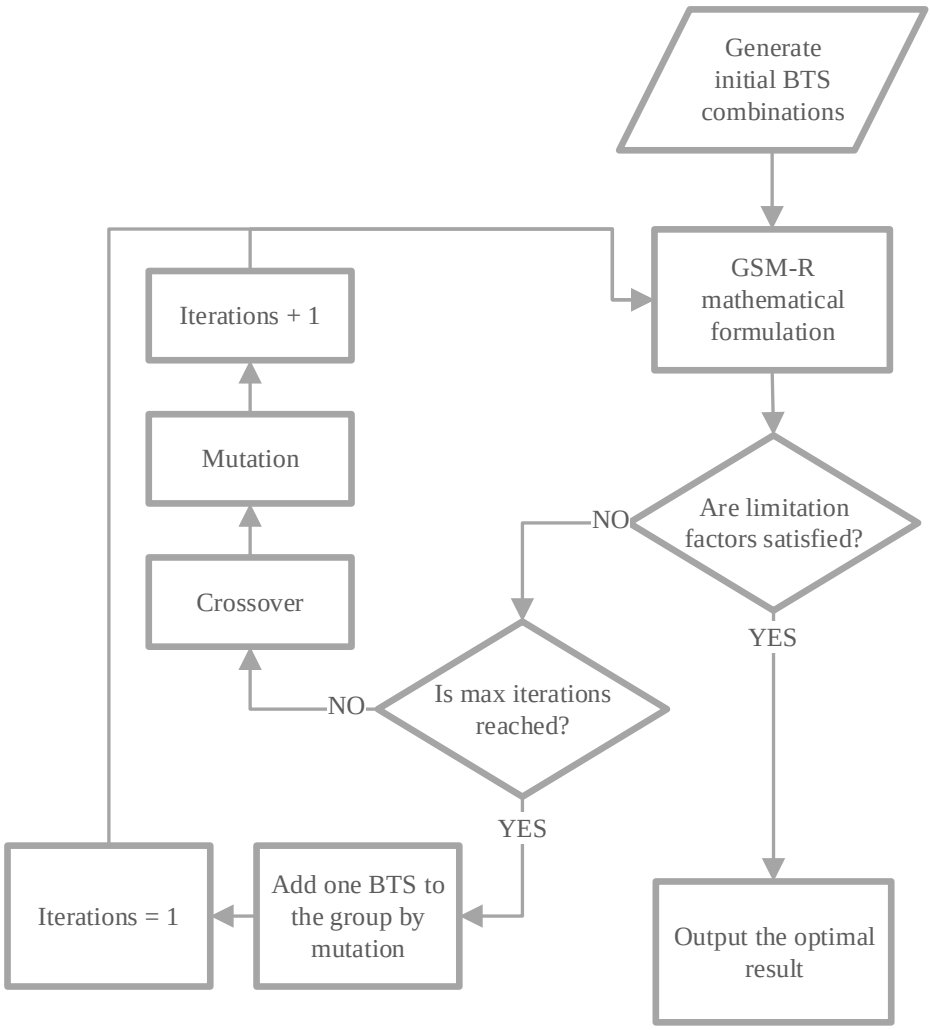

Figure 4.4 Flow chart for the GA applied to the BTS site planning problem

Selection: A mathematical formulation is applied to the selection function, which eliminates the individuals with the unqualified cost function. After the selection of the population, the algorithm shall determine the status of the search function. If the optimal result has not been located and the maximum number of iterations is not reached, then the GA is continued to optimise the population. However, if the maximum number of iterations is reached, which means the optimal result from the given number of the BTSs has not been found, an extra BTS shall be introduced into the population to restart the search with more BTSs in the network.

Crossover: The crossover is used to create the child population by crossing the chromosomes of the parents. This is done by randomly selecting the crossover point and exchanging the genes to create the child element. In the GSM-R optimisation

process, this requires the process of exchanging the BTS position in the location configuration.

Mutation The mutation is performed after the crossover process. The mutation process is applied to ensure the optimisation does not fall into a locally optimal result. In the GSM-R location optimisation, as the number of the BTSs is fixed in each iteration, the behaviour of the mutation process is to change a BTS randomly to another location.

Eventually, by increasing the number of BTSs in the GSM-R network, an optimal individual can be identified by the optimisation algorithm.

4.4 Comparison of the Optimisation Algorithms

In summary, the algorithms illustrated in Section 4.3 have the following advantages and disadvantages.

4.4.1 Brute Force Search

Advantages:

- Available to determine the optimal result;
- Easy to implement.

Disadvantages:

- Massive computation time;
- Unable to perform a global optimisation, since the number of BTS cannot exceed 5;
- Extra interventions are required for the boundaries of the local optimisation.

4.4.2 Adapted Brute Force Search

Advantages:

- Available to implement the BFS algorithm in a local region;
- Can achieve high accuracy while taking account of the coverage in the handover region.

Disadvantages:

- The algorithm is effective for a single railway line, but less effective in a railway network with branches and junctions;
- Requires extra intervention work to configure the direction of the optimisation.

4.4.3 Genetic Algorithm

Advantages:

- Able to provide global optimisation;
- High efficiency.

Disadvantages:

- 'Best-effort' algorithm, which is unable to guarantee that the result is the optimal solution;
- Complex encoding required to perform the optimisation.

4.4.4 Other Optimisation Algorithms

Apart from the genetic algorithms and brute force search algorithms selected in this study, other optimisation algorithms suitable for general base station site planning can also be applied. This includes the simulated annealing algorithm(Chen, Wang and Ouyang, 2023) , K-mean clustering algorithm (Miao, Zhang and Xiao, 2023), immunization algorithm (Tao, 2023). Recent studies also show the utilization of machine learning algorithms in site planning problems(Wang *et al.*, 2021).

4.5 Application to Different Railway Systems

To identify the effectiveness and efficiency of the optimisation algorithms, some typical railway network setups are demonstrated, including a plain line railway, a single line with branches and a meshed network.

4.5.1 **Plain Line Railway**

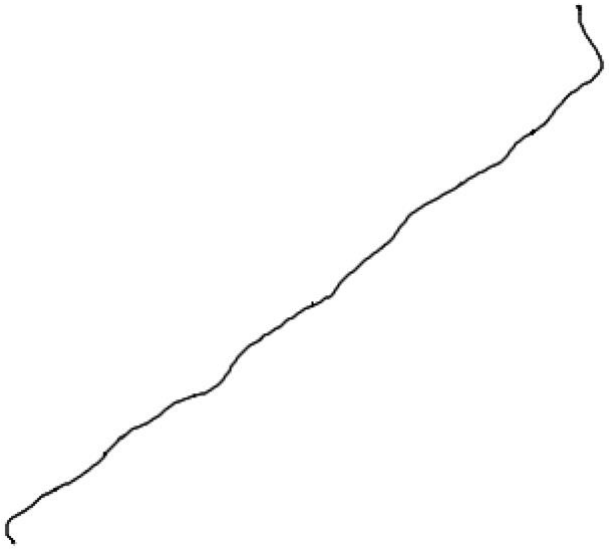

Figure 4.5 The Shanghai-Hangzhou HSR line

Figure 4.5 is a typical high-speed railway line located within a level environment, as the line is located at a plain area and can be designed as a straight line between cities. The line contains entry points at both ends and is designed without any branch. The total length of the railway line is around 150 km, which corresponds to 1500-2000 sampling points. An early estimation indicated that the number of the BTS had to be about 15.

In this system, the application of the BFS requires dividing the line into three sections to implement a local optimisation, leading to a very large search time. On the other hand, by applying the ABFS algorithm, the initialisation area is selected at the edges of the network, and two optimisations starting from each end of the line shall be carried out to ensure the optimisation result is optimal. As for the GA, the global optimisation can be achieved by encoding the railway track as chromosomes. Multiple iterations are required to search the optimal number of BTSs in the network.

In this case, the ABFS can provide the best result with the highest efficiency.

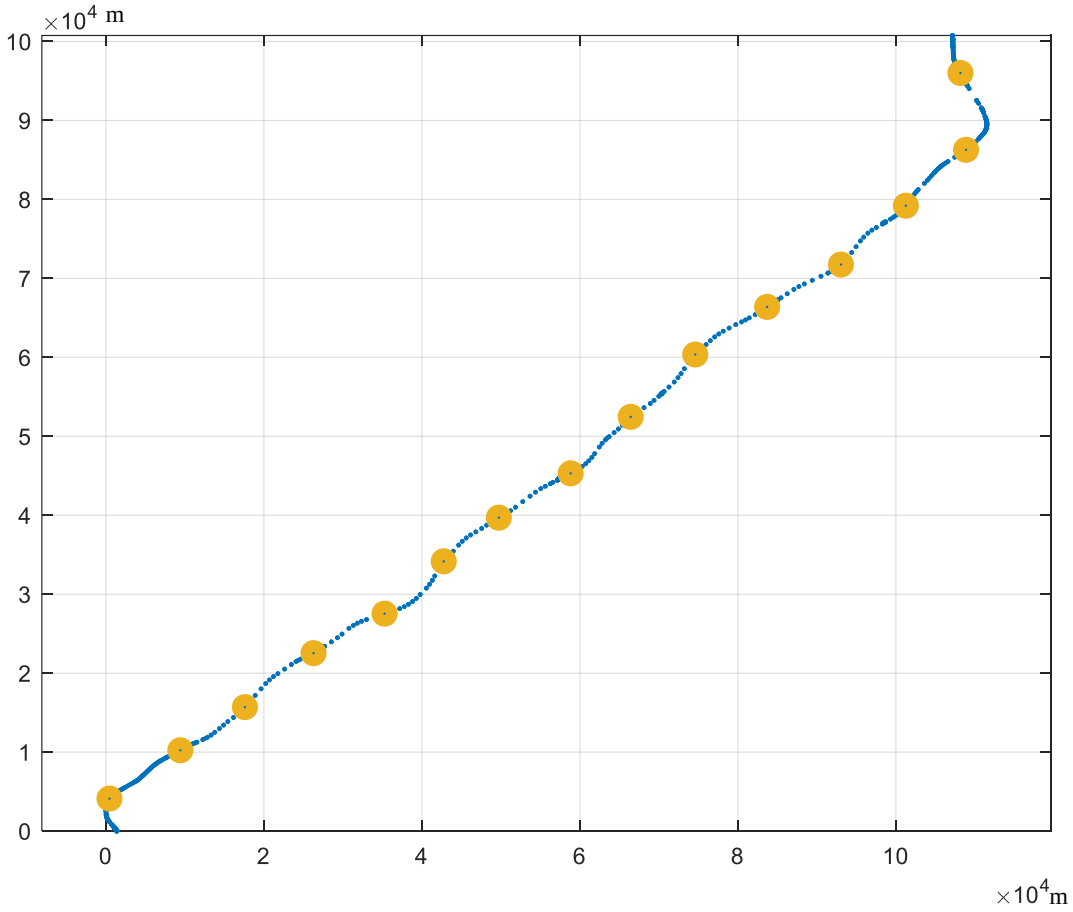

Figure 4.6 BTS locations generated by ABFS optimisation

Figure 4.6 shows the optimisation result generated by the ABFS algorithm. 15 BTSs have been successfully located. The minimum coverage probability validated in the railway line is 96.87%. The railway network has also been validated by GA using only 14 BTSs, which resulted in a minimum coverage probability of 89.96%, which is below the GSM-R requirement of over 95%. Therefore, both ABFS and GA have successfully predicted the minimum number of BTSs required for the network, which is 15.

4.5.2 **Single Line with Branches**

Figure 4.7 The Cambrian Line in Wales, UK

An example of a linear railway line with a branch can be seen in Figure 4.7. In this railway network, a junction exists at the centre of the network, where a branch is connected. The total length of the railway line is around 220 km, which corresponds to 2000-2500 sampling points. An early estimation indicated a requirement for 23 BTSs. The analysis of the Cambrian Line will be discussed in Chapter 5.

In this example, BFS is unable to provide an accurate estimation because of the multiple split sections when applying the BFS for local optimisation. In the ABFS scenario, the optimisation process requires four optimisations, including setting the initialisation area at the three edges of the network, and the junction of the network where the depot of the railway network is located. The application of the GA in this example is the same as the Linear Railway Network scenario.

In this case, both the ABFS and the GA approach can provide efficient optimisations, as will be discussed in Chapter 5.

4.5.3 **Meshed Network**

Figure 4.8 The East Coast Main Line in the UK

Figure 4.8 shows an example of a meshed network, where multiple lines are combined into a railway network. The total length of the railway network is around 500 km, which corresponds to 5500-6000 sampling points.

In this example, the use of BFS is not possible because of the scale of the network. For ABFS, the initialisation area can be selected from the upper and lower edges of the network. However, during the iterations of the optimisation, adding one BTS for each step may not provide sufficient optimisation when processing the multiple junction areas; therefore the algorithm should be adapted to add 2 or 3 BTS in each iteration of the optimisation, which significantly decreases the efficiency of the optimisation. The use of the GA in this network is also the same as the use in a simple network, which is implemented by encoding all the sampling points as the chromosomes.

As a result, in the scenario of the large-scale network, the GA can provide the best efficiency for implementing the global optimisation. Due to the limitation of data available to this railway line, the author did not model this railway network.

4.6 Conclusions

In this chapter, the modelling of communication systems for different railway networks has been illustrated. The ETCS railway line has been modelled as a binary decision system for the siting of the BTSs in a GSM-R network. Based on the features of the railway network, the ABFS method has been proposed, which was developed by improving the BFS to achieve global optimisation. Another two typical algorithms have been discussed in this chapter, including Brute Force Search and the Genetic Algorithm. The applications and the comparison of the three algorithms have also been demonstrated in this chapter.

In the next chapter, the application of the optimisation algorithms will be evaluated to demonstrate the use of the algorithms on a complete network to derive the optimal result for the BTS site plan.

Chapter 5 Case Study of GSM-R BTS Site Planning

5.1 Introduction

In the previous chapters, a mathematical model for a GSM-R communication network and the ETCS railway network has been proposed. The optimisation algorithms have also been evaluated in the context of typical railway networks.

In this chapter, the proposed numeric model is applied to a study case to perform the BTS site planning. This chapter begins with the introduction of the railway network in the study case. Then the GSM-R system is modelled, and the BTS locations are optimised using the Adapted Brute Force Search and the Genetic Algorithm.

5.2 Introduction of the Target Railway Network

The Cambrian Line in the UK was selected for the case study. The Cambrian Line is a 218 km railway line operating with ETCS Level 2 following an upgrade from a conventional signalling system. Figure 5.1 shows the layout of the Cambrian Line, where the junction in the east corner is the entry to the Cambrian Main Line. It provides a connection to the coastal area to the west of the map. At a junction on the western side of the network, the Cambrian Main Line splits into two branches, which are known as the Cambrian Coast Line.

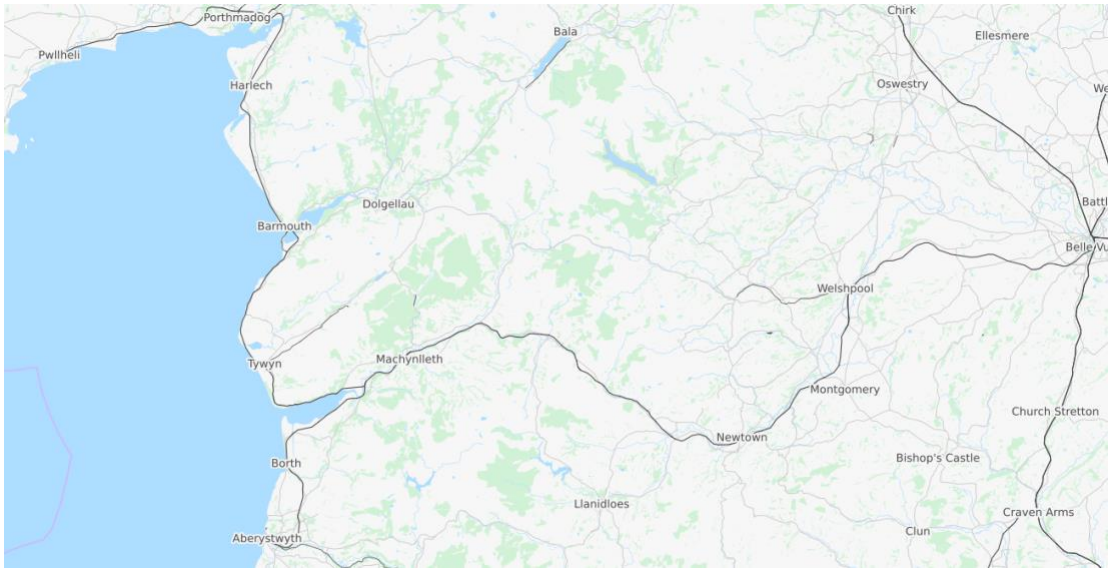

Figure 5.1 Railway layout of the Cambrian Line (OpenSteetMaps)

5.2.1 **System Modelling**

In this case study, OpenStreetMap is used as the database for the Digital Terrain Map (DTM). OpenStreetMap is an open and publicly accessible database containing the data of the public transport including the railway. By converting the Extensible Markup Language (EML) export of the area of the Cambrian Line, it can be used as the vector data containing part of the sampling points. More sampling points are added to ensure the sampling interval is within 50 m. On top of the sampling interval, additional sampling points can be inserted at the sections of the railway where a large volume of traffic may occur.

As an output, the route of the Cambrian Line has been modelled. The total number of sampling points is 3547 for this 218 km network. Figure 5.2 shows the modelled line layout of the Cambrian Line.

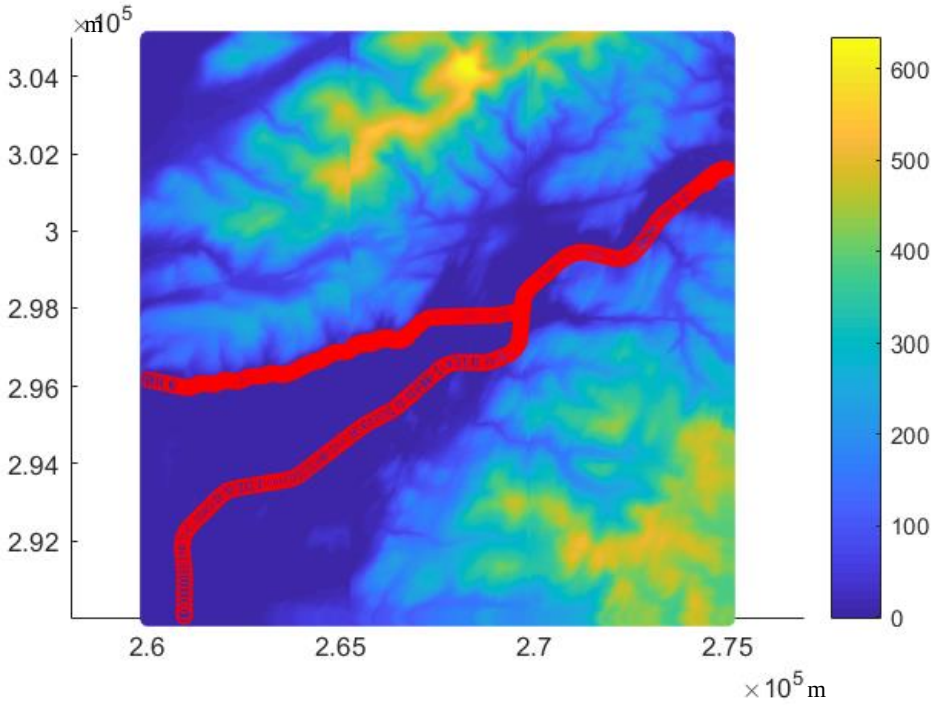

Figure 5.2 Topology Model of the railway at Dovey Junction on the Cambrian Line

5.2.2 **Environment Analysis**

The terrain map of the Cambrian Line is shown in Figure 5.3. A complex topology can be observed, especially in the Cambrian Coast Line area. Therefore, a detailed analysis of the environment is required.

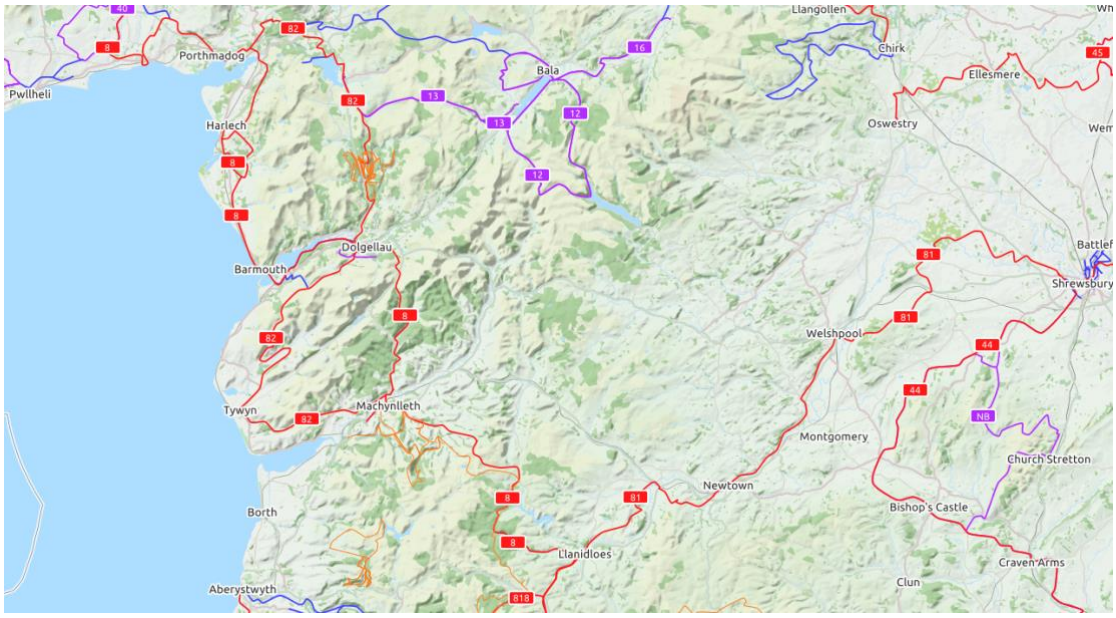

Figure 5.3 Terrain Map of the Cambrian Line

To analyse the terrain data and to categorise it, a Terrain Ruggedness Index (TRI) analysis, as introduced in (Riley, 1999), was performed for the area. During the TRI analysis, a 3D representation of the region was extracted from the DTM with a sampling interval of 25 m. The TRI model uses 1 km^2 as the sample size of a cell; therefore, for each sampling point of the railway network, a 1 km^2 cell is generated by using the sampling point as the centre of the cell. Then Equation (3.21) is applied to the system of squares to calculate the TRI of the area around the sampling point. The summary of the TRI indices associated with the sampling points is shown in Table 5.1.

Table 5.1 TRI of the sampling points in the Cambrian Line

TRI range	TRI categorises	Percentage
0 – 80 m	Level	33.32%
81 – 116 m	Nearly level	11.73%
117 – 161 m	Slightly rugged	18.69%
162 – 239 m	Intermediately Rugged	24.67%
240 – 497 m	Moderately Rugged	11.59%
498 – 958 m	Highly Rugged	0%
959 – 4367 m	Extremely Rugged	0%

Figure 5.4 is the plot of the TRI ranges for the Cambrian Line. The result of the TRI analysis indicates that about 45% of the network is level and nearly level land, which is formed by suburban and rural environments. This can be observed at the entry of the network, as well as the lower branch of the coastal line. 55% of the region is within mountainous regions. This includes the valley located near the junction of the main line, and the upper branch of the coastal line, which can be identified as a complex of mountains and coastal environments.

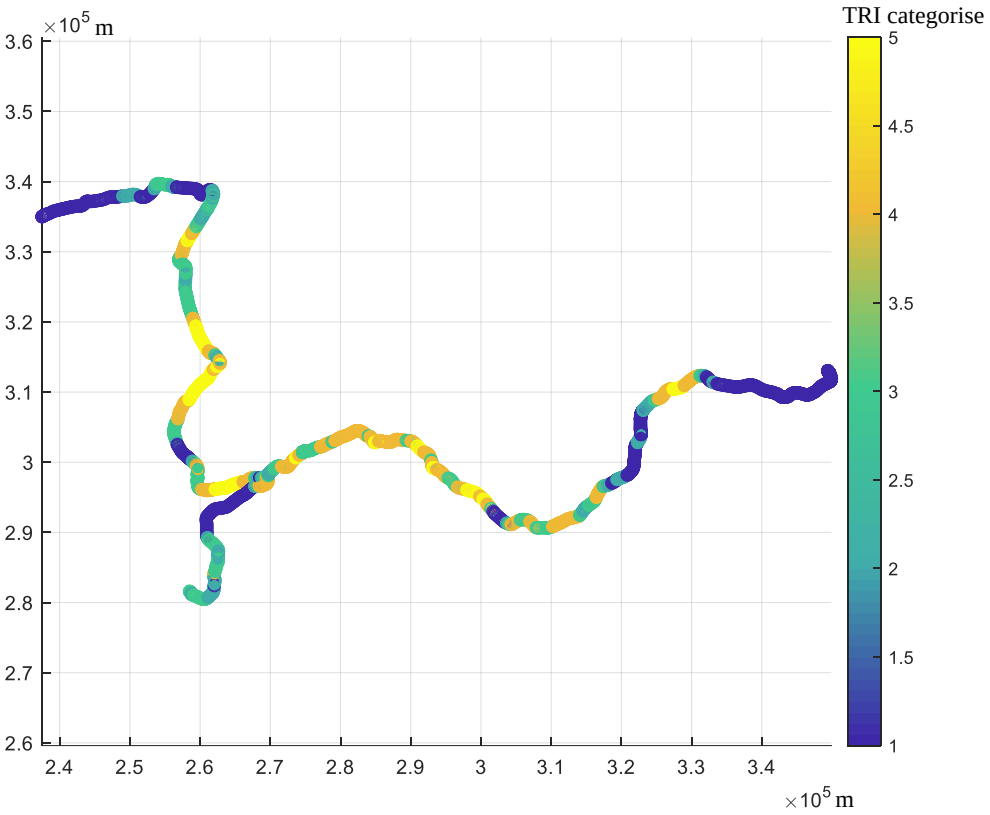

Figure 5.4 TRI of the Cambrian Line

5.3 Case Study on Algorithm Evaluation

To evaluate the performance of the optimisation algorithms, a simple case study is carried out to analyse the characteristic of the optimisation algorithms.

Because of the limitation of the optimisation size in BFS, a local region of the Cambrian Line has been selected for this study case. As shown in Figure 5.5, the junction area is selected to evaluate the accuracy of the optimisation algorithm.

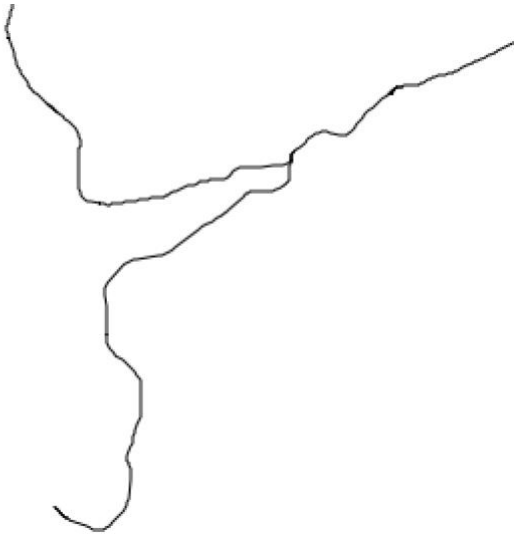

Figure 5.5 Dovey Junction Area of the Cambrian Line

The total length of the railway network in the area is 55 km, which results in 475 sampling points. An early estimation indicates that the number of BTSs required in this section is 4. The BTS and network configuration is summarised in Table 5.2.

Table 5.2 BTS and Network Configuration in the Dovey Junction Area

Parameter	Value
BTS height	15 m
Antenna gain	13 dBi
TX power	+33 dBm
RX threshold	-95 dBm
HO Margin	3 dB
Section speed limit	120 km/h
Station speed limit	50 km/h

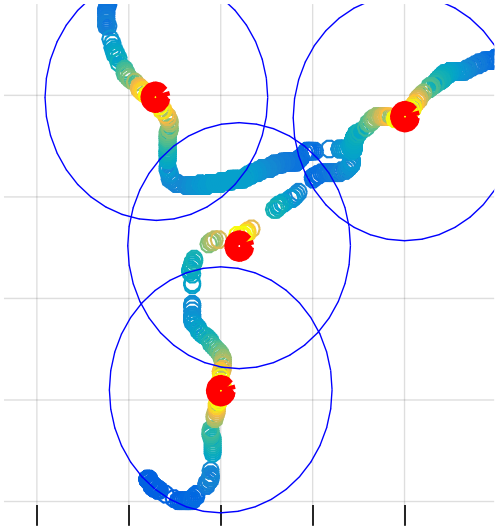

Figure 5.6 Optimisation result in the Dovey Junction Area

The optimisation result is shown in Figure 5.6. In this case study, all three algorithms provide a similar result, with all results within 100 meters of each other for each of the BTS site. The performance of the algorithms is shown in Table 5.3.

Table 5.3 Performance of the algorithms for the Dovey Junction area

Algorithm	Computation Time (seconds)
BFS	32813
ABFS	140
GA	435

As indicated in the performance results, both ABFS and GA solved the local optimisation in this scenario. The ABFS required the least computation time, but a risk of optimisation failure exists in the junction area, where the one additional BTS in the iteration may fail to handle the expansion of the optimisation zone when the junction is reached. Another study test is performed by adding two BTSs in each iteration to resolve this concern. Even though the result is the same as the earlier scenario, the computation time increases significantly, leading to 5325 seconds of ABFS computation time.

As for the GA, the algorithm requires the greatest iteration effort for any number of BTS in the network. Even when selecting the insufficient number of the BTSs for the area, for example by selecting 2 or 3 BTSs for the optimisation, the computation time is still higher than the ABFS.

In conclusion, for the optimisation of this section of the Cambrian Line, both ABFS and GA can provide an effective and efficient method of solution.

5.4 Case Study on BTS Site Planning for the Cambrian Line

5.4.1 Analysis of the Reference Site Plan

After evaluating the feasibility of the optimisation algorithms, the algorithms can be applied to achieve the global optimisation for the complete Cambrian Line. To provide a reference for the optimisation result, the existing BTS distribution in the network is used for the evaluation.

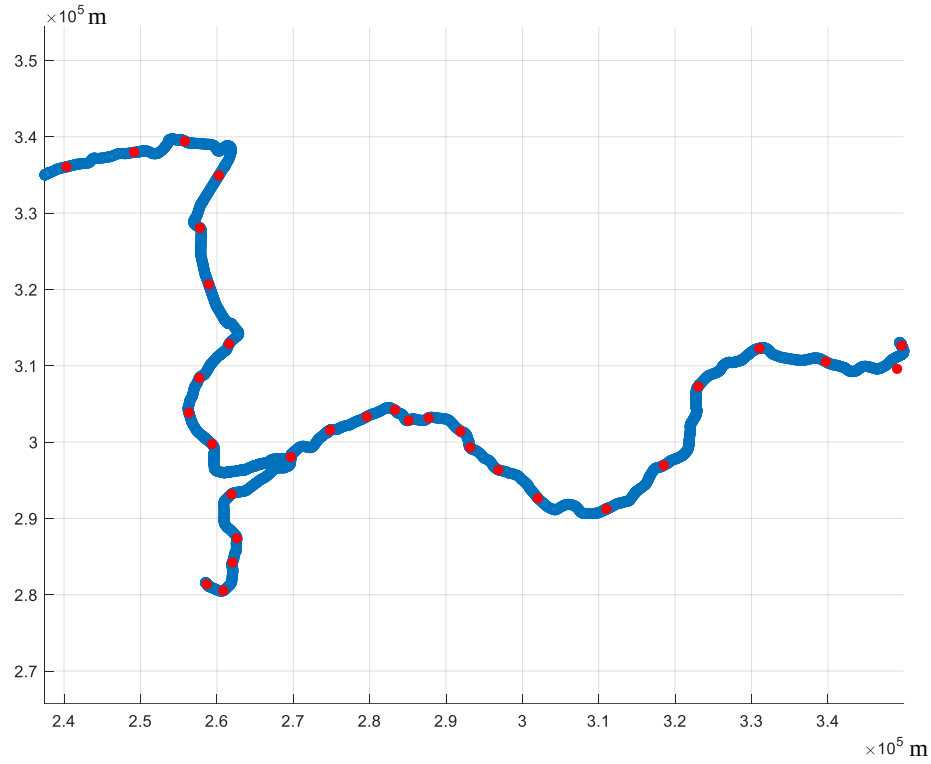

Figure 5.7 GSM-R BTS locations on the Cambrian Line

Figure 5.7 shows the actual BTS locations which have been deployed in the railway network, which provides the coverage that is sufficient to ensure the ETCS operation. In this deployment, 32 BTS have been installed for the GSM-R network. The configurations of the BTS are shown in Table 5.4.

Table 5.4 BTS configurations in the existing GSM-R network

Index	X coordinate	Y coordinate	TX Power (dBm)	Height(m)
1	349654	312629	29	26.5
2	349051	309598	29	28.5
3	339724	310520	20	29
4	331019	312279	20	26.5
5	323023	307263	29	26.5
6	318496	296953	29	26.5
7	310983	291241	29	26.5
8	302008	292654	29	26.5
9	296864	296343	15	29
10	293141	299297	15	29
11	291906	301411	20	26.5
12	287728	303171	15	25
13	285107	302831	29	26.5
14	283302	304211	20	26.5
15	279624	303320	15	29
16	274825	301582	29	26.5
17	269693	298040	29	25
18	261908	293174	15	26.5
19	262623	287401	29	26.5
20	262043	284230	15	26.5
21	260838	280540	20	29
22	258670	281370	3	8
23	259364	299742	15	26.5
24	256323	303857	15	26.5
25	257696	308404	15	26.5
26	261616	312877	29	25
27	258939	320664	15	26.5
28	257779	328064	15	26.5
29	260259	334927	15	29
30	255810	339420	15	26.5

31	249169	337974	20	26.5
32	240302	336072	15	26.5

In this table, two additional BTSs have been included to provide the redundancy at the east and south boundaries of the network. BTS No.22 is the redundant BTS for providing coverage within the terminus station, which is located at the lower left corner of the network. BTS No.1 is a junction BTS for providing the extended coverage for another railway network connected to the junction, which is not used to provide service for the Cambrian Line. Therefore, by eliminating the additional BTS which are not used to provide service for the Cambrian Line, there are 30 BTS installed in this network.

The propagation models are applied to the railway network for analysing the coverage of the GSM-R signal in the existing railway network. Figure 5.8 shows the receiving power across the railway network. The minimum receiving power in the scattered plot is -88.3 dBm, and the mean power is -64.7 dBm.

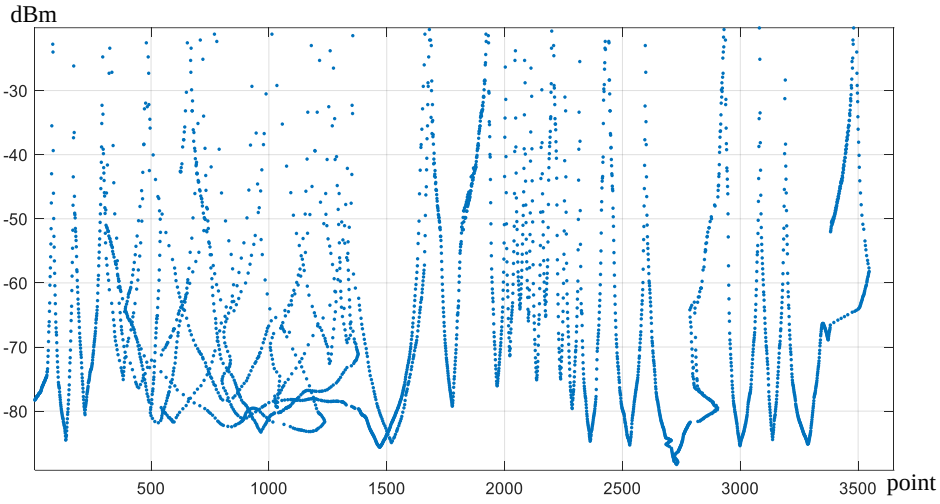

Figure 5.8 Receiving power in the Cambrian Line

5.4.2 **BTS Location Optimisation**

5.4.2.1 The Railway Network Configuration

To ensure that the optimisation is aligned with the railway's properties, the speed of the trains must be determined in the target network. The train speed at the sampling point is used for deriving the handover time in the region. For each of the sampling points in

the modelled system, the potential train speed when passing the sampling point can be derived by the speed limit of the section, as well as the characteristics of the train, including its acceleration rate and the maximum speed.

5.4.2.2 The GSM-R network configuration

The GSM-R network configuration is defined in Table 5.5, extended from Table 5.2. The propagation parameters are selected from (C. X. Wang *et al.*, 2016) and (Chen *et al.*, 2015) and summarised in Table 5.6

Table 5.5 Network Configuration for the Cambrian Line

Parameter	Value
BTS height	15 m
Antenna gain	13 dBi
TX power	+30 dBm
RX threshold	-95 dBm
HO Margin	3 dB

Table 5.6 Propagation Model Configuration

Catalogue	PL exponent	Correction Factor	Standard Deviation
Plain	3.4	46.17 dB	3.5 - 4 dB
Mountain	3.88	-11.6 dB	3.3 - 4.2 dB

5.4.2.3 Optimisation Algorithms

Both the ABFS and the GA algorithms are selected for the BTS optimisation.

a) Adapted Brute Force Search

The application of the ABVS algorithm requires dividing the railway network into two sections, the Cambrian Coast Line and the Cambrian Main Line. This is because a division into two entities is introduced at the junction connecting the Coast Line to the Main Line. At start up of the algorithm, the initial section is selected at one of the three significant points: the upper edge of the coastal line, the lower edge of the coastal line and the junction connecting the coastal line with the main line. The second step is to perform the optimisation on the coastal line until all the sampling points are covered.

Then the optimisation area is expanded onto the Cambrian Main Line, which concludes the optimisation. The pseudo code of the algorithm can be expressed as:

Table 5.7 Pseudo code for the ABFS Algorithm

	Algorithm 1: ABFS Algorithm
1	Set the initial area of the Cambrian Coast Line;
2	**While** (optimisation area not reached to all boundaries of the network) {
3	Insert one BTS into the optimisation area;
4	Expand the optimisation area to evaluate the capability of BTS;
5	**While** (limitation factor not satisfied) {
6	Decrease optimisation area, then re-evaluate;
7	Locate the last correct size of the area when terms are satisfied;
8	Fix the location of the existing BTS;
9	} }

b) Genetic Algorithm

The standard GA algorithm can be selected for the optimisation for this network. The size of the population in the GA can be determined by the number of sampling points and the estimated number of the BTS. For the medium-sized network in this study case, a population of 500 can be defined for optimising around 30 BTSs on a network with 3547 sampling points.

The pseudo code of the algorithm can be expressed as:

Table 5.8 Pseudo code for the Genetic Algorithm

	Algorithm 2: Genetic Algorithm
1	Generate initial population;
2	**While** (optimal result not found){
3	Iteration = iteration +1;
4	Fitness evaluation;
5	**If** (optimal result has found){
6	Output the optimal result;
7	Conclude the algorithm;
8	}
9	**If** (max iteration has reached){

```
10          Iteration = 0;
11          Number of BTS = Number of BTS +1;
12          Mutate the population with the additional BTS;
13       }
14    Crossover;
15    Mutation;
16    }
```

5.4.2.4 Performing the Optimisation

After the processes of system modelling, configuration determination and the algorithm implementation, the optimisation can be performed on the modelled railway network.

The optimal result derived by ABFS is shown in Figure 5.9.

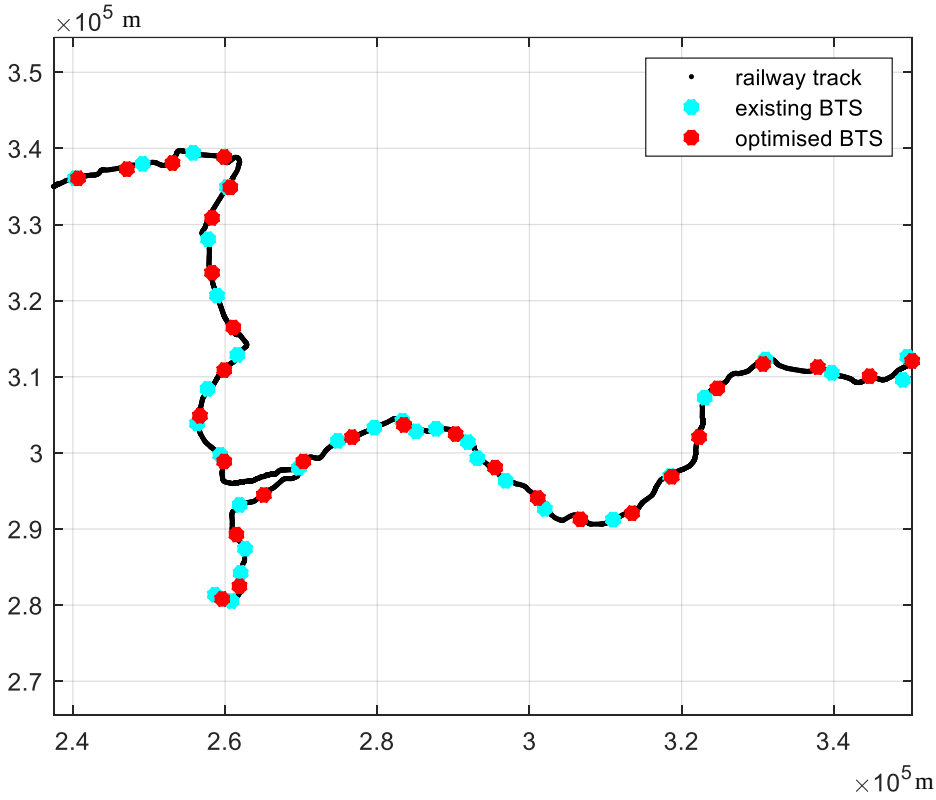

Figure 5.9 Optimal result derived by ABFS

In the figure, the red coloured dots represent the BTS locations of the optimised result generated by ABFS, and the cyan coloured plot are the locations of the transmitters of

the existing network. The result generated by the ABFS shows that a total number of 30 BTSs is required on the Cambrian Line, which is identical to the reference design in the existing layout but with slightly different positions along the lines.

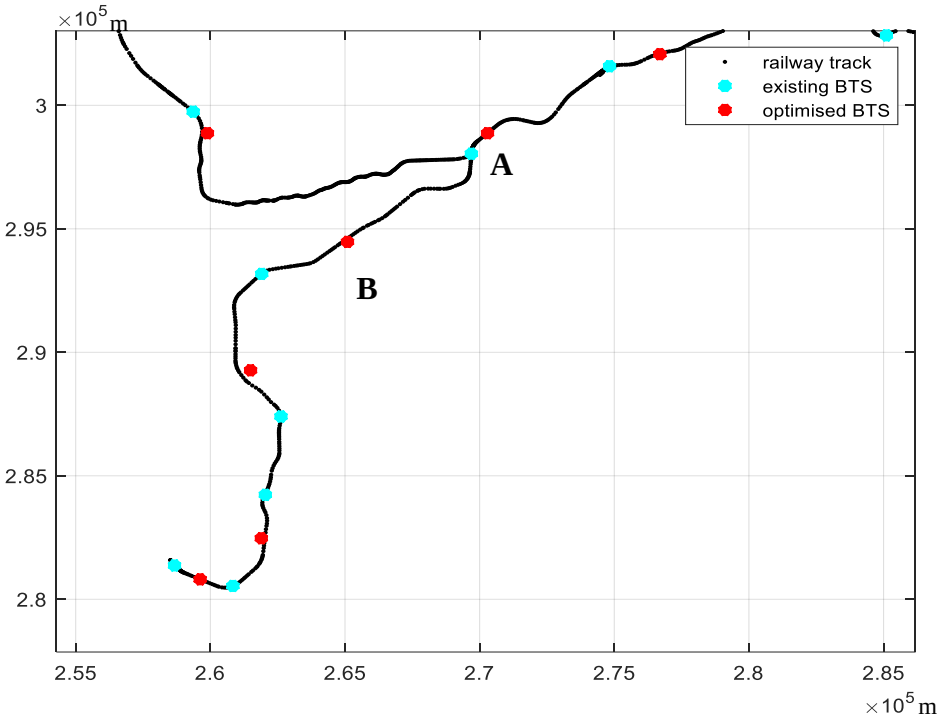

Figure 5.10 BTS locations in the Dovey Junction area

In Figure 5.10, for the Dovey Junction area marked with Point A, the ABFS algorithm successfully provides the estimation in the connection region between the Cambrian Main Line and the Cambrian Coast Line, with a distance margin of less than 1 km compared with the reference BTSs. On the southern branch, the coastal line, the algorithm derives one less BTS required in this region. This is because the area is located within a level environment, which leads to better coverage for the BTSs in this region. The algorithm also identifies that the BTS at Point B shall be closer to Point A, as the area is in a valley environment, leading to a high TRI index.

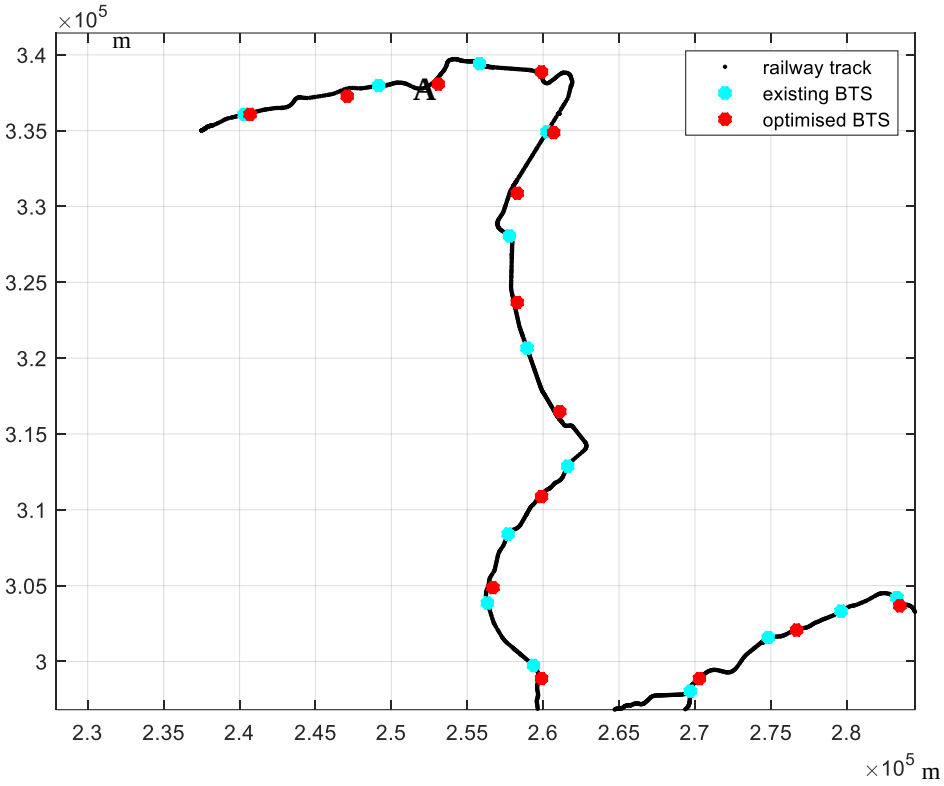

Figure 5.11 BTS locations on the northern branch of the Coast Line

In Figure 5.11, on the northern branch of the coastal line, even though the BTS at the terminus of the network is accurately predicted, one additional BTS is predicted in the region of Point A. This is because, when performing the optimisation by the ABFS algorithm, the height of the BTS was fixed at 15 m, while in the real-world design, the two BTS at the Point A are installed with a height of 30 m, which can provide a better coverage compared to a 15 m BTS. This indicates that after deriving the optimal result by applying system modelling and optimisation, extra configurations can be applied manually to further optimise the BTS site plan.

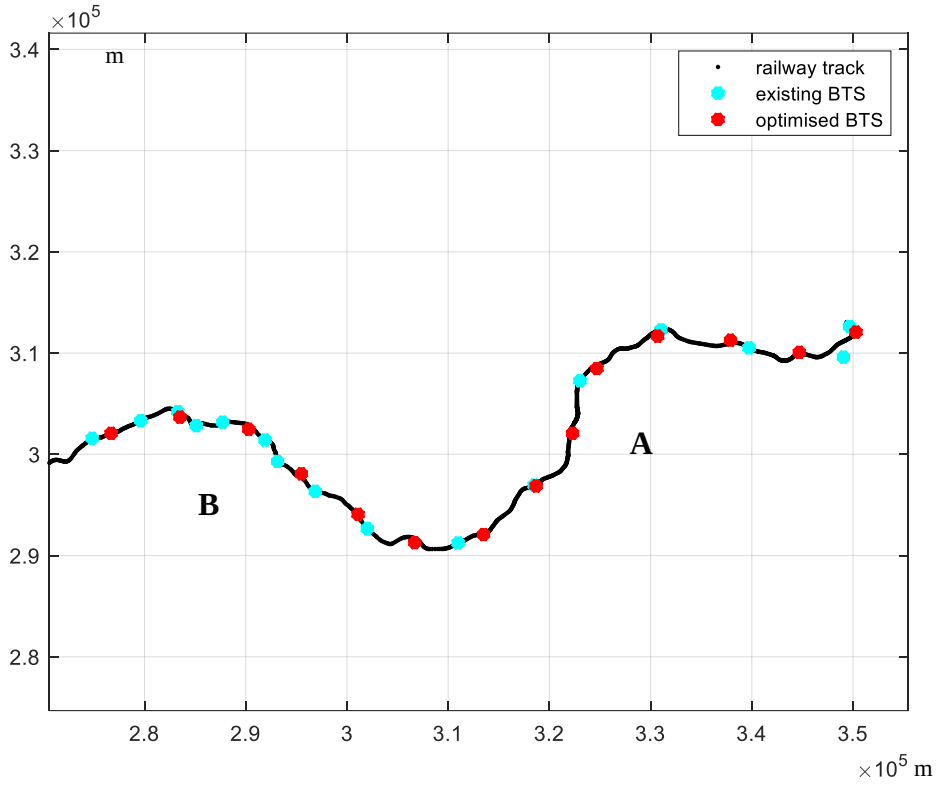

Figure 5.12 BTS location on the Cambrian Main Line

Figure 5.12 shows the result for the main line of the network. The estimation in the level area is relatively accurate, where Point A is located. However, the estimation at Point B is significantly different from the actual design where, in existing transmission network, more BTS are deployed. This is because of the following two reasons: The first reason is because of the accuracy of the terrain analysis. The terrain analysis is based on the 1 km^2 cell, which is not able to fully model the small scale mountains in the region. The second reason is the extra configurations applied in the actual design. As indicated by the satellite image shown in Figure 5.13, the area includes significant tree cover. As a result, extra installations were implemented in the actual site plan to overcome the extra loss caused by the vegetation in the surrounding area.

Figure 5.13 Satellite Image of the mountain region (Google Maps)

Figure 5.14 is the scatter plot of the received power provided by the optimised BTS arrangements. The mean received power is -68.1 dBm, and the minimum received power at the sampling points is -82.4 dBm, which is above the required -95 dBm ETCS operation standard.

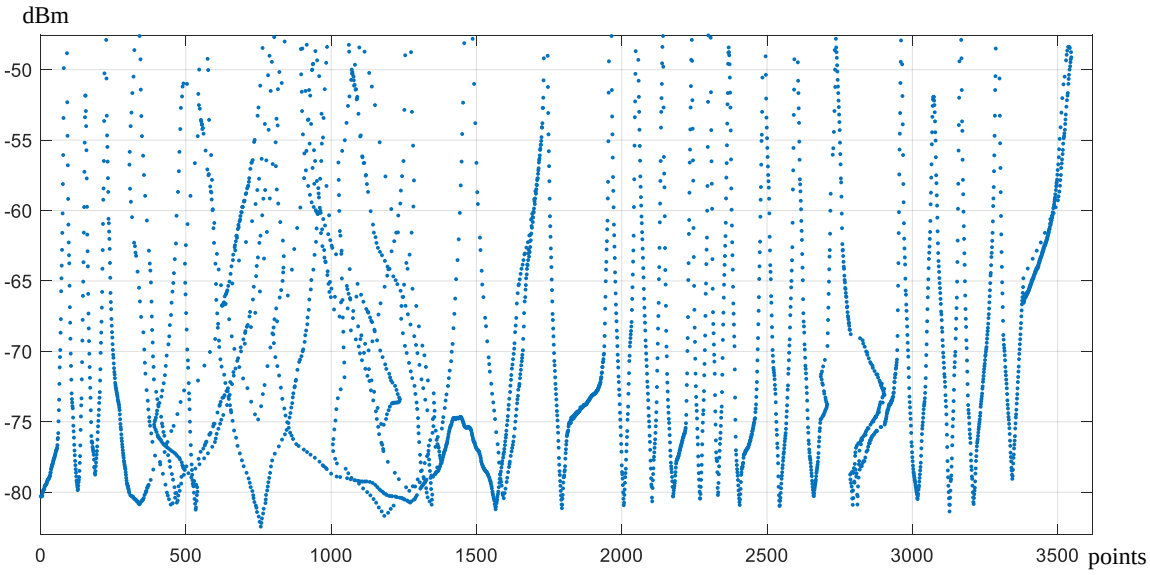

Figure 5.14 Received power in the ABFS scenario

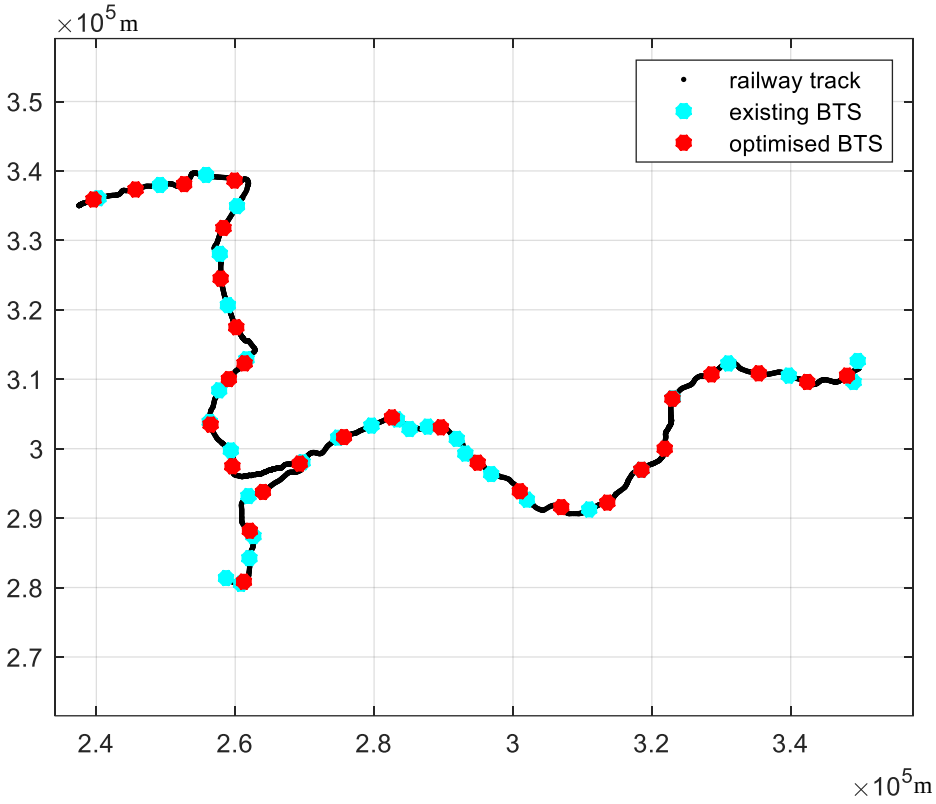

Figure 5.15 Optimal result derived by GA

The optimal result derived by GA is shown in Figure 5.15. In this optimised result, most of the BTS locations are the same as with the result of ABFS. Even higher accuracy of prediction is indicated in the level area of the Cambrian Main Line, where the optimised result is nearly aligned with the actual site plan, see Figure 5.16.

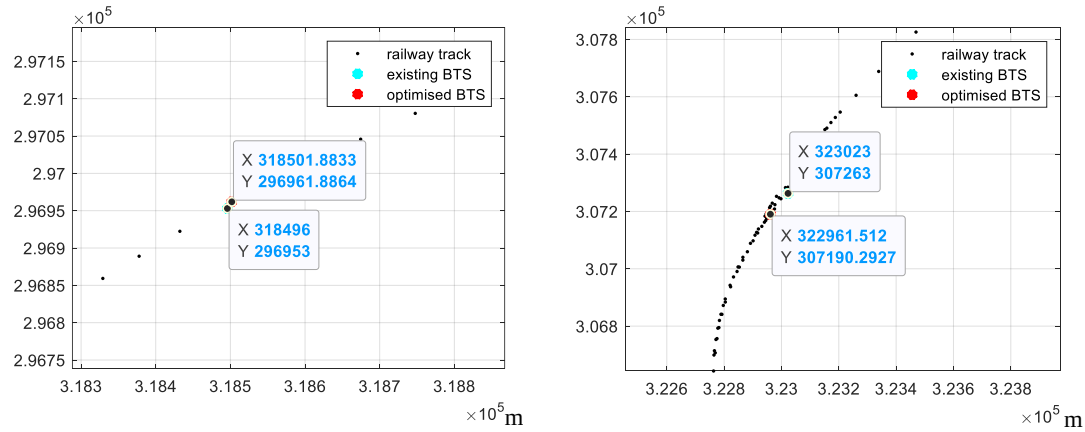

Figure 5.16 Accurate estimation of the GA

Figure 5.17 is the scatter plot of the received power provided by the optimised BTS arrangements. The mean receivin power is -67.0 dBm, and the minimum receiving

power at the sampling points is -81.8 dBm, which is 1 dB higher than the result provided by the ABFS.

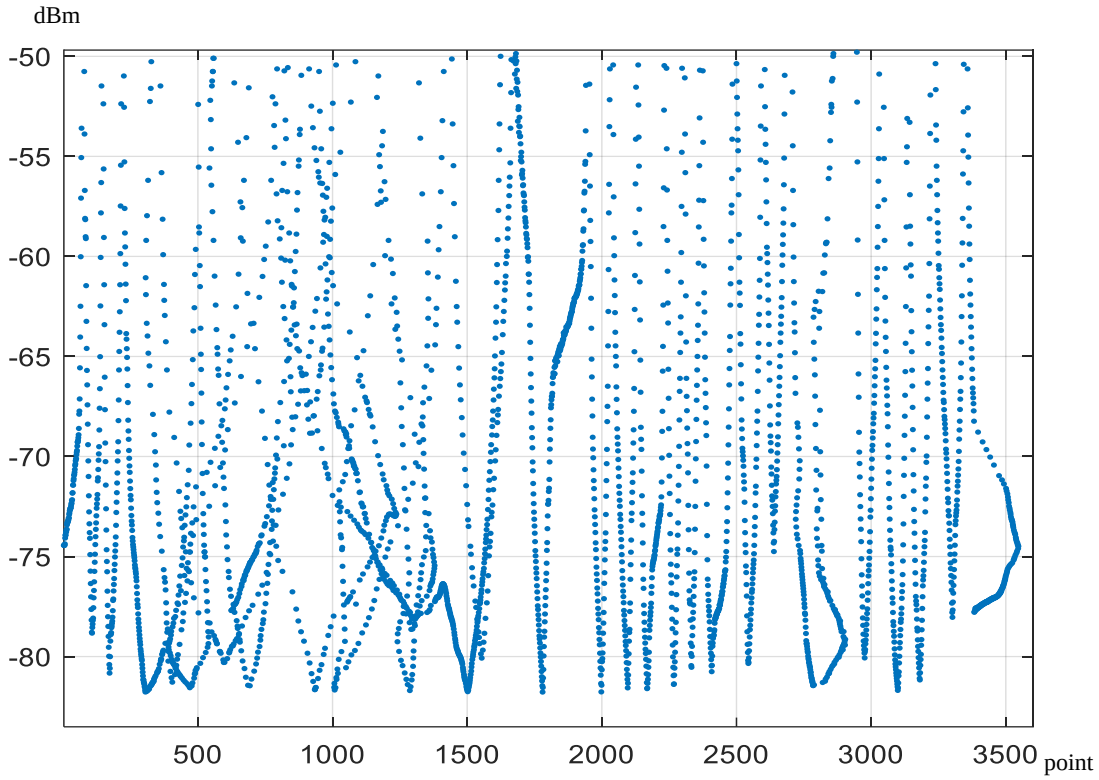

Figure 5.17 Receiving power in the GA scenario

5.4.3 **Algorithm Evaluation**

Based on the analysis of the results, both ABFS and GA can provide an optimised prediction for the BTS site plan, with the accuracy of the GA being slightly higher than most of the ABFS.

As for the efficiency of the simulation algorithm, the time for ABFS to derive the result is 3030 seconds, but more than 50% of the time is required to derive the location of the two BTSs at the junction of the network, which significantly increases the computation time.

In the GA scenario, by deploying 8-thread parallel computing, it takes 4680 seconds to derive an optimal result from one iteration of setting the BTS number. This means the computation time would be multiplied if the initial number of BTS is not identical to the optimal number of the BTS.

Table 5.9 is a summary of the performance of the algorithms. The performance test was made on a workstation PC equipped with an Intel Core i9-9900K 5.0 GHz processor, and MATLAB R2018a was selected for executing the optimisation study. Therefore, the ABFS algorithm can achieve the same accuracy level as GA but with much less computation time.

Table 5.9 Summary of the performance of ABFS and GA

Algorithm	Duration [s]	BTS number	Mean power	Minimum power
ABFS	3030	30	-67.0 dBm	-81.8 dBm
GA	4680×n *	30	-68.1 dBm	-82.4 dBm

* Where n is the possible attempts required in GA, n=2 was applied in the study case.

5.5 Conclusions

In this chapter, the proposed numeric model is applied to a real-world network to optimise the BTS locations. Two algorithms were applied to the study case, namely, the ABFS algorithm and the genetic algorithm. The comparison showed that both algorithms can provide effective optimisation of the GSM-R network. When excluding the extra configuration applied in the actual network, the optimisation result is close to the actual deployment of the existing railway network. The performance evaluation is also demonstrated, which shows that a greater computation time is required to perform the GA optimisation. On the other hand, the accuracy of the GA optimisation is the best.

In the next chapter, an integrated simulation platform is proposed, which is developed for validating the optimisation result.

Chapter 6 Simulation Platform Development for the GSM-R Network

6.1 Introduction

In the previous chapters, a study case conducted of implementing a solution for the GSM-R BTS site planning problem. Two typical algorithms were applied to a modelled railway network and produced optimal results for the siting of the BTSs.

The aim of this chapter is to develop an evaluation tool, which can validate the feasibility of the optimal result generated by the algorithms. In this chapter, an integrated simulation platform is introduced, which can simulate the communication in the GSM-R network while performing railway operations simulations. Then the optimal result generated in Chapter 5 is implemented in the simulation platform for validation.

6.2 Introduction to the Integrated Simulation Platform

As introduced in Chapter 2, the main constraints for the existing simulation tools for GSM-R transmission simulation are:

- Lack of railway features in the simulation platform.
- Commercial use, not academically available.

To overcome the limitations, an integrated simulation platform is developed. The platform includes a communication simulator to process the GSM-R communication, and a railway simulator to handle the operation of ETCS controlled services.

6.2.1 Communication Simulator

The selection of the communication simulator shall follow the principles below:

- Either open source or free for public use;
- Available with long-term support, or maintained by the community;
- Available with multiple communication models;
- Has the potential to be adapted for future communication technology;
- Ease of development and modelling.

By following these principles, the OMNeT++ simulator was selected for developing the integrated simulation platform for this research.

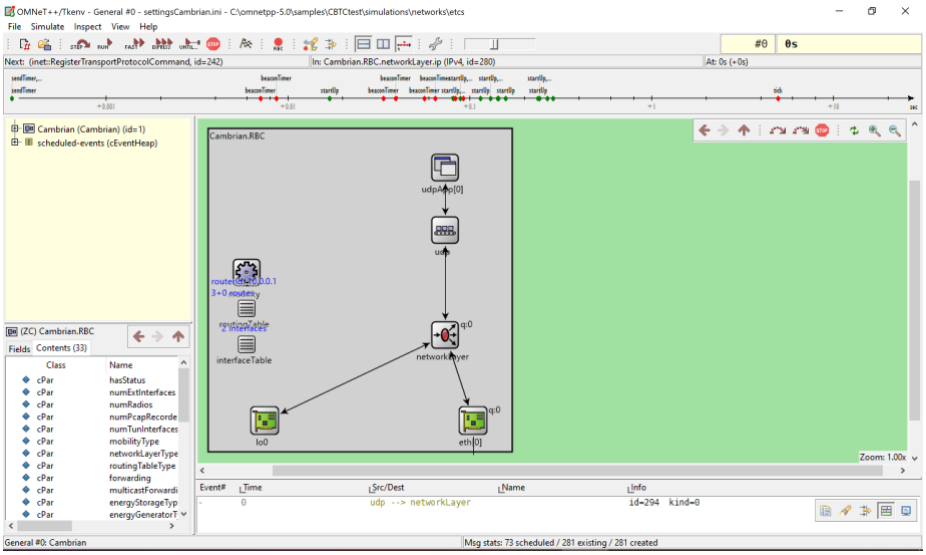

Figure 6.1 OMNeT++ Communication Simulator

OMNeT++ is an event-based discrete network modelling environment which can simulate the multiple communication layers of the network. As OMNeT++ features a modular design, many simulation models and components are available in the simulator. The main advantages of OMNeT++ are:

- The simulation library provided by OMNeT++ as default is based on the Open Systems Interconnection (OSI) model, which allows modification of the components in the OSI layers depending on the requirements of the simulation;
- The network can be defined using a high-level language, which also supports the User Interface (UI) interactions;
- Positive community support introduces a large variety of simulation models, including IEEE standard communication systems, Long-Term Evolution (LTE) model and 5G models.

To model the GSM-R network in OMNeT++, the communication network is created with the RBC, BTS and the ETCS train. Figure 6.2 is the structure of the ETCS train modelled in OMNeT++.

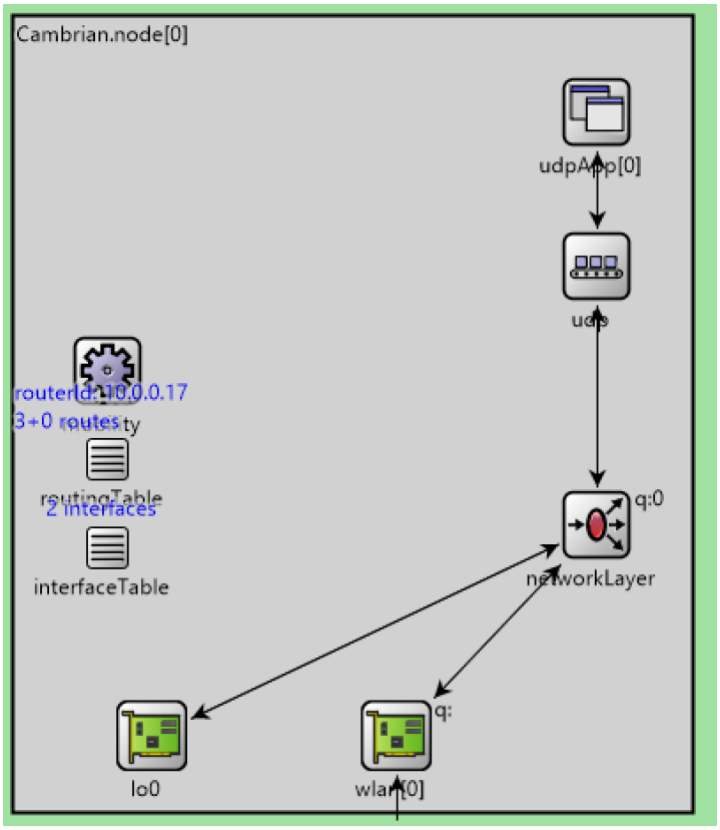

Figure 6.2 ETCS train in OMNeT++

Within the ETCS train element, the application layer, network layer and physical layer of the OSI model are configured. In the application layer, a User Datagram Protocol (UDP) application is configured, which simulates the operation of the on-board computer. The location report is generated by the UDP application at 1 second interval to simulate the ETCS messages. The network layer simulates the EURORADIO

protocol in GSM-R communication. It is used for coordinating the transmitted and received packets. The data link layer provides the wireless interface, where the GSM-R data packet is transmitted into the radio medium.

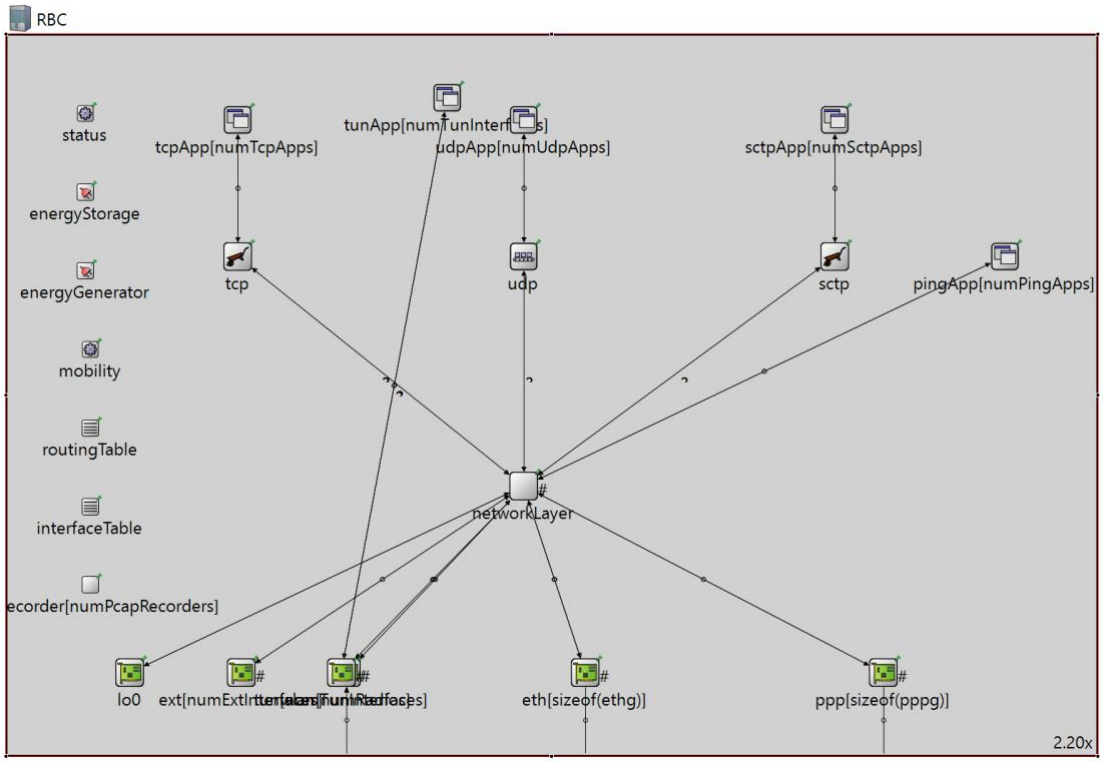

Figure 6.3 RBC structure in OMNeT++

The implementation of the RBC is shown in Figure 6.3. Similar to the structure of the ETCS train, the RBC also consists of three layers of the OSI model. The main difference compared to the train entity is the application layer, where the UDP application of the RBC is used to generate Movement Authority (MA) data, the permissive messages for the ETCS trains. In the physical layer, the RBC uses the Ethernet (eth) interfaces as the primary network interface, which are connected to the BTSs in the network. During a simulation, the railway simulator can interface with the UDP application to handle the MA data, then the RBC will create the MA data packets and transmit through the communication system.

The BTS is the wireless interface of the RBC. As shown in Figure 6.4, the role of the BTS is to provide an Ethernet interface to the RBC, then forward the MA message to the GSM-R wireless interface using a relay unit.

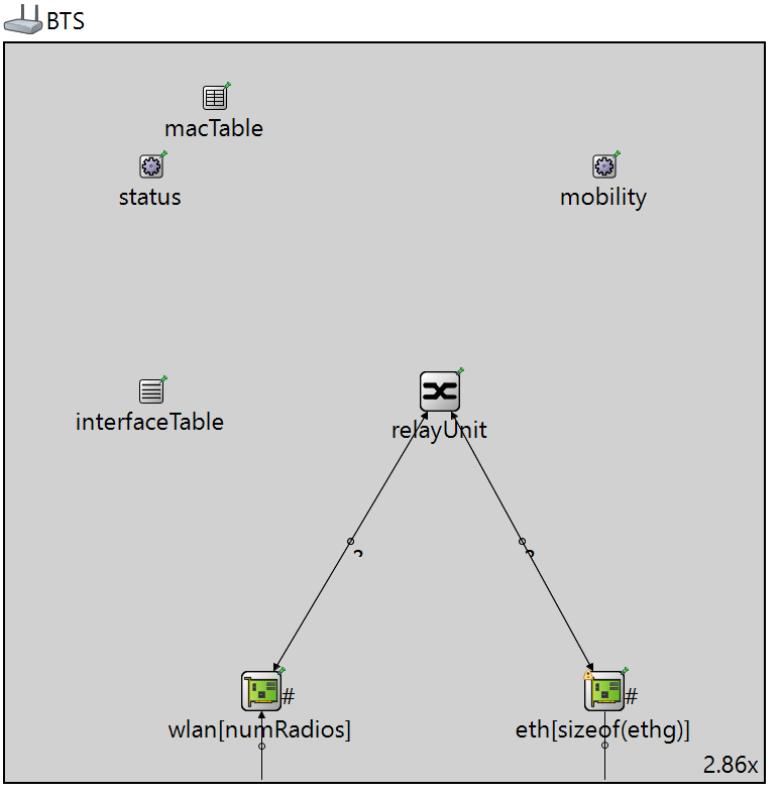

Figure 6.4 Structure of the BTS in OMNeT++

By assembling the main components into a network configurator, the GSM-R network simulation framework can be established, which is pictured in Figure 6.5.

Figure 6.5 GSM-R network in OMNeT++

6.2.2 **Railway Simulator**

In order to provide dynamic movement information to OMNeT++, a railway simulator is integrated into the simulation platform. For this research, the railway simulator BRaVE has been selected, which is a microscopic railway simulator developed by the Birmingham Centre for Railway Research and Education at the University of Birmingham, UK. Figure 6.6 is an example of the user interface of BRaVE.

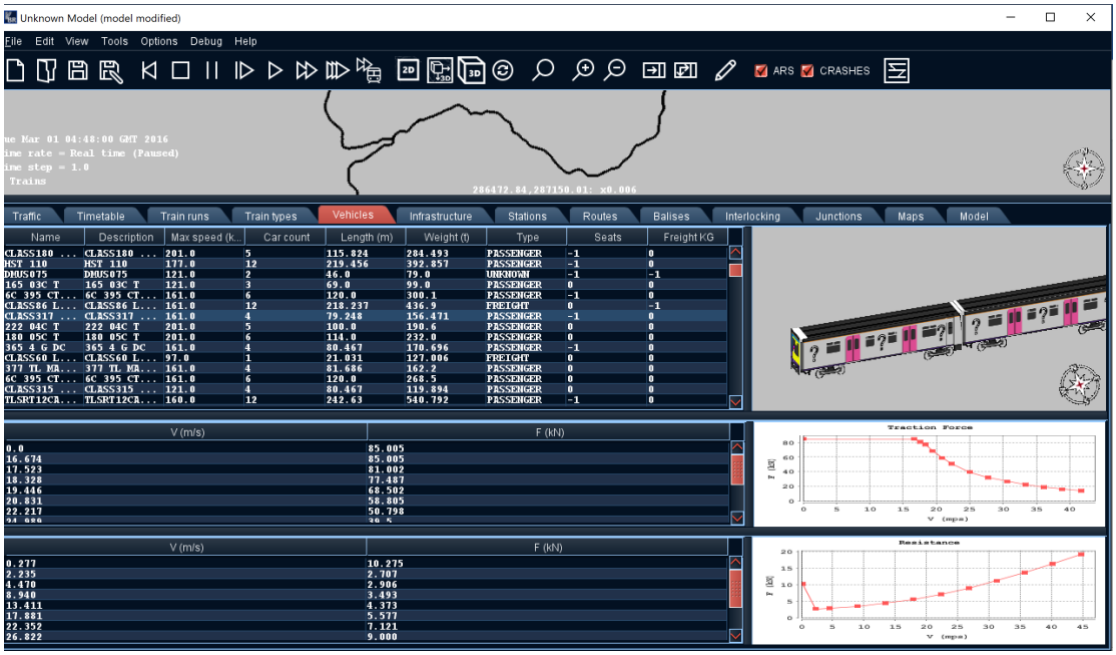

Figure 6.6 The railway simulator BRaVE

Similar to the network simulator, the railway simulator is also a modular design. Figure 6.7 demonstrates the structure of the railway simulator. In BRaVE, the components can be categorised as follows: static components, dynamic components, executors and user interface. The static components are integrated to provide the model data for the railway, including infrastructure, timetable and vehicle data to configure the characteristics of the trains. The role of the dynamic components is the simulator for the signalling and operation system. In particular, the interlocking module is the component for simulating the operation of ETCS. The executor components and UI components are supplementary components for improving the usability of the simulator.

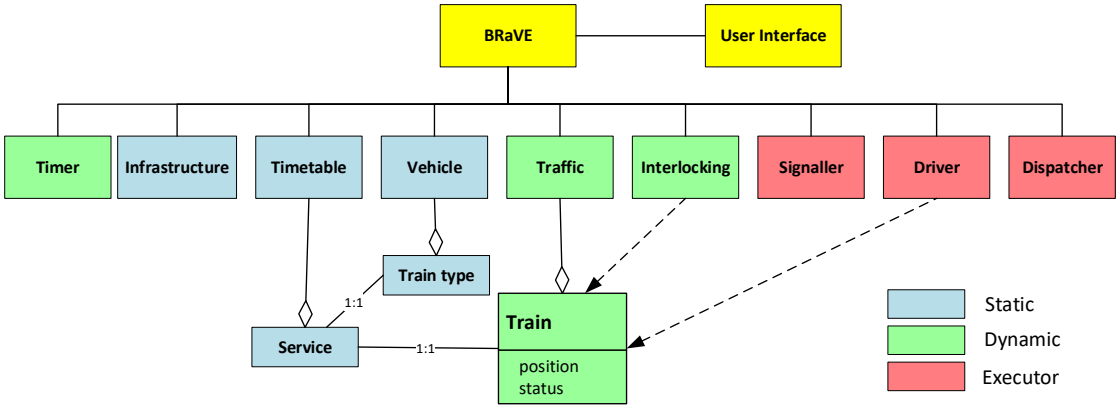

Figure 6.7 Structure of the railway simulator

The main reason for choosing BRaVE as the railway simulator is the usability of the simulation software. Only a limited number of railway simulators are available, but most of them cannot be reconfigured or integrated with add-on components. For example, as shown in Figure 6.8, the modelling of a railway network into a railway simulator takes massive effort to implement, especially for the modelling based on a DTM, where the railway track is located on a Geographic Information System (GIS) map. In BRaVE, this can be resolved by implementing an import tool, which can convert the XML output of the DTM database into a railway model in the simulator.

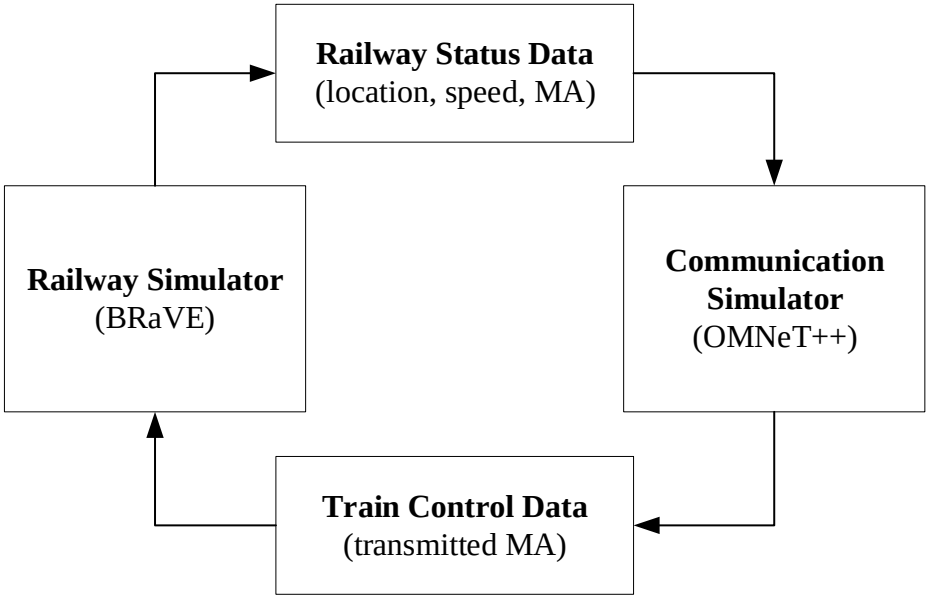

Figure 6.8 Integrated simulation platform

6.2.3 **Platform Integration**

As the railway simulator assumes the communication channel to be ideal, the network simulator is integrated with BRaVE to model and simulate the characteristics of a wireless network. To develop the integrated simulation platform, the communication simulator requires the dynamic information of the trains, including location and speed; meanwhile, the railway simulator requires the feedback of the transmission of the Movement Authority (MA). Therefore, a closed-loop design can be implemented to bind the two simulators into the simulation platform.

Figure 6.8 shows the integration mechanism of the platform. For both simulators in the platform, the same railway network is modelled in both software tools to achieve the different aspects of the simulation. During the simulation process, the railway simulator processes the movement of the train and sends the location and speed information to the communication simulator as a UDP packet. Then the communication simulator updates the location of the train in the GSM-R environment.

Meanwhile, the simulation of the ETCS operation is also implemented during the process. The interlocking module in the railway simulator generates the MA packet which is to be passed to the train. Then the MA is sent as a UDP packet together with the movement packet. On the OMNeT++ side, the communication simulator receives the MA packet, and transmits the packet in the simulated GSM-R environment within the simulator. This is implemented by the RBC within the GSM-R network. In the next step, the BTS transmits the MA packet into the radio medium, where the MA packet is propagated in the GSM-R radio environment and received by the train. Finally, the train receives the MA packet and forwards the packet back to the railway simulator to finish the simulation loop.

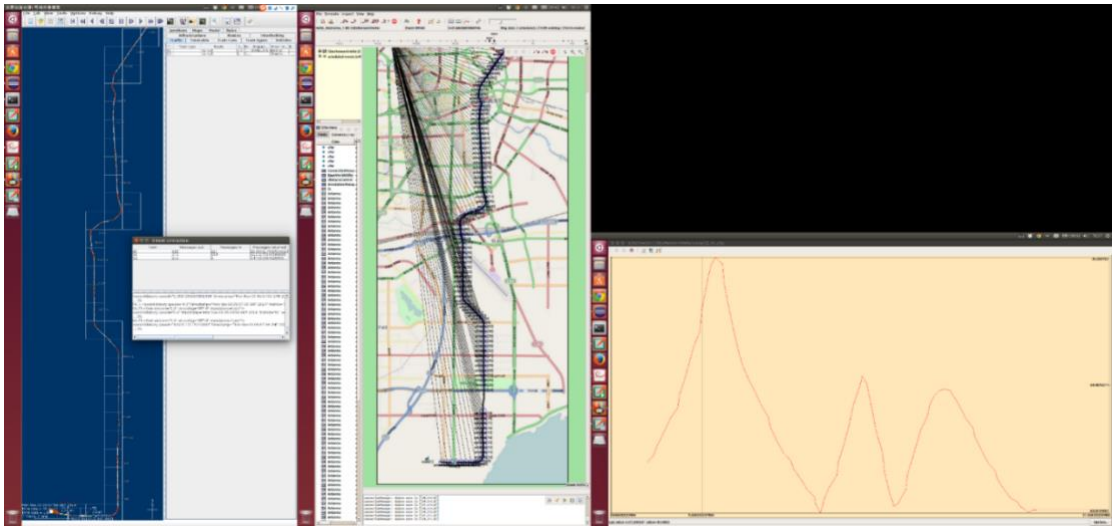

Figure 6.9 Integrated simulation platform for GSM-R network

Figure 6.9 shows an example of a GSM-R simulation in the integrated platform, where the small window located on the left side of the screen is the UDP client for linking the two simulation software tools. The primary window on the left side is the railway simulator. The two windows located at the centre and the right side of the figure represents the communication software, while the centre window is the user interface of OMNeT++ simulation and the right window is the monitor for the receiving power of a train.

The main advantage of the integrated simulation platform is that it can provide an accurate simulation of the behaviour of the overall system, including the operation of the ETCS service, and the MA packet forwarding mechanism in the GSM-R network.

Another advantage can be identified in the synchronisation mechanism. The closed-loop simulation mechanism can also be used for the time synchronisation. By defining the time interval of sending the MA packet, the clock tick of the timer can be received by the communication simulator; therefore, only one timer module is required in the simulation platform. Moreover, the synchronising mechanism can ensure the deterministic nature of the simulation result. As the secondary simulator in the simulation loop is not able to lose the synchronisation, the result of the simulation can be guaranteed by the synchronisation mechanism.

6.2.4 **Evaluation of the Simulation Platform**

To evaluate the functionality of the integrated platform, a test case was introduced in the platform (Wen *et al.*, 2015).

The test case is based on the Hefei Urban Rail Transit Line 1 with a length of 29 km. A 2.4 GHz CBTC system has been deployed on the metro line. The network configuration of the CBTC system is shown in Table 6.1. The reason for choosing a metro line for the platform validation is because metro lines use a more condensed communications network compared to the GSM-R, which can provide a better test case for validating the simulation platform. This is because the IEEE 802.11 system used for metros has less coverage on each cell, normally within a radius of 200m for each cell. Therefore, more handovers can occur during the simulation compared to the GSM-R. Meanwhile, the metro CBTC system requires a 1-second communication interval during operation, while the GSM-R only communicate when the movement authority is updated, which can be once every few minutes.

Table 6.1 CBTC Network Configuration in Hefei Line 1

Parameter	Value
Carrier frequency	2.412 GHz
Antenna gain	13 dBi
TX power	+3 dBm
RX threshold	-84 dBm
Path loss exponent	3 dB
Fading standard deviation	2.75 dB

The setup of the test scenario is shown in Figure 6.10. A coverage gap is introduced to simulate s connection loss of the wireless communication. In the railway simulator, two services are planned, with Train A entering the railway network, followed by Train B.

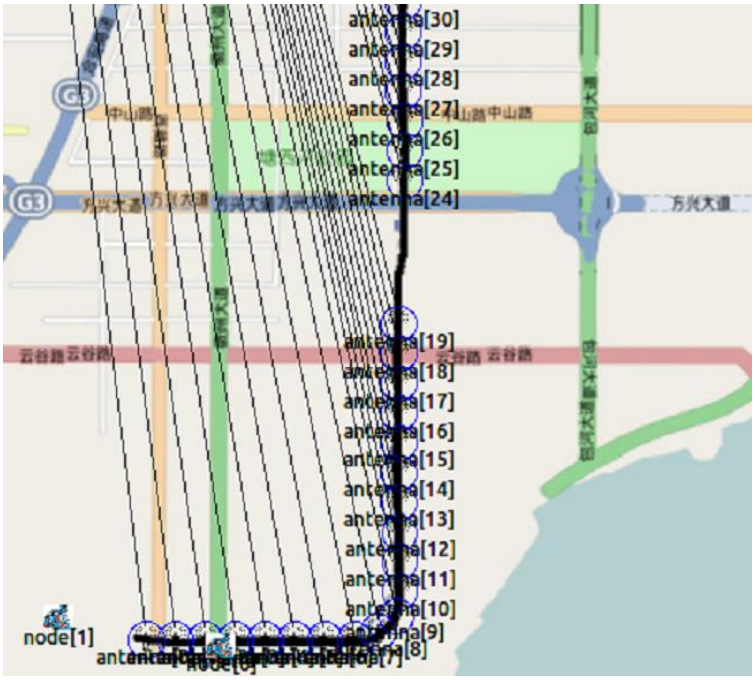

Figure 6.10 Test scenario for an integrated platform

The simulation result of the integrated simulation platform is demonstrated in Figure 6.11. At the beginning of the simulation, Train A receives the MA for the whole route as all tracks ahead are clear. Therefore, Train A can pass the no-coverage area without any intervention by the onboard Automatic Train Protection (ATP) system. However, Train A is unable to update its current position to the signalling system during the time.

As a result, when Train B enters the network, the MA is given with the ATP stopping point located in rear of the tail of Train A. The signalling system is unable to update the MA of Train B, as the location of Train A has not been updated via wireless communication. When Train B reaches the end of the MA, the ATP system of Train B still assumes that Train A is at the previously reported location; therefore the ATP applies the brakes to avoid a potential collision.

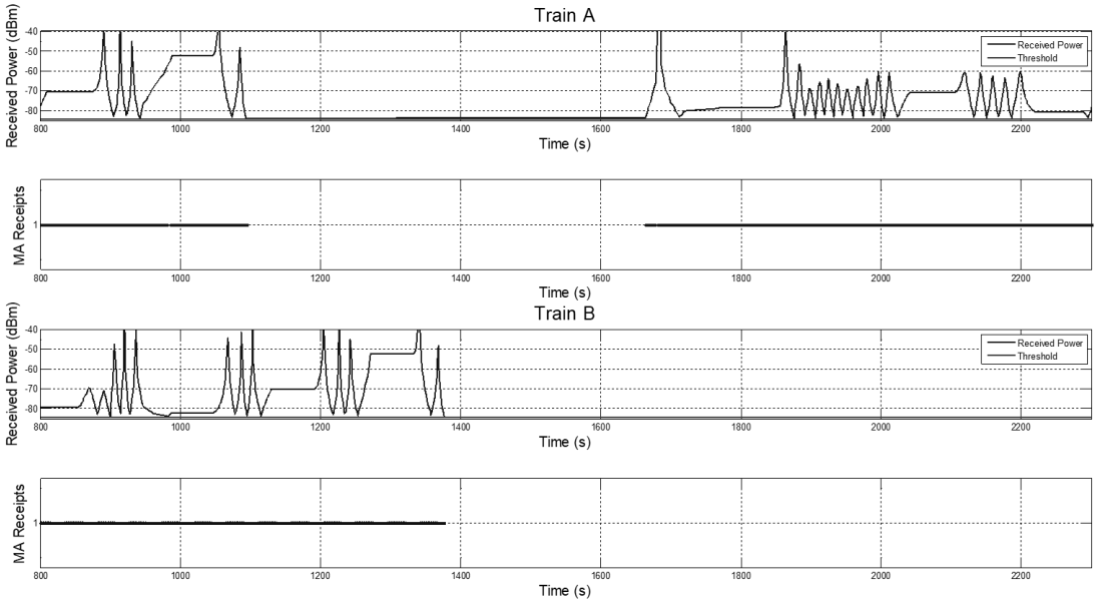

Figure 6.11 Simulation result of the test scenario

6.3 Validation of the Optimisation Result with the Integrated Simulation Platform

In the validation process, the optimisation result obtained in Chapter 5 is imported into the communication simulator, which is used to perform the coverage analysis in the GSM-R network.

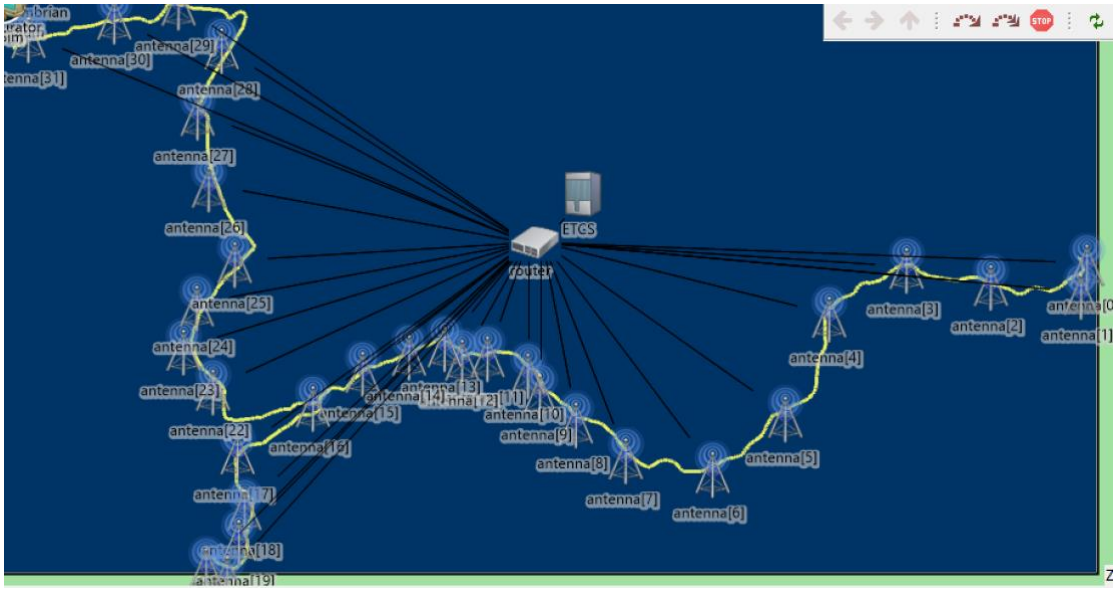

Figure 6.12 OMNeT++ simulation for the Cambrian Line

As for the railway simulator, a non-stop service is configured in the simulation, which starts from the boundary of the main line and ends at the terminus of the Cambrian

Coast Line. Since the train in the simulator runs at the maximum speed permitted on this line, this validation scenario is the representation of the worst-case scenario.

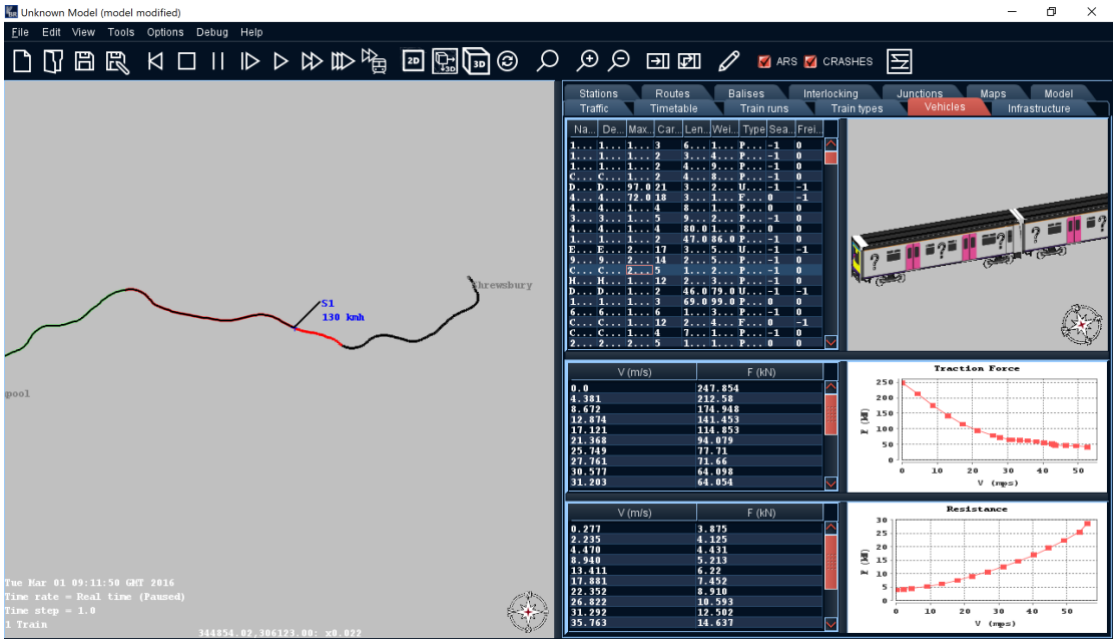

Figure 6.13 BRaVE simulation for the Cambrian Line

The performance in the physical layer has been evaluated in Chapter 5, which is the propagation evaluation for the optimised result. The simulation in the integrated platform is mainly focused on the performance of the network layer.

The validation of the simulation result took 8720 simulation seconds in the integrated environment. During the simulation, 13043 packets were injected into the GSM-R radio environment, including the transmission of MA and the location report. The result of the communication shows the mean Packet Error Rate (PER) of the GSM-R communication is 1.43%, where 10 of the 13043 packets were lost during the transmission and unable to be corrected, which accounts to 0.08% of the total transmission. The plot of the PER shown in Figure 6.14 indicates the distribution of packet error probability for all the packets transmitted in a simulation session, a slower decay of the distribution curve indicates a noisier transmission occurred in the simulation.

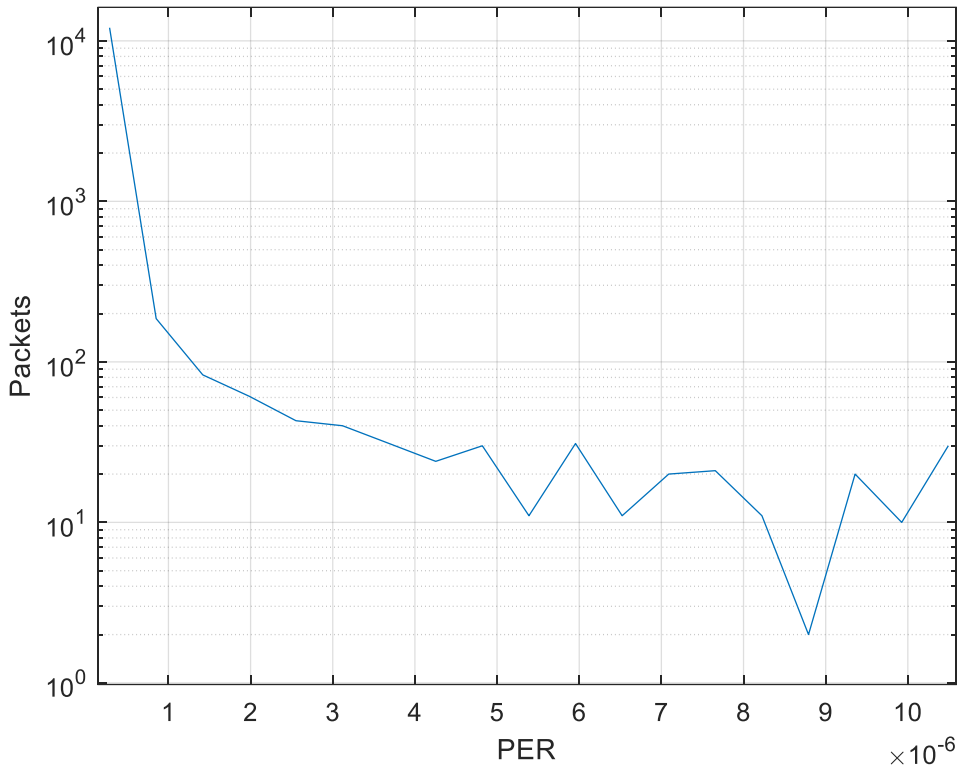

Figure 6.14 Packet Error Rate of the optimisation result

During the railway simulation, no interruption was observed in the whole process of the integrated simulation. Another service level of the simulation was also implemented by deactivating the communication simulator in the integrated platform. The railway simulation was proceeded by regarding the GSM-R communication as an ideal radio medium. The result shows that when using the standalone railway simulation as the reference of the service, no delay was introduced during the simulation of the GSM-R transmission. This means the optimisation result would not affect the operation of the railway service even in the worst-case scenario.

To compare the optimisation result with the reference BTS configuration, the locations of the existing BTSs in the Cambrian Line were imported into the network simulator to provide the reference result in the same railway environment. The result of the communication shows the mean Packet Error Rate (PER) of the GSM-R communication is 1.21%, which is slightly lower than the 1.43% provided by the optimisation result. The plot of the PER is shown in Figure 6.15, where a more rapid decay of the PER is shown in the PER distribution curve, which indicates a more reliable communication channel measured during the transmission.

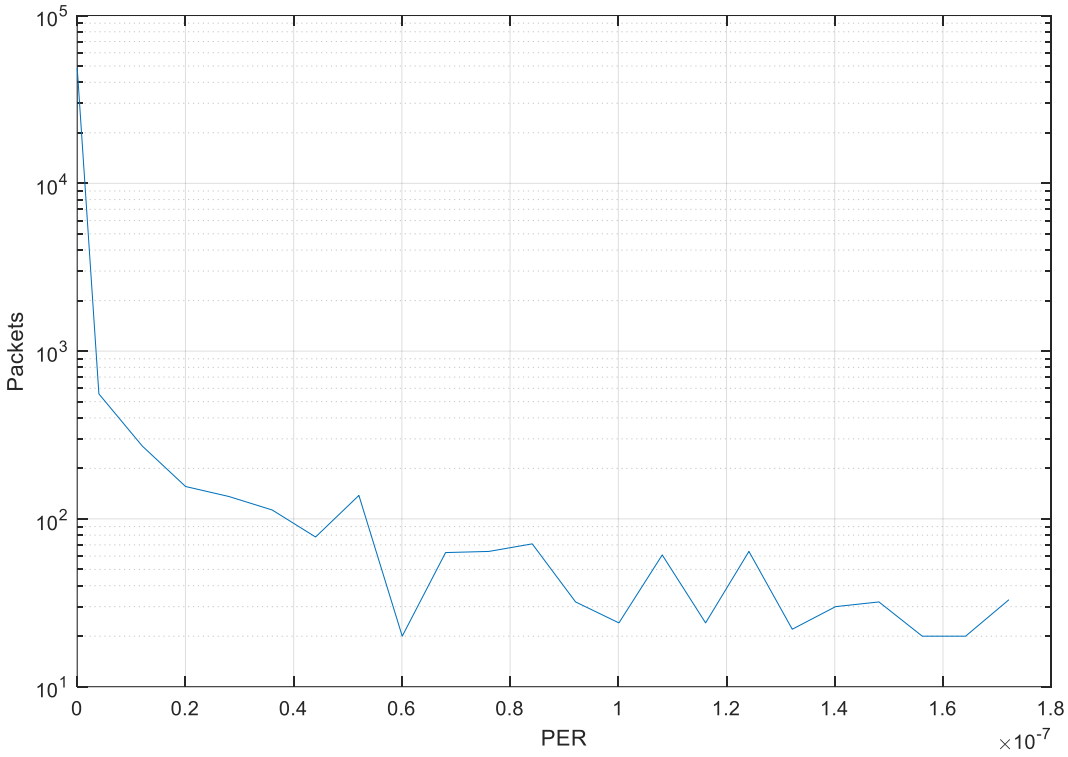

Figure 6.15 Packet Error Rate of the reference design

In conclusion, compared to the reference BTS design in the Cambrian Line, the BTS locations generated by the mathematical optimisation can provide an estimate that is close to the reference design. The PER of the optimisation result is slightly higher than the result of the reference BTS location, which can be further optimised by site surveys in the later processes of the GSM-R BTS site planning.

6.4 Conclusions

In this chapter, by integrating the communication simulator with the railway simulator using the closed-loop simulation mechanism, an integrated simulation platform has been developed for the simulation and verification of the GSM-R system in an ERTMS network. The optimisation result is further validated using the integrated simulation platform, which verified the feasibility of the proposed numeric optimisation method.

Chapter 7 Conclusions and Future Work

7.1 Conclusions

In modern railway signalling systems, wireless communication has a critical role in the railway operations, especially in high-speed railway networks where communication-based operation is mandatory. Therefore, the development of a robust wireless data communication system in the railway signalling system is exceptionally important. Unlike the deployment of the classical colour light based railway signalling which can be visually inspected, the deployment of the GSM-R wireless communication system requires the prediction of EMW propagation and the optimisation of the BTS locations to provide reliability for the railway operation, while reducing the construction and maintenance cost.

In order to understand the requirements and configuration of the GSM-R BTS site planning problem, the typical site planning process was evaluated, which is divided into the subject of geometry, communication and railway. Based on the system requirement specification of the GSM-R network, as well as the characteristics of the railway system, a mathematical modelling method was introduced to provide numeric modelling of the BTS site planning problem. Additionally, as railway networks are normally located in open space, the data preparation process was also illustrated in this thesis.

The next section of the thesis was used to derive the algorithms which can provide the optimal solution for the mathematical model formulated in the GSM-R network. Brute Force Search was investigated to determine the feasibility of the application. Due to the extremely low efficiency and the shortcomings when processing a large-scale network, an adapted brute force search algorithm was developed by adapting the BFS to step-by-step network optimisation. A typical genetic algorithm was also developed to solve the BTS site planning problem. The three algorithms were evaluated in a simple case study to validate the usability of the algorithms in the GSM-R network.

After developing the mathematical model and the optimisation algorithm, the modelling and optimisation method was applied to an existing GSM-R network. In the case study, the existing GSM-R BTS locations were selected as a reference. The evaluation of the optimisation result indicated that the GA could provide the most accurate optimisation result, while the ABFS can provide the best efficiency in solving the BTS site planning problem.

The next step was to validate the accuracy of the optimisation result. As the existing GSM-R network simulators have the disadvantage of being inaccessible for academic use, as well as a lack of essential railway features, an integrated simulation platform was developed to link an academic free-to-use communication simulator with the railway simulator BRaVE. The integrated simulation platform can provide a deterministic closed-loop simulation of the GSM-R network with the operation of the ETCS railway network, which can be used for simulating the dynamic behaviour of the GSM-R network on the railway and the service level. The optimisation of the BTS site planning problem was implemented on the simulation platform, which demonstrates the accuracy of the modelling and the optimising method.

7.2 Future Work

The research in this thesis was focused on the modelling and optimisation of GSM-R networks for the railway industry. Further work is suggested to extend the work, including:

1. The modelling of the GSM-R handover was implemented by setting a fixed handover time window as the limitation factor, which did not consider the optimisation of the handover algorithm. In the future, optimisation of the handover algorithm can be included in the mathematical formulation to improve the optimisation result.
2. The GSM-R system has a number of constraints, including limited lifetime with the technical support not being guaranteed after 2025 (Ai *et al.*, 2014), and the limited performance in terms of the communication rate and the delay. Application of LTE-R and 5G-R are to be expected in the railway industry. Due to the different mechanisms of multiple access and the different characteristic

of the propagation models in 4G and 5G communication, future work on the application of the optimisation method to the 5G-R network is recommended.

References

Adriano, R. *et al.* (2008) ‘Prediction of the BER on the GSM-R communications provided by the EM transient disturbances in the railway environment’, *IEEE International Symposium on Electromagnetic Compatibility* [Preprint], (1). Available at: https://doi.org/10.1109/EMCEUROPE.2008.4786913.

Ai, B. *et al.* (2012) ‘Radio wave propagation scene partitioning for high-speed rails’, *International Journal of Antennas and Propagation*, 2012. Available at: https://doi.org/10.1155/2012/815232.

Ai, B. *et al.* (2014) ‘Challenges toward wireless communications for high-speed railway’, *IEEE Transactions on Intelligent Transportation Systems*, 15(5), pp. 2143–2158. Available at: https://doi.org/10.1109/TITS.2014.2310771.

Ai, B. *et al.* (2017) ‘Determination of cell coverage area and its applications in high-speed railway environments’, *IEEE Transactions on Vehicular Technology*, 66(5), pp. 3515–3525. Available at: https://doi.org/10.1109/TVT.2016.2599113.

Akhoondzadeh-Asl, L. and Noori, N. (2007) *Modification and Tuning of the Universal Okumura-Hata Model for Radio Wave Propagation Predictions*.

Alamoud, M. a. and Schütz, W. (2012) ‘Okumura-Hata model tuning for TETRA mobile radio networks in Saudi Arabia’, *2012 2nd International Conference on Advances in Computational Tools for Engineering Applications, ACTEA 2012*, pp. 47–51. Available at: https://doi.org/10.1109/ICTEA.2012.6462901.

ALCATEL *et al.* (2005) ‘GSM-R Interfaces Class 1 Requirements’, pp. 1–26.

Binningsbø, J., Baldersheim, R. and P., Lauvstad.J. (2006) ‘GSM-R Radio Planning Guidelines’, p. 40.

Bouaziz, M. *et al.* (2016) *Evaluating TCMS Train-to-Ground Communication Performances Based on the LTE Technology and Discreet Event Simulations*, *Lecture Notes in Computer Science (including subseries Lecture Notes in Artificial Intelligence and Lecture Notes in Bioinformatics)*. Available at: https://doi.org/10.1007/978-3-319-38921-9_11.

Briso, C. *et al.* (2002) ‘Requirements of GSM Technology for The Train Control of High Speed Trains’, pp. 792–793.

Briso-rodríguez, C., Cruz, J.M. and Alonso, J.I. (2007) ‘Measurements and Modeling of Distributed Antenna Systems in Railway Tunnels’, 56(5), pp. 2870–2879.

Cai, Z. (2017) *Study on Doppler Shift Estimation and Compensation of High Speed Railway in GSM-R System*.

Cecchetti, G. *et al.* (no date) ‘An implementation of EURORADIO protocol for ERTMS/ETCS systems’.

Chen, B. *et al.* (2015) ‘Channel Characteristics in High-Speed Railway: A Survey of Channel Propagation Properties’, *IEEE Vehicular Technology Magazine*, pp. 67–78.

Chen, L. *et al.* (2011) ‘Performance analysis and verification of safety communication protocol in train control system’, *Computer Standards & Interfaces*, 33(5), pp. 505–518. Available at: https://doi.org/10.1016/j.csi.2011.02.006.

Chen, Y., Wang, Q. and Ouyang, X. (2023) ‘Communication Base Station Site Planning Based on Improved Simulated Annealing Algorithm’, in *2023 IEEE 3rd International Conference on Electronic Technology, Communication and Information, ICETCI 2023*. Institute of Electrical and Electronics Engineers Inc., pp. 1319–1323. Available at: https://doi.org/10.1109/ICETCI57876.2023.10176555.

Cota, N. *et al.* (2013) ‘On the use of Okumura-Hat a propagation model on railway communications’, in *International Symposium on Wireless Personal Multimedia Communications, WPMC*.

Djomadji Eric Michel, D. and Emmanuel, T. (2015) ‘Optimization of Okumura Hata Model in 800MHz based on Newton Second Order algorithm. Case of Yaoundé, Cameroon’, *IOSR Journal of Electrical and Electronics Engineering Ver. I*, 10(2), pp. 2278–1676. Available at: https://doi.org/10.9790/1676-10211624.

Du, Q. *et al.* (2012) ‘ICI mitigation by Doppler frequency shift estimation and pre-compensation in LTE-R systems’, *2012 1st IEEE International Conference on Communications in China, ICCC 2012*, pp. 469–474. Available at: https://doi.org/10.1109/ICCChina.2012.6356928.

Dudoyer, S. *et al.* (2011) ‘Reliability of the GSM-R Communication System against Railway Electromagnetic Interferences’, *World congress of Railway Research* [Preprint].

Dudoyer, S. *et al.* (2012) ‘Study of the susceptibility of the GSM-R communications face to the electromagnetic interferences of the rail environment’, *IEEE Transactions on Electromagnetic Compatibility*, 54(3), pp. 667–676. Available at: https://doi.org/10.1109/TEMC.2011.2169677.

Evolution of GSM-R (2015). Available at: www.idate.org.

GSM-R Operations Group (2012) ‘System Requirements Specification Version 15.3.0’, (March).

Guan, K., Zhong, Z. and Ai, B. (2011) ‘Assessment of LTE-R Using High Speed Railway Channel Model’, *2011 Third International Conference on Communications and Mobile Computing*, 2, pp. 461–464. Available at: https://doi.org/10.1109/CMC.2011.34.

Hammoud, M., Prof, A. and Abdelouahab, A. (2012) ‘LTE-ADVANCED SIMULATION FRAMEWORK BASED ON OMNeT ++’, 2012, pp. 8–10.

Hata, M. (1980) ‘Empirical formula for propagation loss in land mobile radio services’, *Vehicular Technology, IEEE Transactions on*, 29(3), pp. 317–325. Available at: https://doi.org/10.1109/T-VT.1980.23859.

He, D. *et al.* (2017) ‘Ray-tracing simulation and analysis of propagation for 3GPP high speed scenarios’, *2017 11th European Conference on Antennas and Propagation, EUCAP 2017*, pp. 2890–2894. Available at: https://doi.org/10.23919/EuCAP.2017.7928437.

He, R. *et al.* (2011) ‘Propagation measurements and analysis for high-speed railway cutting scenario’, *Electronics Letters*, 47(21), p. 1167. Available at: https://doi.org/10.1049/el.2011.2383.

He, R., Zhong, Z., Ai, B. and Guan, K. (2015) ‘Reducing the Cost of High-Speed Railway Communications : From the Propagation Channel View’, 16(4), pp. 1–11.

He, R., Zhong, Z., Ai, B. and Oestges, C. (2015) ‘Shadow Fading Correlation in High-Speed Railway Environments’, *IEEE Transactions on Vehicular Technology*, 64(7), pp. 2762–2772. Available at: https://doi.org/10.1109/TVT.2014.2351579.

He, R. *et al.* (2016a) ‘High-Speed Railway Communications: From GSM-R to LTE-R’, *IEEE Vehicular Technology Magazine*, 11(3), pp. 49–58. Available at: https://doi.org/10.1109/MVT.2016.2564446.

He, R. *et al.* (2016b) ‘High-Speed Railway Communications: From GSM-R to LTE-R’, *IEEE Vehicular Technology Magazine*, 11(3), pp. 49–58. Available at: https://doi.org/10.1109/MVT.2016.2564446.

Helgason, O. and Kouyoumdjieva, S. (2012) ‘Enabling Multiple Controllable Radios in OMNeT++ Nodes’, in. Institute for Computer Sciences, Social Informatics and Telecommunications Engineering (ICST). Available at: https://doi.org/10.4108/icst.simutools.2011.245502.

Hillenbrand, W. (ICN C.C.A. (1999) ‘GSM-R. The Railways Integrated Mobile Communication System’, p. 50.

Hsiao, L.S. and Lin, I.L. (2023) ‘Discussion on Integrating 5G and TETRA Applied to Railway Safety and Information Security-Related Issues’, in *2023 IEEE 3rd International Conference on Electronic Communications, Internet of Things and Big Data, ICEIB 2023*. Institute of Electrical and Electronics Engineers Inc., pp. 17–21. Available at: https://doi.org/10.1109/ICEIB57887.2023.10170585.

Hu, J. *et al.* (2022) ‘Off-Network Communications for Future Railway Mobile Communication Systems: Challenges and Opportunities’, *IEEE Communications Magazine*. Institute of Electrical and Electronics Engineers Inc., pp. 64–70. Available at: https://doi.org/10.1109/MCOM.001.2101081.

Jin, X., Jiang, L. and Wu, D. (2010) ‘A study of wireless channel on GSM-R network’, *2nd International Conference on Information Science and Engineering, ICISE2010 - Proceedings*, pp. 1782–1785. Available at: https://doi.org/10.1109/ICISE.2010.5691139.

Kastell, K. *et al.* (2006) ‘Improvments in Railway Communication via GSM-R’, 00(c), pp. 3026–3030.

Khan, S.N., Kalil, M. a. and Mitschele-Thiel, A. (2013) 'crSimulator: A discrete simulation model for cognitive radio ad hoc networks in OMNeT ++', *6th Joint IFIP Wireless and Mobile Networking Conference (WMNC)*, pp. 1–7. Available at: https://doi.org/10.1109/WMNC.2013.6549029.

Köpke, a *et al.* (2008) 'Simulating wireless and mobile networks in OMNeT++ the MiXiM vision', *Proceedings of the 1st international conference on Simulation tools and techniques for communications, networks and systems & workshops*, pp. 71:1--71:8. Available at: https://doi.org/10.4108/ICST.SIMUTOOLS2009.5555.

Kyösti, P. *et al.* (2008) 'IST-4-027756 WINNER II D1. 1.2 V1. 2 WINNER II Channel Models.pdf', *Projectscelticinitiativeorg*, 1(82), p. 82. Available at: http://projects.celtic-initiative.org/winner+/WINNER2-Deliverables/D1.1.2v1.2.pdf.

Lefrancq, M. (2016) 'D5 : FINAL REPORT Coexistence of GSM-R with other Communication Systems ERA 2015 04 2 SC Made for European Union Agency for Railways', 49(0).

Lijie, C. *et al.* (2012) 'Verification of the safety communication protocol in train control system using colored Petri net', *Reliability Engineering and System Safety*, 100, pp. 8–18. Available at: https://doi.org/10.1016/j.ress.2011.12.010.

Lin, S. *et al.* (2012) 'Finite state Markov modelling for high speed railway wireless communication channel', *GLOBECOM - IEEE Global Telecommunications Conference*, pp. 5421–5426. Available at: https://doi.org/10.1109/GLOCOM.2012.6503983.

Liu, Y. *et al.* (2017) 'Channel measurements and models for high-speed train wireless communication systems in tunnel scenarios: a survey', *Science China Information Sciences*, 60(10). Available at: https://doi.org/10.1007/s11432-016-9014-3.

Lu, J., Zhu, G. and Briso-Rodríguez, C. (2011) 'Fading characteristics in the railway terrain cuttings', *IEEE Vehicular Technology Conference*, pp. 1–5. Available at: https://doi.org/10.1109/VETECS.2011.5956605.

Lu, J.S. and Bertoni, H.L. (2011) 'Simulation of Fading Statistics in Hilly / Mountainous Terrain', *Terrain*, pp. 3440–3444.

Luan, F. *et al.* (2013) ‘Fading Characteristics of Wireless Channel on High-Speed Railway in Hilly Terrain Scenario’, *International Journal of Antennas and Propagation*, 2013, pp. 1–9. Available at: https://doi.org/10.1155/2013/378407.

Ma, Y. *et al.* (2014) ‘Dynamic estimation of local mean power in GSM-R networks’, *Wireless Networks*, 20(2), pp. 289–302. Available at: https://doi.org/10.1007/s11276-013-0601-1.

Martens, D. and Schattschneider, D. (2014) ‘Assessment report on GSM-R current and future radio environment’, pp. 1–24.

Martí Pallarés, F. *et al.* (2001) *Analysis of Path Loss and Delay Spread at 900 MHz and 2.1 GHz While Entering Tunnels*, *IEEE TRANSACTIONS ON VEHICULAR TECHNOLOGY*.

Medeisis, a. and Kajackas, A. (2000) ‘On the use of the universal Okumura-Hata propagation prediction model in rural areas’, *VTC2000-Spring. 2000 IEEE 51st Vehicular Technology Conference Proceedings (Cat. No.00CH37026)*, 3, pp. 4–7. Available at: https://doi.org/10.1109/VETECS.2000.851585.

Miao, X., Zhang, J. and Xiao, H. (2023) ‘Research on Base Station Siting Based on K-Means Clustering Algorithm’, in *2023 IEEE International Conference on Image Processing and Computer Applications, ICIPCA 2023*. Institute of Electrical and Electronics Engineers Inc., pp. 974–978. Available at: https://doi.org/10.1109/ICIPCA59209.2023.10257904.

Miao, Z., Tang, T. and Liu, J. (2013) ‘Performance Analysis of High Speed Rail Wireless Communication Network’, *2013 International Conference on Cyber-Enabled Distributed Computing and Knowledge Discovery*, pp. 483–489. Available at: https://doi.org/10.1109/CyberC.2013.89.

Nemţoi, L.M., Alexandrescu, C.M. and Stanciu, E.A. (2010) ‘GSM-R radio planning for the Bucureşti-Constanţa railway corridor - Case study’, *2010 IEEE 16th International Symposium for Design and Technology of Electronics Packages, SIITME 2010*, pp. 219–224. Available at: https://doi.org/10.1109/SIITME.2010.5652907.

Priebe, S. and Kurner, T. (2013) ‘Stochastic modeling of THz indoor radio channels’, *IEEE Transactions on Wireless Communications*, 12(9), pp. 4445–4455. Available at: https://doi.org/10.1109/TWC.2013.072313.121581.

Quan, H., Zhao, H. and Zhou, G. (2013) ‘Analysis on EURORADIO safety critical protocol by probabilistic model checking’, *IEEE ICIRT 2013 - Proceedings: IEEE International Conference on Intelligent Rail Transportation*, pp. 75–78. Available at: https://doi.org/10.1109/ICIRT.2013.6696271.

Railway Signalling EU (2013) ‘The ERTMS/ETCS signalling system’.

Riley, S. (1999) ‘Index that quantifies topographic heterogeneity’, *intermountain Journal of sciences*, pp. 23–27.

Riley, S.J., DeGloria, S.D. and Elliot, R. (1999) ‘A Terrain Rouggedness Index that Quantifies Topographic Heterogeneity’, *International Journal of Science*, 5(1–4), pp. 23–27.

Sharma, L., Pathak, B.K. and Sharma, R. (2012) ‘Breaking of Simplified Data Encryption Standard Using Genetic Algorithm’, 12(5).

Shi, J., Zhang, X. and Gao, T. (2010) ‘Performance analysis of GSM-R network structure in China train control system’, *ICEIE 2010 - 2010 International Conference on Electronics and Information Engineering, Proceedings*, 2(Iceie), pp. 214–218. Available at: https://doi.org/10.1109/ICEIE.2010.5559767.

Siemens (2004) *Tunnel System Guidelines*.

Siemens (no date) ‘Trainguard’, *siemens.com/mobility* [Preprint].

Sniady, A., Sønderskov, M. and Soler, J. (2015) ‘VOLTE Performance in Railway Scenarios’, (September).

Sousa, T. and Jorge, P. (2013) ‘Evaluation of Analytic Interference, Reception and Detection Modeling for IEEE 802.15.4 Networks with the MiXiM Omnet++ Framework’, *Thesis* [Preprint]. Available at: http://kth.diva-portal.org/smash/record.jsf?pid=diva2:597800.

Tao, H. (2023) ‘5G Base Station Deployment Based on Improved Hierarchical Co-Evolutionary Immunization Algorithm’, in *2023 IEEE International Conference on*

Image Processing and Computer Applications, ICIPCA 2023. Institute of Electrical and Electronics Engineers Inc., pp. 183–188. Available at: https://doi.org/10.1109/ICIPCA59209.2023.10257984.

Tingting, G. and Bin, S. (2010) 'A high-speed railway mobile communication system based on LTE', *2010 International Conference on Electronics and Information Engineering*, 1(Iceie), pp. V1-414-V1-417. Available at: https://doi.org/10.1109/ICEIE.2010.5559665.

UIC (2009) *GSM-R Procurement & Implementation Guide*.

UIC (2015) *EIRENE: GSM-R System Requirements Specification Version 16.0.0*.

UNISIG, E.I.G. (2012) 'Radio Transmission FFFIS for EuroRadio', (March), pp. 1–56.

Usman, A.U., Sadiq, J.M. and Ozovehe, A. (2012) 'Investigating the Applicability of Okumura-Hata Model for GSM 900 Networks of Yola Suburbs in Nigeria', pp. 7–16.

Wang, C. *et al.* (2016) 'Channel Measurements and Models for High-Speed Train Communication Systems: A Survey', *IEEE Communications Surveys & Tutorials*, 18(2), pp. 974–987. Available at: https://doi.org/10.1109/COMST.2015.2508442.

Wang, C.X. *et al.* (2016) 'Channel Measurements and Models for High-Speed Train Communication Systems: A Survey', *IEEE Communications Surveys and Tutorials*, 18(2), pp. 974–987. Available at: https://doi.org/10.1109/COMST.2015.2508442.

Wang, D. *et al.* (2021) 'Base Station Prediction Analysis Scheme Based on Lasso Regression Machine Learning Algorithm', in *Proceedings - 2021 IEEE 20th International Conference on Trust, Security and Privacy in Computing and Communications, TrustCom 2021*. Institute of Electrical and Electronics Engineers Inc., pp. 1406–1411. Available at: https://doi.org/10.1109/TrustCom53373.2021.00198.

Wang, S., Liu, K.Z. and Hu, F.P. (2005) 'Simulation of Wireless Sensor Networks Localization with OMNeT', *2005 2nd Asia Pacific Conference on Mobile Technology, Applications and Systems* [Preprint]. Available at: https://doi.org/10.1109/MTAS.2005.207141.

Wei, H. *et al.* (2010) 'Path loss models in viaduct and plain scenarios of the High-speed Railway', *2010 5th International ICST Conference on Communications and Networking in China*, pp. 1–5.

Wei, M. *et al.* (2012) ‘Base station electromagnetic simulation using ray-tracing method’, *Proceedings - 2012 6th Asia-Pacific Conference on Environmental Electromagnetics, CEEM 2012*, pp. 360–362. Available at: https://doi.org/10.1109/CEEM.2012.6410643.

Wei Qi *et al.* (2012) ‘Design of TETRA-based dedicated radio communication system for urban rail transit’, in *2012 3rd International Conference on System Science, Engineering Design and Manufacturing Informatization*.

Wen, T. *et al.* (2015) ‘Co-simulation Testing of Data Communication System Supporting CBTC’, *IEEE Conference on Intelligent Transportation Systems, Proceedings, ITSC*, 2015-Octob, pp. 2665–2670. Available at: https://doi.org/10.1109/ITSC.2015.428.

Wen, T. *et al.* (2018) ‘Access Point Deployment Optimization in CBTC Data Communication System’, *IEEE Transactions on Intelligent Transportation Systems*, 19(6), pp. 1985–1995. Available at: https://doi.org/10.1109/TITS.2017.2747759.

Xue, R. *et al.* (2020) ‘5G Enabling Technologies in Rail’, in *Proceedings - 2020 2nd International Conference on Information Technology and Computer Application, ITCA 2020*. Institute of Electrical and Electronics Engineers Inc., pp. 372–375. Available at: https://doi.org/10.1109/ITCA52113.2020.00084.

Yu, X., Ni, D. and Wang, W. (2006) ‘An omnidirectional high-gain antenna element for TD-SCDMA base station’, *ISAPE 2006 - 2006 7th International Symposium on Antennas, Propagation and EM Theory, Proceedings*, pp. 377–380. Available at: https://doi.org/10.1109/isape.2006.353347.

Zhang, L. *et al.* (2017) ‘Propagation modeling for outdoor-to-indoor and indoor-to-indoor wireless links in high-speed train’, *Measurement: Journal of the International Measurement Confederation*, 110, pp. 43–52. Available at: https://doi.org/10.1016/j.measurement.2017.06.014.

Zhang, X. (2013) ‘Research on the propagation characteristic of control signal of high-speed train’.

Zhang, X. *et al.* (2015) ‘Calibration of a 3-D ray-tracing model in railway environments’, *IEEE Antennas and Propagation Society, AP-S International*

Symposium (Digest), 2015-Octob, pp. 89–90. Available at: https://doi.org/10.1109/APS.2015.7304430.

Zhou, Y. *et al.* (2011) 'Broadband Wireless Communications on High Speed Trains'.

Adriano, R. *et al.* (2008) 'Prediction of the BER on the GSM-R communications provided by the EM transient disturbances in the railway environment', *IEEE International Symposium on Electromagnetic Compatibility* [Preprint], (1). Available at: https://doi.org/10.1109/EMCEUROPE.2008.4786913.

Ai, B. *et al.* (2012) 'Radio wave propagation scene partitioning for high-speed rails', *International Journal of Antennas and Propagation*, 2012. Available at: https://doi.org/10.1155/2012/815232.

Ai, B. *et al.* (2014) 'Challenges toward wireless communications for high-speed railway', *IEEE Transactions on Intelligent Transportation Systems*, 15(5), pp. 2143–2158. Available at: https://doi.org/10.1109/TITS.2014.2310771.

Ai, B. *et al.* (2017) 'Determination of cell coverage area and its applications in high-speed railway environments', *IEEE Transactions on Vehicular Technology*, 66(5), pp. 3515–3525. Available at: https://doi.org/10.1109/TVT.2016.2599113.

Akhoondzadeh-Asl, L. and Noori, N. (2007) *Modification and Tuning of the Universal Okumura-Hata Model for Radio Wave Propagation Predictions*.

Alamoud, M. a. and Schütz, W. (2012) 'Okumura-Hata model tuning for TETRA mobile radio networks in Saudi Arabia', *2012 2nd International Conference on Advances in Computational Tools for Engineering Applications, ACTEA 2012*, pp. 47–51. Available at: https://doi.org/10.1109/ICTEA.2012.6462901.

ALCATEL *et al.* (2005) 'GSM-R Interfaces Class 1 Requirements', pp. 1–26.

Binningsbø, J., Baldersheim, R. and P., Lauvstad.J. (2006) 'GSM-R Radio Planning Guidelines', p. 40.

Bouaziz, M. *et al.* (2016) *Evaluating TCMS Train-to-Ground Communication Performances Based on the LTE Technology and Discreet Event Simulations*, *Lecture Notes in Computer Science (including subseries Lecture Notes in Artificial Intelligence and Lecture Notes in Bioinformatics)*. Available at: https://doi.org/10.1007/978-3-319-38921-9_11.

Briso, C. *et al.* (2002) ‘Requirements of GSM Technology for The Train Control of High Speed Trains’, pp. 792–793.

Briso-rodríguez, C., Cruz, J.M. and Alonso, J.I. (2007) ‘Measurements and Modeling of Distributed Antenna Systems in Railway Tunnels’, 56(5), pp. 2870–2879.

Cai, Z. (2017) *Study on Doppler Shift Estimation and Compensation of High Speed Railway in GSM-R System*.

Cecchetti, G. *et al.* (no date) ‘An implementation of EURORADIO protocol for ERTMS/ETCS systems’.

Chen, B. *et al.* (2015) ‘Channel Characteristics in High-Speed Railway: A Survey of Channel Propagation Properties’, *IEEE Vehicular Technology Magazine*, pp. 67–78.

Chen, L. *et al.* (2011) ‘Performance analysis and verification of safety communication protocol in train control system’, *Computer Standards & Interfaces*, 33(5), pp. 505–518. Available at: https://doi.org/10.1016/j.csi.2011.02.006.

Chen, Y., Wang, Q. and Ouyang, X. (2023) ‘Communication Base Station Site Planning Based on Improved Simulated Annealing Algorithm’, in *2023 IEEE 3rd International Conference on Electronic Technology, Communication and Information, ICETCI 2023*. Institute of Electrical and Electronics Engineers Inc., pp. 1319–1323. Available at: https://doi.org/10.1109/ICETCI57876.2023.10176555.

Cota, N. *et al.* (2013) ‘On the use of Okumura-Hat a propagation model on railway communications’, in *International Symposium on Wireless Personal Multimedia Communications, WPMC*.

Djomadji Eric Michel, D. and Emmanuel, T. (2015) ‘Optimization of Okumura Hata Model in 800MHz based on Newton Second Order algorithm. Case of Yaoundé, Cameroon’, *IOSR Journal of Electrical and Electronics Engineering Ver. I*, 10(2), pp. 2278–1676. Available at: https://doi.org/10.9790/1676-10211624.

Du, Q. *et al.* (2012) ‘ICI mitigation by Doppler frequency shift estimation and pre-compensation in LTE-R systems’, *2012 1st IEEE International Conference on Communications in China, ICCC 2012*, pp. 469–474. Available at: https://doi.org/10.1109/ICCChina.2012.6356928.

Dudoyer, S. *et al.* (2011) ‘Reliability of the GSM-R Communication System against Railway Electromagnetic Interferences’, *World congress of Railway Research* [Preprint].

Dudoyer, S. *et al.* (2012) ‘Study of the susceptibility of the GSM-R communications face to the electromagnetic interferences of the rail environment’, *IEEE Transactions on Electromagnetic Compatibility*, 54(3), pp. 667–676. Available at: https://doi.org/10.1109/TEMC.2011.2169677.

Evolution of GSM-R (2015). Available at: www.idate.org.

GSM-R Operations Group (2012) ‘System Requirements Specification Version 15.3.0’, (March).

Guan, K., Zhong, Z. and Ai, B. (2011) ‘Assessment of LTE-R Using High Speed Railway Channel Model’, *2011 Third International Conference on Communications and Mobile Computing*, 2, pp. 461–464. Available at: https://doi.org/10.1109/CMC.2011.34.

Hammoud, M., Prof, A. and Abdelouahab, A. (2012) ‘LTE-ADVANCED SIMULATION FRAMEWORK BASED ON OMNeT ++’, 2012, pp. 8–10.

Hata, M. (1980) ‘Empirical formula for propagation loss in land mobile radio services’, *Vehicular Technology, IEEE Transactions on*, 29(3), pp. 317–325. Available at: https://doi.org/10.1109/T-VT.1980.23859.

He, D. *et al.* (2017) ‘Ray-tracing simulation and analysis of propagation for 3GPP high speed scenarios’, *2017 11th European Conference on Antennas and Propagation, EUCAP 2017*, pp. 2890–2894. Available at: https://doi.org/10.23919/EuCAP.2017.7928437.

He, R. *et al.* (2011) ‘Propagation measurements and analysis for high-speed railway cutting scenario’, *Electronics Letters*, 47(21), p. 1167. Available at: https://doi.org/10.1049/el.2011.2383.

He, R., Zhong, Z., Ai, B. and Guan, K. (2015) ‘Reducing the Cost of High-Speed Railway Communications : From the Propagation Channel View’, 16(4), pp. 1–11.

He, R., Zhong, Z., Ai, B. and Oestges, C. (2015) ‘Shadow Fading Correlation in High-Speed Railway Environments’, *IEEE Transactions on Vehicular Technology*, 64(7), pp. 2762–2772. Available at: https://doi.org/10.1109/TVT.2014.2351579.

He, R. *et al.* (2016a) ‘High-Speed Railway Communications: From GSM-R to LTE-R’, *IEEE Vehicular Technology Magazine*, 11(3), pp. 49–58. Available at: https://doi.org/10.1109/MVT.2016.2564446.

He, R. *et al.* (2016b) ‘High-Speed Railway Communications: From GSM-R to LTE-R’, *IEEE Vehicular Technology Magazine*, 11(3), pp. 49–58. Available at: https://doi.org/10.1109/MVT.2016.2564446.

Helgason, O. and Kouyoumdjieva, S. (2012) ‘Enabling Multiple Controllable Radios in OMNeT++ Nodes’, in. Institute for Computer Sciences, Social Informatics and Telecommunications Engineering (ICST). Available at: https://doi.org/10.4108/icst.simutools.2011.245502.

Hillenbrand, W. (ICN C.C.A. (1999) ‘GSM-R. The Railways Integrated Mobile Communication System’, p. 50.

Hsiao, L.S. and Lin, I.L. (2023) ‘Discussion on Integrating 5G and TETRA Applied to Railway Safety and Information Security-Related Issues’, in *2023 IEEE 3rd International Conference on Electronic Communications, Internet of Things and Big Data, ICEIB 2023*. Institute of Electrical and Electronics Engineers Inc., pp. 17–21. Available at: https://doi.org/10.1109/ICEIB57887.2023.10170585.

Hu, J. *et al.* (2022) ‘Off-Network Communications for Future Railway Mobile Communication Systems: Challenges and Opportunities’, *IEEE Communications Magazine*. Institute of Electrical and Electronics Engineers Inc., pp. 64–70. Available at: https://doi.org/10.1109/MCOM.001.2101081.

Jin, X., Jiang, L. and Wu, D. (2010) ‘A study of wireless channel on GSM-R network’, *2nd International Conference on Information Science and Engineering, ICISE2010 - Proceedings*, pp. 1782–1785. Available at: https://doi.org/10.1109/ICISE.2010.5691139.

Kastell, K. *et al.* (2006) ‘Improvments in Railway Communication via GSM-R’, 00(c), pp. 3026–3030.

Khan, S.N., Kalil, M. a. and Mitschele-Thiel, A. (2013) 'crSimulator: A discrete simulation model for cognitive radio ad hoc networks in OMNeT ++', *6th Joint IFIP Wireless and Mobile Networking Conference (WMNC)*, pp. 1–7. Available at: https://doi.org/10.1109/WMNC.2013.6549029.

Köpke, a *et al.* (2008) 'Simulating wireless and mobile networks in OMNeT++ the MiXiM vision', *Proceedings of the 1st international conference on Simulation tools and techniques for communications, networks and systems & workshops*, pp. 71:1--71:8. Available at: https://doi.org/10.4108/ICST.SIMUTOOLS2009.5555.

Kyösti, P. *et al.* (2008) 'IST-4-027756 WINNER II D1. 1.2 V1. 2 WINNER II Channel Models.pdf', *Projectscelticinitiativeorg*, 1(82), p. 82. Available at: http://projects.celtic-initiative.org/winner+/WINNER2-Deliverables/D1.1.2v1.2.pdf.

Lefrancq, M. (2016) 'D5 : FINAL REPORT Coexistence of GSM-R with other Communication Systems ERA 2015 04 2 SC Made for European Union Agency for Railways', 49(0).

Lijie, C. *et al.* (2012) 'Verification of the safety communication protocol in train control system using colored Petri net', *Reliability Engineering and System Safety*, 100, pp. 8–18. Available at: https://doi.org/10.1016/j.ress.2011.12.010.

Lin, S. *et al.* (2012) 'Finite state Markov modelling for high speed railway wireless communication channel', *GLOBECOM - IEEE Global Telecommunications Conference*, pp. 5421–5426. Available at: https://doi.org/10.1109/GLOCOM.2012.6503983.

Liu, Y. *et al.* (2017) 'Channel measurements and models for high-speed train wireless communication systems in tunnel scenarios: a survey', *Science China Information Sciences*, 60(10). Available at: https://doi.org/10.1007/s11432-016-9014-3.

Lu, J., Zhu, G. and Briso-Rodríguez, C. (2011) 'Fading characteristics in the railway terrain cuttings', *IEEE Vehicular Technology Conference*, pp. 1–5. Available at: https://doi.org/10.1109/VETECS.2011.5956605.

Lu, J.S. and Bertoni, H.L. (2011) 'Simulation of Fading Statistics in Hilly / Mountainous Terrain', *Terrain*, pp. 3440–3444.

Luan, F. *et al.* (2013) ‘Fading Characteristics of Wireless Channel on High-Speed Railway in Hilly Terrain Scenario’, *International Journal of Antennas and Propagation*, 2013, pp. 1–9. Available at: https://doi.org/10.1155/2013/378407.

Ma, Y. *et al.* (2014) ‘Dynamic estimation of local mean power in GSM-R networks’, *Wireless Networks*, 20(2), pp. 289–302. Available at: https://doi.org/10.1007/s11276-013-0601-1.

Martens, D. and Schattschneider, D. (2014) ‘Assessment report on GSM-R current and future radio environment’, pp. 1–24.

Martí Pallarés, F. *et al.* (2001) *Analysis of Path Loss and Delay Spread at 900 MHz and 2.1 GHz While Entering Tunnels*, *IEEE TRANSACTIONS ON VEHICULAR TECHNOLOGY*.

Medeisis, a. and Kajackas, A. (2000) ‘On the use of the universal Okumura-Hata propagation prediction model in rural areas’, *VTC2000-Spring. 2000 IEEE 51st Vehicular Technology Conference Proceedings (Cat. No.00CH37026)*, 3, pp. 4–7. Available at: https://doi.org/10.1109/VETECS.2000.851585.

Miao, X., Zhang, J. and Xiao, H. (2023) ‘Research on Base Station Siting Based on K-Means Clustering Algorithm’, in *2023 IEEE International Conference on Image Processing and Computer Applications, ICIPCA 2023*. Institute of Electrical and Electronics Engineers Inc., pp. 974–978. Available at: https://doi.org/10.1109/ICIPCA59209.2023.10257904.

Miao, Z., Tang, T. and Liu, J. (2013) ‘Performance Analysis of High Speed Rail Wireless Communication Network’, *2013 International Conference on Cyber-Enabled Distributed Computing and Knowledge Discovery*, pp. 483–489. Available at: https://doi.org/10.1109/CyberC.2013.89.

Nemţoi, L.M., Alexandrescu, C.M. and Stanciu, E.A. (2010) ‘GSM-R radio planning for the Bucureşti-Constanţa railway corridor - Case study’, *2010 IEEE 16th International Symposium for Design and Technology of Electronics Packages, SIITME 2010*, pp. 219–224. Available at: https://doi.org/10.1109/SIITME.2010.5652907.

Priebe, S. and Kurner, T. (2013) ‘Stochastic modeling of THz indoor radio channels’, *IEEE Transactions on Wireless Communications*, 12(9), pp. 4445–4455. Available at: https://doi.org/10.1109/TWC.2013.072313.121581.

Quan, H., Zhao, H. and Zhou, G. (2013) ‘Analysis on EURORADIO safety critical protocol by probabilistic model checking’, *IEEE ICIRT 2013 - Proceedings: IEEE International Conference on Intelligent Rail Transportation*, pp. 75–78. Available at: https://doi.org/10.1109/ICIRT.2013.6696271.

Railway Signalling EU (2013) ‘The ERTMS/ETCS signalling system’.

Riley, S. (1999) ‘Index that quantifies topographic heterogeneity’, *intermountain Journal of sciences*, pp. 23–27.

Riley, S.J., DeGloria, S.D. and Elliot, R. (1999) ‘A Terrain Rouggedness Index that Quantifies Topographic Heterogeneity’, *International Journal of Science*, 5(1–4), pp. 23–27.

Sharma, L., Pathak, B.K. and Sharma, R. (2012) ‘Breaking of Simplified Data Encryption Standard Using Genetic Algorithm’, 12(5).

Shi, J., Zhang, X. and Gao, T. (2010) ‘Performance analysis of GSM-R network structure in China train control system’, *ICEIE 2010 - 2010 International Conference on Electronics and Information Engineering, Proceedings*, 2(Iceie), pp. 214–218. Available at: https://doi.org/10.1109/ICEIE.2010.5559767.

Siemens (2004) *Tunnel System Guidelines*.

Siemens (no date) ‘Trainguard’, *siemens.com/mobility* [Preprint].

Sniady, A., Sønderskov, M. and Soler, J. (2015) ‘VOLTE Performance in Railway Scenarios’, (September).

Sousa, T. and Jorge, P. (2013) ‘Evaluation of Analytic Interference, Reception and Detection Modeling for IEEE 802.15.4 Networks with the MiXiM Omnet++ Framework’, *Thesis* [Preprint]. Available at: http://kth.diva-portal.org/smash/record.jsf?pid=diva2:597800.

Tao, H. (2023) ‘5G Base Station Deployment Based on Improved Hierarchical Co-Evolutionary Immunization Algorithm’, in *2023 IEEE International Conference on*

Image Processing and Computer Applications, ICIPCA 2023. Institute of Electrical and Electronics Engineers Inc., pp. 183–188. Available at: https://doi.org/10.1109/ICIPCA59209.2023.10257984.

Tingting, G. and Bin, S. (2010) 'A high-speed railway mobile communication system based on LTE', *2010 International Conference on Electronics and Information Engineering*, 1(Iceie), pp. V1-414-V1-417. Available at: https://doi.org/10.1109/ICEIE.2010.5559665.

UIC (2009) *GSM-R Procurement & Implementation Guide*.

UIC (2015) *EIRENE: GSM-R System Requirements Specification Version 16.0.0*.

UNISIG, E.I.G. (2012) 'Radio Transmission FFFIS for EuroRadio', (March), pp. 1–56.

Usman, A.U., Sadiq, J.M. and Ozovehe, A. (2012) 'Investigating the Applicability of Okumura-Hata Model for GSM 900 Networks of Yola Suburbs in Nigeria', pp. 7–16.

Wang, C. *et al.* (2016) 'Channel Measurements and Models for High-Speed Train Communication Systems: A Survey', *IEEE Communications Surveys & Tutorials*, 18(2), pp. 974–987. Available at: https://doi.org/10.1109/COMST.2015.2508442.

Wang, C.X. *et al.* (2016) 'Channel Measurements and Models for High-Speed Train Communication Systems: A Survey', *IEEE Communications Surveys and Tutorials*, 18(2), pp. 974–987. Available at: https://doi.org/10.1109/COMST.2015.2508442.

Wang, D. *et al.* (2021) 'Base Station Prediction Analysis Scheme Based on Lasso Regression Machine Learning Algorithm', in *Proceedings - 2021 IEEE 20th International Conference on Trust, Security and Privacy in Computing and Communications, TrustCom 2021*. Institute of Electrical and Electronics Engineers Inc., pp. 1406–1411. Available at: https://doi.org/10.1109/TrustCom53373.2021.00198.

Wang, S., Liu, K.Z. and Hu, F.P. (2005) 'Simulation of Wireless Sensor Networks Localization with OMNeT', *2005 2nd Asia Pacific Conference on Mobile Technology, Applications and Systems* [Preprint]. Available at: https://doi.org/10.1109/MTAS.2005.207141.

Wei, H. *et al.* (2010) 'Path loss models in viaduct and plain scenarios of the High-speed Railway', *2010 5th International ICST Conference on Communications and Networking in China*, pp. 1–5.

Wei, M. *et al.* (2012) ‘Base station electromagnetic simulation using ray-tracing method’, *Proceedings - 2012 6th Asia-Pacific Conference on Environmental Electromagnetics, CEEM 2012*, pp. 360–362. Available at: https://doi.org/10.1109/CEEM.2012.6410643.

Wei Qi *et al.* (2012) ‘Design of TETRA-based dedicated radio communication system for urban rail transit’, in *2012 3rd International Conference on System Science, Engineering Design and Manufacturing Informatization*.

Wen, T. *et al.* (2015) ‘Co-simulation Testing of Data Communication System Supporting CBTC’, *IEEE Conference on Intelligent Transportation Systems, Proceedings, ITSC*, 2015-Octob, pp. 2665–2670. Available at: https://doi.org/10.1109/ITSC.2015.428.

Wen, T. *et al.* (2018) ‘Access Point Deployment Optimization in CBTC Data Communication System’, *IEEE Transactions on Intelligent Transportation Systems*, 19(6), pp. 1985–1995. Available at: https://doi.org/10.1109/TITS.2017.2747759.

Xue, R. *et al.* (2020) ‘5G Enabling Technologies in Rail’, in *Proceedings - 2020 2nd International Conference on Information Technology and Computer Application, ITCA 2020*. Institute of Electrical and Electronics Engineers Inc., pp. 372–375. Available at: https://doi.org/10.1109/ITCA52113.2020.00084.

Yu, X., Ni, D. and Wang, W. (2006) ‘An omnidirectional high-gain antenna element for TD-SCDMA base station’, *ISAPE 2006 - 2006 7th International Symposium on Antennas, Propagation and EM Theory, Proceedings*, pp. 377–380. Available at: https://doi.org/10.1109/isape.2006.353347.

Zhang, L. *et al.* (2017) ‘Propagation modeling for outdoor-to-indoor and indoor-to-indoor wireless links in high-speed train’, *Measurement: Journal of the International Measurement Confederation*, 110, pp. 43–52. Available at: https://doi.org/10.1016/j.measurement.2017.06.014.

Zhang, X. (2013) ‘Research on the propagation characteristic of control signal of high-speed train’.

Zhang, X. *et al.* (2015) ‘Calibration of a 3-D ray-tracing model in railway environments’, *IEEE Antennas and Propagation Society, AP-S International*

Symposium (Digest), 2015-Octob, pp. 89–90. Available at: https://doi.org/10.1109/APS.2015.7304430.

Zhou, Y. *et al.* (2011) ‘Broadband Wireless Communications on High Speed Trains’.

Source Code: Genetic Algorithm, Adaptive BFS, OMNeT++ Models

https://github.com/xinnanlyu/GSM-R-Optimisation-Cambrian